*Russian Original Vol. 38, No. 4, April, 1975*

October, 1975

SATEAZ 38(4) 263–360 (1975)

# SOVIET ATOMIC ENERGY

**АТОМНАЯ ЭНЕРГИЯ**
**(ATOMNAYA ÉNERGIYA)**

**TRANSLATED FROM RUSSIAN**

**CONSULTANTS BUREAU, NEW YORK**

# SOVIET ATOMIC ENERGY

*Soviet Atomic Energy* is a cover-to-cover translation of *Atomnaya Énergiya*, a publication of the Academy of Sciences of the USSR.

An agreement with the Copyright Agency of the USSR (VAAP) makes available both advance copies of the Russian journal and original glossy photographs and artwork. This serves to decrease the necessary time lag between publication of the original and publication of the translation and helps to improve the quality of the latter. The translation began with the first issue of the Russian journal.





Consultants Bureau journals appear about six months after the publication of the original Russian issue. For bibliographic accuracy, the English issue published by Consultants Bureau carries the same number and date as the original Russian from which it was translated. For example, a Russian issue published in December will appear in a Consultants Bureau English translation about the following June, but the translation issue will carry the December date. When ordering any volume or particular issue of a Consultants Bureau journal, please specify the date and, where applicable, the volume and issue numbers of the original Russian. The material you will receive will be a translation of that Russian volume or issue.

Subscription
$87.50 per volume (6 issues)

Single Issue: $50
Single Article: $15

Prices somewhat higher outside the United States.

**CONSULTANTS BUREAU, NEW YORK AND LONDON**

c/b

227 West 17th Street
New York, New York 10011

4a Lower John Street
London W1R 3PD
England

Published monthly. Second-class postage paid at Jamaica, New York 11431.

*Soviet Atomic Energy* is abstracted or indexed in *Applied Mechanics Reviews, Chemical Abstracts, Engineering Index, INSPEC—Physics Abstracts and Electrical and Electronics Abstracts, Current Contents,* and *Nuclear Science Abstracts.*

# SOVIET ATOMIC ENERGY

A translation of *Atomnaya Énergiya*

October, 1975

Volume 38, Number 4 April, 1975

## CONTENTS

# CONTENTS

(continued)



The Russian press date (podpisano k pechati) of this issue was 3/25/1975. Publication therefore did not occur prior to this date, but must be assumed to have taken place reasonably soon thereafter.

# CZECHOSLOVAKIAN HEAVY-WATER REACTOR OF ZERO POWER

M. Gron and M. Voříšek

UDC 621.039.55:621.039.524.46

The TR-0 reactor may be regarded as the first nuclear reactor constructed principally by Czechoslovakian undertakings. Great help was received from the Soviet Union, which supplied the necessary amount of heavy-water and various special items of equipment as well as the corresponding expertise.

The supply of modern experimental equipment for the reactor and automation of its control offered extensive prospects for a variety of physical measurements. The large size of the active zone and the negligible influence of the side and end reflectors enabled us to carry out precision critical experiments. These qualities of the TR-0 reactor make it unique not only in the Comecon countries but also on a world wide scale, as has already been indicated by experts from a number of other countries.

The starting of the TR-0 reactor offered the possibility of making a careful check on the validity of the computing methods commonly used in reactor design and obtaining valuable information as to the physical properties of reactors (chiefly heavy-water reactors) of the A-1 type (the reactor of the first Czechoslovakian Nuclear Power Station in Yaslovski Bogunici [1-3]). The basic program of the experimental work designed to be carried out on the TR-0 reactor [3-5] up to 1975 was one of providing assistance in the starting, optimization, and perfection of the A-1 reactor, and in also estimating the practical potentialities of reactors of this type.

## Fundamental Parameters of the TR-0 Reactor

The TR-0 operates with rod-type fuel elements of the A-1 class; it is intended for the rapid realization of accurate physical experiments. The following are the main characteristics of the system.

| | |
|---|---|
| Maximum reactor power | 1 kW (briefly 3 kW) |
| Maximum thermal-neutron flux in the center of the active zone | $10^9$ neutrons/cm$^2$·sec |
| Moderator | $D_2O$ (99.87%) |
| Fuel | Natural uranium |
| Diameter of active zone | 350 cm |
| Maximum height of active zone | 400 cm |
| Maximum amount of $D_2O$ | 42 tons |
| Maximum charge of natural uranium | 39 tons |
| Reactor tank | Made of aluminum, wall thickness 16 mm, bottom thickness 25 mm, max. excess pressure 100 mm water |
| Taper of tank bottom | 15 mm |
| Outer coating of wall and tank base | Cadmium sheet 1 mm thick |
| Type of fuel | Rod, A-1 type, with hermetically closed bushing |
| Diameter of rod (uranium part) | 6.5 mm |
| Coating of rod (thickness) | Magnesium (1 mm) |
| Material of fuel-element screen tube (wall thickness) | Aluminum 99.99% (3mm) |

Institute of Nuclear Research, Rzez, Czechoslovakia. Translated from Atomnaya Énergiya, Vol. 38, No. 4, pp. 203-208, April, 1975. Original article submitted October 2, 1973; revision submitted December 28, 1974.

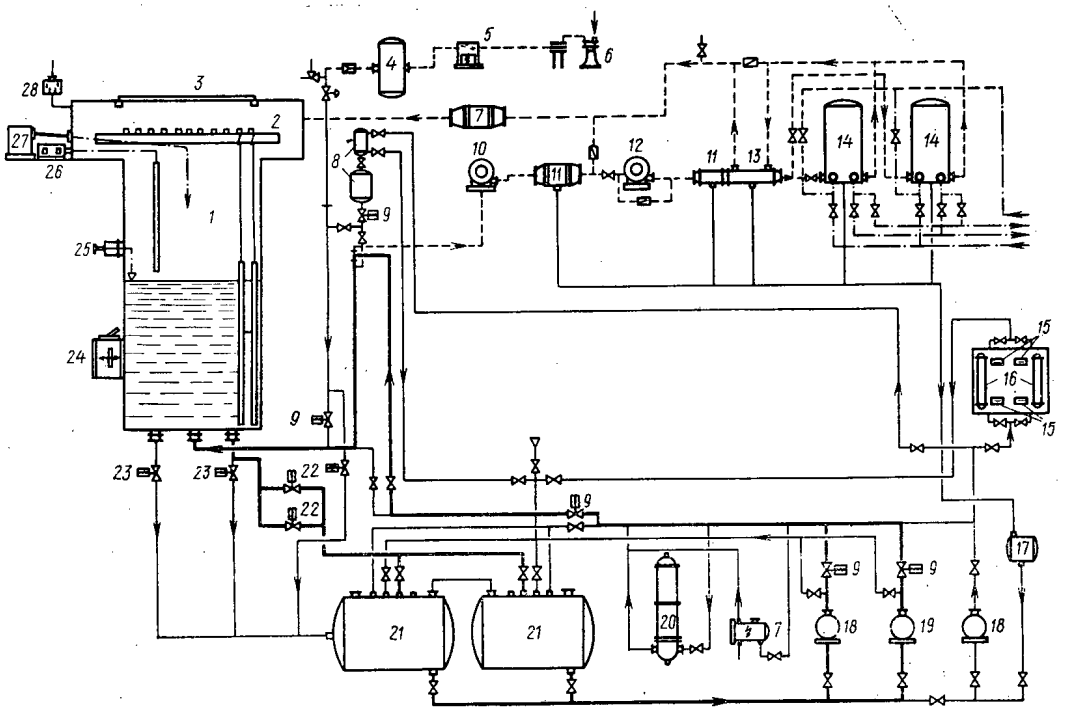

Fig. 1. Arrangement of the technological circuits of the TR-0 reactor. 1) Reactor tank; 2) carrying lattice; 3) rotating cover with hydraulic sealing; 4) dry-air reservoir; 5) silica gel drying apparatus; 6) compressor; 7) electric heater; 8) measuring tanks; 9) shut-off valves; 10) fan; 11) air cooler; 12) fan of freezing circuit; 13) heat exchanger; 14) freezing-out tanks; 15) mechanical filters; 16) ionic-exchange columns; 17) collecting tank; 18), 19) pumps with deliveries of 100 and 600 liter /min respectively; 20) heat exchanger with an intermediate layer; 21) store tanks; 22) control valves; 23) emergency valves; 24) mobile automatic-control detectors; 25) level gages; 26) drives of control and emergency rods; 27) neutron-source container; 28) hydraulic shutter.

| | |
|---|---|
| Internal diameter of fuel-element screen tubes (uranium occupation factor) | 110 mm (0.264); 123 mm (0.246); 156 mm (0.196); 183 mm (0.179) |
| Length of active part of fuel element | Max. 400 (comprising sections of 300 and 100 cm), 300 cm, or 200 cm (two sections of 100 cm) |
| Basic geometry of the lattice | Square |
| Range of automatic adjustment of the lattice step (in both perpendicular directions) | 180–275 mm; 204–316 mm; 230–320 mm; 320–520 mm; 408–632 mm; 460–640 mm; |
| Reflectors | |
| side | A $D_2O$ reflector may be provided inside the tank, with a corresponding reduction in the diameter of the active zone; outside the tank any reflector may be provided up to a thickness of about 100 cm |
| lower | Thickness referred to $D_2O$ 0–50 cm (either without cavities or containing cavities having the same diameter as the screen tubes of the fuel elements) |

| | |
|---|---|
| Temperature of moderator | |
| while cooling | Roughly 15°C |
| while heating | Roughly 90°C |
| Thermal insulation of tank | Glass wool 20 cm thick |
| Maximum rate of filling with $D_2O$ (two pumps) | 600 and 100 liters/min |
| Reactor cooling | None |
| Protective atmosphere over $D_2O$ | Dry air, dew point −40°C (excess pressure up to 35 mm water) |
| Main access to active zone | Rotating circular top and experimental openings therein |
| Upper shielding of reactor | Movable shielding slabs, total thickness ~60 cm, including ~50 cm of concrete (2.5 tons/$m^3$), 6 cm mixture of polyethylene with $B_2O_3$ |
| Side shielding of reactor | Concrete bunker 2.3 tons/$m^3$ with wall thickness 100 cm, roughly 3 m from the reactor rank |
| Reactor control | Automatic-control device working on two-out-of-three principle |
| Automatic control sensors | Three tracking fission chambers, three stationary neutron ionization chambers, three coarse level gages |
| Regulating organs (control devices) of the automatic control system | Cadmium control rod or control valves |
| Emergency executive organs | Three cadmium rods, two valves |
| Rate of emergency discharge of $D_2O$ | Roughly 15 mm/sec for a $D_2O$ level of ~300 cm; 30 tons of $D_2O$ may be discharged in 350 sec |
| Neutron source | Ra–Be, 1 Ci |
| Monitoring and measurement of the $D_2O$ level | Three working level gages connected to the emergency circuit of the automatic control; measuring accuracy ±1 mm in the range 0.5–430 cm |

## Brief Characteristics of the Basic Equipment

The technological equipment of the TR-0 reactor was described in detail in [5]. Here we shall present some basic data relating to the technological circuits. The simplified scheme and general view of the reactor are illustrated in Figs. 1 and 2.

The reactor tank is placed in a concrete shielding bunker. The lower cylindrical part of the tank, with an internal diameter of 350 cm, constitutes the active zone, 400 cm high; above this is a space, also roughly 400 cm high. Through this space pass the fuel channels and also the control and emergency rods. The upper part of the reactor tank is made in the form of a square housing, which accommodates the lattice carrying the fuel elements and a beam for the channels of the control and emergency rods. In the demountable square top of the tank is a rotating round cover with hydraulic sealing. In the cover are four eccentrically-placed round holes 50 cm in diameter and two reactangular holes 40 cm wide and 240 and 100 cm long. Fuel elements and experimental equipment may be passed in and out through these holes (without removing the cover) to any part of the active zone. The wall and conical base of the tank (15 mm on the axis of the reactor) are covered with cadmium sheets 1 mm thick.

The fuel assembly of the TR-0 reactor (Fig. 3) is a model of the fuel assembly of the A-1 reactor, which consists mainly of rod-type fuel elements and a screen tube. The fuel rods, made of natural metallic uranium, 6.3 mm in diameter and 300 and 100 cm long, are coated with 1 mm of magnesium. By means of the spacing lattices the rods are assembled into two fuel sections, which are arranged in the aluminum screen tube, hermetically closed with a lid.

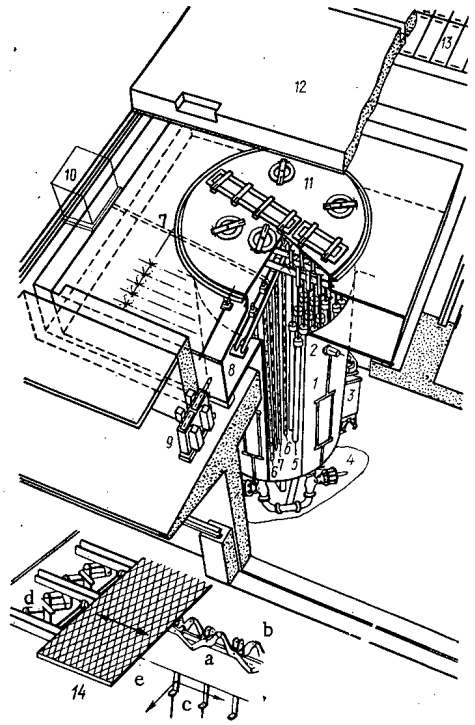


Fig. 2

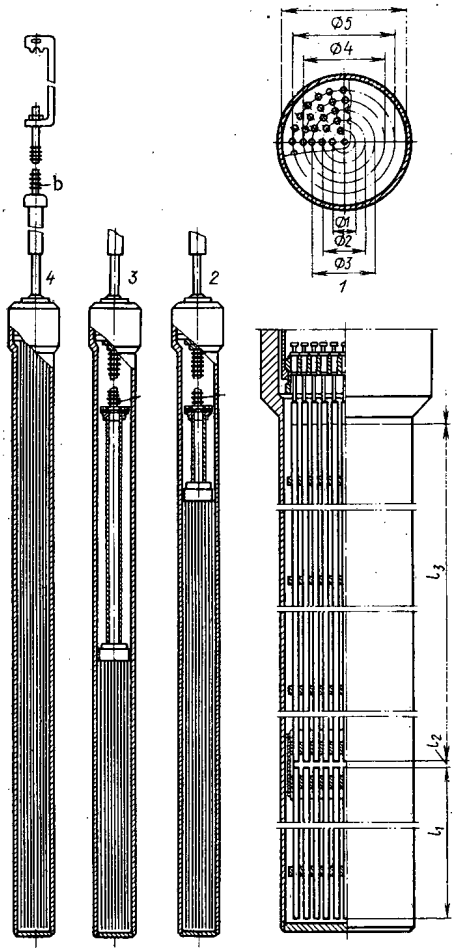


Fig. 3

Fig. 2. General view of the TR-0 reactor: 1) Cylindrical part of the tank; 2) working level gages; 3) thermal column with mobile fission chambers (automatic-control sensors); 4) emergency valves; 5) fuel element; 6) control and emergency rods; 7) neutron-source channel; 8) square part of tank; 9) rod drives; 10) neutron-source container; 11) rotating cover with hydraulic sealing; 12) mobile shielding slabs; 13) fuel element store; 14) part of carrying lattice: a) beams; b) vertical hinged lever mechanism; c) suspension hook; d) mobile mouting plate.

Fig. 3. Fuel element. 1) Cross section of a fuel element of the central type $l_1$ = 1000 mm; $l_2$ = 5 mm; $l_3$ = 3000 mm; internal diameter $\varnothing$ = 120 mm; $\varnothing 1$ = 19.6 mm; $\varnothing 2$ = 39.2 mm; $\varnothing 3$ = 59.7 mm; $\varnothing 4$ = 78.9 mm; $\varnothing 5$ = 99.6 mm; 2) one three-meter section; 3) two one-meter sections; 4) one three-meter and one one-meter section; a) internal supporting rod; b) external supporting rod. Number of rods on the circles 5, 10, 15, 20, and 25.

The special construction of the fuel-section couplings enables us to suspend a one-meter section from a three-meter (or another one-meter) section. For siting the three-meter (or two one-meter) sections in the screen tube, (supporting) rods are provided; these enable us to simulate a lower reflector (with cavities) 0-48 cm thick arranged in steps of 2 cm.

The external supporting rods fixed in the caps of the fuel assembly enable us to arrange the fuel elements at various heights above the bottom of the reactor tank and to create a reflector (without cavities) 0-52 cm thick arranged in steps of 2 cm. The fuel assemblies are set up automatically in both directions in the carrying lattice, with a square step of 180-640 mm (positioning accuracy ±0.2 mm).

The control rod and the three emergency rods have an analogous construction. The absorbing material is cadmium of cruciform profile, covered with aluminum. The length of the active part of the rod is 200 cm, the width 6 cm, and the thickness of the cadmium sheet 1 mm. The rods are placed in perforated aluminum channels furnished with shock absorbers in the lower part. The channels are sited in a special structure under the carrying lattice.

The heavy-water circuits are designed for filling and emptying the reactor tank, storing the $D_2O$ in the storage (reserve) tanks, heating, cooling, and purifying the moderator, and so forth.

In order to carry out experiments at high temperatures, provision is made for the electrical heating of the $D_2O$ (to 90°C). For cooling the moderator there is a heat exchanger with an intermediate layer (inlet temperature of the $D_2O$ 20-90°C, cooling water 15°C). The circulation of the $D_2O$ is achieved by means of three glandless stainless-steel pumps: two of these (delivery 600 and 100 liters/min) are used in the main $D_2O$ circuit and one (100 liters/min) in the purification circuit. Rapid filling of the reactor with $D_2O$ (1-100 liters in less than 0.1 sec) is achieved by means of exactly calibrated measuring tanks.

In order to purify the $D_2O$ from soluble and insoluble impurities, two parallel circuits with mechanical filters and ion-exchange columns filled with deuterized resin are provided. In order to prevent contact with light water vapor, a slight excess pressure of dry air is automatically maintained in the heavy-water circuit. In order to avoid the loss of $D_2O$ as a result of the evaporation of the remaining traces of moderator after emptying the reactor tank, the remaining $D_2O$ is passed into a special freezing apparatus by means of a stream of heated dry air. Dry air is also used for heating the reactor before filling the tank with the heated moderator.

A novel automatic control device is used for controlling the reactor power and providing emergency protection; it is designed to carry out the following operations:

1) automatic verification of the state of readiness for operation;

2) automatic (or manual) achievement and stabilization of the critical state; this process consists of three stages: a) raising the level of $D_2O$ to a specified minimum height; b) increasing the neutron flux in accordance with a specified program by changing the level of heavy-water while automatically regulating the reactor period until the specified neutron flux is attained; c) achieving and stabilizing the critical state while automatically regulating the steady neutron flux and automatically extracting the neutron source;

3) automatic maintenance of a specified neutron flux by means of the control rod or the $D_2O$ level;

4) automatic (or manual) variation of the neutron flux in accordance with a specific program;

5) automatic continuous monitoring of the reactor in the steady and transient states, i.e., a determination of the actual state of the reactor and comparison with the specified state;

6) emission of warning signals;

7) emission of emergency signals for the rapid shutting down of the reactor.

The basic concept of the automatic-control device is the generally-accepted logical principle of two-out-of-three. Three independent systems fulfil the function of tracking devices. For low neutron fluxes these operate without moving the fission chambers, while for high fluxes the automatic control sensors are moved within the water-filled thermal column. All three automatic-control systems operate in the tracking mode. One of the two systems may be used as regulator. If one system becomes faulty the second automatically assumes the function of regulator.

The working equipment includes (and these are extremely vital features) a set of level gages: three working ("coarse") gages and one of much higher accuracy (experimental). These are placed in special perforated channels on the periphery of the active zone. The working level gages, which have an error of ±1 mm in the range 0.5-430 cm, are connected to the automatic control device. These monitor the $D_2O$ level and emit a signal when the moderator has reached a specified height. The main function of the working gages is to prevent the level of $D_2O$ from exceeded the specified position; this is ensured by connecting the gages to the emergency circuit of the automatic control device, using the two-out-of-three principle. The accurate level gage is intended for experimental purposes; its error is ±0.05 mm over a few centimeters and ±0.2 mm over the range 30-400 cm.

## Experimental Equipment

In addition to instruments for activation, spectrometric, and time measurements, neutron detectors, and so forth, the TR-0 reactor also contains an experimental device for measuring the neutron distribution in the active zone of the reactor; this is placed on the reactor cover and is intended for the smooth or stepped movement (in 2 mm steps) of the detector in the vertical and horizontal directions. The position of the detector is measured to an accuracy of ±1 mm. The motion of the detector may be controlled manually or by means of a specialized controlling computer (the "ESTIMATOR") in accordance with a preselected program. This computer is designed for controlling various pieces of experimental equipment (for example, it is used in varying the level of the moderator) periodically, measuring the reactor period, analyzing experimental data, and so on.

By using the equipment for varying the $D_2O$ level we may study the influence of periodic changes of reactivity due to changes in the height of the $D_2O$ level close to the critical state. In order to vary the level, the filling and emptying valves are periodically opened and closed; this is effected by means of the "HETRO" system controlled by the ESTIMATOR computer or by a time converter.

The HETRO system gives a $D_2O$ level fluctuation period of 4-400 sec; we may specify 1-10 fluctuations, or any unlimited number. The change in level over one period may reach as much as ±2 cm (the corresponding change in reactivity is about $\pm 2 \cdot 10^{-3}$).

The main aim of the experiments carried out with the cadmium fluctuator is to determine the influence of periodic perturbations on the state of the reactor. A change in reactivity is achieved by rotating one of two cadmium plates of special form (a rotor and a stator); these reside in an aluminum shell inside the reactor. The number of revolutions of the interchangeable rotor may be varied over the range 20-1800 rpm; the maximum change in reactivity is $2 \cdot 10^{-3}$.

The absorbing rods (24) serve to imitate the influence of the absorbing properties of the emergency, control, and compensating rods of the A-1 reactor on the reactivity and neutron field.

The absorbing part is made of cadmium, and has the shape of a tube with an external diameter of 53 mm and a wall thickness of 1.5 mm. The tube is held in a hermetic can (internal diameter 56 mm, wall thickness 2 mm). The rod drives situated on the carrying lattice execute the following functions: facilitating the free fall of one to four rods into the active zone; remote control of the position of the rods to an error of ±2 mm; manual variation of rod position.

For measuring those characteristics of the lattice which depend on the fuel temperature, four special fuel assemblies are provided, with electric heating to 350°C.

A model of the experimental loop of the A-1 serves for studying the physical properties of this loop in the TR-0 reactor. This consists of suspension equipment, an outer casing, and inner tubes filled with 3%-enriched metallic uranium. The suspension equipment and the outer casing are made of the same construction elements as the fuel assemblies of the TR-0. The inner tubes of the model are made of steel, their diameters are 115 and 79 mm, the wall thickness is 6.5 and 2 mm respectively. The model consists of 31 fuel elements with a diameter of 6.3 mm (thickness of magnesium coating 1 mm).

The model is intended for carrying out the following experiments: measuring the reactivity of the model at various points and for various configurations of the active zone, and measuring the neutron-flux distribution around and inside the model.

In order to determine the efficiency of the absorbing rods, the dynamic characteristics of the lattice, and so forth, the pulsed-source method is also employed in the TR-0 reactor. The neutron intensity in the pulse is $10^{10}$ neutrons/sec for a mean value of $2 \cdot 10^8$ neutrons/sec. The pulse length may be smoothly varied from 5 to 8 μsec, the frequency being varied in the range $1\text{-}5 \cdot 10^4$ pulses/sec.

Thus from the very onset of its experimental activities (which began in July 1972) the TR-0 reactor has been undergoing a wide range of experiments, mainly associated with the program of realizing physical initiation of the A-1 reactor, the central feature in the first Czechoslovakian Nuclear Power Station. Some of these experiments were actually carried out before the physical initiation of the A-1 began and were continued during the whole period of physical and power initiation.

The results obtained in the TR-0 for a number of parameters [6, 7] supplement the information obtained in the physical initiation of the A-1, provide a more accurate theoretical description of the reactor, and help in effecting a reliable extrapolation of the resultant data in the range corresponding to the working state of the reactor.

Experiments with the neutron converter carried out in cooperation with Soviet specialists and ZVJE –ŠKODA workers enabled us to calibrate the detectors of the A-1 reactor and to carry out unique measurements of fast-neutron fluxes. Great attention was also paid to experiments with a pulsed neutron source, carried out in cooperation with Nuclear Power Station workers. These experiments were carried out in order to develop methods of measuring reactivities, breeding factors, and neutron-migration areas.

After carrying out the first part of the experimental program, measurements which had proved impossible to realize in the A-1 were continued in the TR-0 reactor. These measurements may have an important significance not only from the point of view of verifying theoretical methods and programs of calculating the physical parameters of heavy-water reactors but also from that of the efficient use of the A-1 power station and the assessment of the practical potentialities of reactors of this type.

## LITERATURE CITED

1. A. Sevcik, Second Geneva Conference, Paper No. R/2092, Czechoslovakia (1958).
2. J. Holubec et al., Third Geneva Conference, Paper No. R/523, Czechoslovakia (1964).
3. I. Paulička et al., ibid., Paper No. R/542.
4. J. Bárdoš et al., ÚJV-2737/R (1971).
5. M. Voříšek, ÚJV-2845/R (1972).
6. M. Voříšek, ÚJV-2967-F/R (1973); M. Voříšek, F. Hudec, and Z. Turzík, ÚJV 2968-F (1973); Z. Turzik, ÚJV-2969-F (1973); Ć. Svoboda, ÚJV-2970-F/R (1973); Ć. Svoboda, ÚJV-2971-F/R (1973); J. Mikus and F. Kryl, UJV-3067/R (1973).
7. I. Paulička, A. Zbytovský, and M. Voříšek, Jaderna Energie, 19, 291 (1973).

# THERMAL AND RESONANCE NEUTRON SPECTRA IN A GRAPHITE CUBE

Yu. M. Odintsov, A. S. Koshelev, and A. A. Malinkin

UDC 539.125.5:162.2.3

In view of the ever-increasing demands for greater accuracy in the measurement of neutron spectra in nuclear reactors, a great deal of attention has lately been paid to the metrological problems involved in this process [1].

The creation of standard sources of resonance neutrons is an extremely important problem at the present time, yet the development of such sources is still in its infancy. In referring to resonance neutrons, most papers [3, 4] only indicate the ratio of the resonance neutrons to those of the thermal type. In actual practice it is often essential to study the characteristics of resonance neutrons in media in which their spectra differ from the simple 1/E form. Clearly the study of neutron characteristics in these media would be greatly simplified if we had a standard source with a set of known spectra not obeying the 1/E law. The spectral characteristics of resonance neutrons in graphite prisms were studied in [6, 7]; it was shown that, depending on the distance from the primary neutron source, the resonance neutron spectrum could be expressed in the form $E^{-(1+\beta)}$, where $|\beta| \ll 1$.

In order to create a calibrated source of thermal and resonance neutrons in the present investigation, we studied the characteristics of thermal and resonance neutrons in a graphite cube with a side of 1 m, which showed that there were a number of regions in the graphite cube in which the resonance neutron spectra differed considerably from the 1/E form and could better be expressed in the form $1/E^{\alpha}$ (here $0.8 < \alpha < 1$). The neutron characteristics studied in the graphite tube subsequently justified us in using the latter as a calibrated source of thermal and resonance neutrons with different spectral characteristics.

## Construction of the Cube

The cube was made up of reactor graphite blocks with a density of 1.6 g/cm$^3$ and placed on a scaffold so that the center of the cube lay at a height of 2 m from the floor, on a level with the center of a 28-cm-diameter sphere of 90%-enriched metallic uranium. The front face of the cube lay at 3 m from the center of the uranium assembly. The cube was placed in a room 6.5 × 7.5 × 4.5 m in size with concrete walls.

Along the central axis of the cube in the direction of the assembly, an open channel 10 × 10 cm in section was provided; this was filled with graphite blocks containing cells for indicating instruments. The cells were placed along one face of the blocks in steps of 3 cm, and took the form of cylinders 20 mm in diameter and 5 mm deep.

No protective screens (cadmium or boron) were placed on the faces of the cube.

## Characteristics of the Detectors

In order to reconstruct the spectra we used the reactions indicated in Table 1. The range of measurable neutron energies for the system chosen was 1.46 eV to 8.7 keV. All the materials of the indicators had a natural isotopic composition. The indium, tungsten, and copper indicators were metal foil disks 5-15 cm in diameter. The indicators for the reactions $^{139}$La(n, $\gamma$) and $^{164}$Dy(n, $\gamma$) were prepared from films made of a mixture of powdered lanthanum or dysprosium oxides with saponlac (cellulose nitrate). The indicators for the reactions $^{23}$Na(n, $\gamma$) and $^{37}$Cl(n, $\gamma$) were made by pressing 15 mm diameter tablets of $Na_2CO_3$ and $C_6Cl_6$ respectively.

Translated from Atomnaya Énergiya, Vol. 38, No. 4, pp. 209-212, April, 1975. Original article submitted March 19, 1974.

TABLE 1. Characteristics of the Reactions and Indicators Used

| Reaction | Thickness of indicator referred to the isotope, nuclei/cm² | $T_{1/2}$ | σ(2200 m/sec), G | $E_0$, eV | Recorded energy of γ quanta, MeV |
|---|---|---|---|---|---|
| $^{115}In$ (n, γ) | $1{,}01\cdot10^{20}$ | 54,0 min | 160±2 | 1,46 | 1,3 |
| $^{197}Au$ (n, γ) | $2{,}86\cdot10^{19}$ | 2,7 days | 98,8±0,3 | 4,9 | 0,412 |
| $^{186}W$ (n, γ) | $8{,}35\cdot10^{19}$ | 24 h | 38±2 | 18,8 | 0,687 |
| $^{139}La$ (n, γ) | $2{,}39\cdot10^{19}$ | 40,2 h | 8,2±08 | 72,4 | 1,597 |
| $^{63}Cu$ (n, γ) | $4{,}97\cdot10^{20}$ | 12,88h | 4,51±0,23 | 577 | 0,511 |
| $^{23}Na$ (n, γ) | $2{,}46\cdot10^{21}$ | 15,05h | 0,531±0,008 | 2900 | 1,37 |
| $^{37}Cl$ (n, γ) | $4{,}60\cdot10^{21}$ | 37,12 min | 0,56±0,12 | 8700 | 1,65 |
| $^{164}Dy$ (n, γ) | $1{,}90\cdot10^{18}$ | 2,36h | 800±100 | 1/v- detector | 0,412—0,511 |

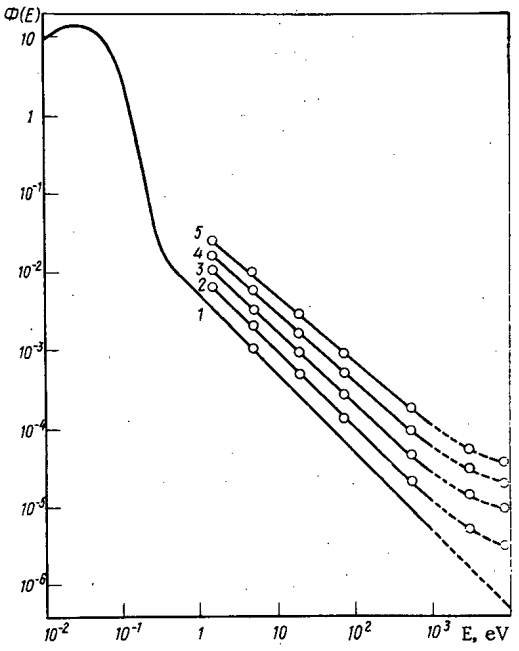


Fig. 1. Thermal and resonance neutron spectra in a graphite cube at the following distances from the front face: 1) 65 cm, $\varphi_r = 1/E$ (taken); 2) 41 cm, $\varphi_r = 1/E^{0.96}$; 3) 28 cm, $\varphi_r = 1/E^{0.93}$; 4) 16 cm, $\varphi_r = 1/E^{0.86}$; 5) 4 cm, $\varphi_r = 1/E^{0.84}$.

The indicators were employed in conjunction with a scintillation gamma spectrometer containing an NaI(Tl) crystal 80 × 80 mm in size, calibrated with standard γ sources; the error in the activity was ±3% (for a 95% confidence interval). The absolute activity of gold was determined in a $\beta-\gamma$ coincidence installation, which was calibrated by comparison with the $4\pi\beta-\gamma$ and $\beta-\gamma$ systems of the All-Union Scientific-Research Institute of Metrology. The error in the determination of the absolute activity of gold in our apparatus was ±1.5% for a 95% confidence range.

## Determination of Neutron Temperature

The effective neutron temperature was determined using a "double sandwich" of gadolinium and dysprosium (method described in [8]). The filters were prepared by spraying gadolinium oxide on a polyethylene substrate 0.05 mm thick. The thickness of the filters varied: from $6.8\cdot10^{18}$ to $3.8\cdot10^{19}$ nuclei/cm², referred to the $^{155}Ga$ isotope. The thickness of the indicator for the reaction $^{164}Dy(n, \gamma)$ was 1 mg/cm². The error in determining the temperature (±6%) was mainly due to the inaccuracy of the $^{155}Ga(n, \gamma)$ cross section and the thickness of the filters.

## Determination of the Absolute Flux of the Thermal and Resonance Neutrons

In measuring the density of the reactions we found that the neutron spectrum was thermalized to the greatest extent at 65 cm from the front face of the cube.

The energy distribution of the neutron flux at this distance may be expressed in the form [9]

$$\Phi(E)=\Phi_{th}\frac{E}{(kT)^2}e^{-E/kT}+\Phi_{epi}\frac{\Delta(E/kT)}{E}, \quad (1)$$

where k is Boltzmann's constant, T is the absolute temperature, Δ(E/kT) is a transitional function between the Maxwell and Fermi distributions, $\Phi_{epi}$ is the flux density of the resonance neutrons, $\Phi_{th}$ is the flux density of the thermal neutrons ($\Phi_{tn} = n\bar{v} = 2nv_t/\sqrt{\pi}$, n is the neutron density, $\bar{v}$ is average neutron velocity, $v_t$ is the most probable velocity of the neutrons at temperature T).

It should be noted that the form of the intermediate neutron spectrum – see Eq. (1) – may differ from the generally-accepted one in the range 1-10 keV. Thus it was indicated in [7] that the resonance neutron spectrum in a graphite cube with a side of 70 cm obeyed the 1/E law up to 1 keV but fell more sharply than 1/E at higher energies.

TABLE 2. Characteristics of Thermal and Resonance Neutrons in a Graphite Cube

| R,* cm | $n\bar{v}\cdot 10^8$ neut./(cm²·sec) | $n\bar{v}/\Phi_{epi}$ | $T_{eff}$, K | $\alpha$ |
|---|---|---|---|---|
| 4 | 3,40±0,14 | 54±3 | 378±22 | 0,84 |
| 16 | 4,70±0,19 | 68±3 | 352±21 | 0,86 |
| 28 | 5,25±0,21 | 92±4 | 324±19 | 0,93 |
| 41 | 5,22±0,15 | 135±6 | 315±18 | 0,96 |
| 65 | 3,06±0,09 | 195±10 | 309±18 | 1,0 (taken) |

*Distance from the front face of the cube.

The absolute thermal neutron flux was determined from the activation of gold in a cadmium filter, and also in the absence of a filter. The value of $\Phi_{th}$ was found from the equation

$$\Phi_{th}=N_{th}/n_{nu}^{Au}\bar{\sigma}_{th}^{Au}. \quad (2)$$

Here $n_{nu}^{Au}$ is the number of $^{197}Au$ nuclei in 1 mg of indicator; $N_{th} = N - F_{Cd}N_{Cd}$; N and $N_{Cd}$ are the saturation activities referred to the end of the gold-irradiation period in the absence of the cadmium filter and after the inclusion of the latter, respectively; $F_{Cd}$ is the cadmium correction, equal to 1.07 for cadmium 0.6 mm thick, calculated in accordance with [9. 10]; $\bar{\sigma}_{th}^{Au} = \sqrt{\pi}\, 2^{-1}(T)\sqrt{293.6/T}\,\sigma_{th}^{Au}$ (2200 m/sec) is the gold activation cross section averaged over a thermal neutron spectrum with a Maxwell distribution; g(T) is a factor allowing for the deviation of the gold activation cross section from the law $\sigma \approx 1/v$; $\sigma_{th}^{Au}$(2200 m/sec) is the activation cross section for a velocity of 2200 m/sec.

The absolute value of the resonance neutron flux was determined from the reactions $^{197}Au(n, \gamma)$ and $^{164}Dy(n, \gamma)$ both in a cadmium filter and in the absence of the filter. For a thin resonance indicator we may write

$$(R_{Cd}-F_{Cd})_{res}=\frac{\Phi_{th}}{\Phi_{epi}}\frac{\bar{\sigma}_{th}}{\int_{E_{Cd}}^{\infty}\sigma_{act}(E)\frac{dE}{E}}. \quad (3)$$

Here $E_{Cd}$ is the cadmium boundary, equal to 0.58 eV for cadmium 0.6 mm thick [9]; $R_{Cd}$ is the cadmium ratio; $\int_{E_{Cd}}^{\infty}\sigma_{act}(E)dE/E$ is the resonance integral. The resonance integral for gold is taken as 1534 ± 40 b [9]. A correction was introduced into the measured value of the cadmium ratio, since the gold indicator was insufficiently thin with respect to the resonance neutrons. The extent of this correction was determined from the tabulated values of [10].

For a thin 1/v detector we may write

$$(R_{Cd}-F_{Cd})_{1/v}=\frac{\Phi_{th}}{\Phi_{epi}}\frac{\sqrt{\pi}}{4}\sqrt{\frac{E_{Cd}}{kT}}. \quad (4)$$

The unknown quantity $\Phi_{epi}$ was determined from Eqs. (3) and (4). The values obtained from these relationships agreed closely.

For known values of $\Phi_{th}$, $\Phi_{epi}$, $\Delta(E/kT)$, T [9] we used Eq. (1) to determine the absolute value and spectral distribution of the thermal and resonance neutron fluxes.

## Calibration of Resonance Detectors and Determination of the Resonance Neutron Spectra along the Central Axis of the Cube

The calibration of the indicators was carried out at a distance of 65 cm from the front face of the cube, at which the spectrum was taken in the form of the 1/E relationship, while the absolute neutron flux was determined in the manner already indicated.

For the irradiation of indicator i and the gold indicator in a thermal neutron flux, the saturation activities referred to the end of the irradiation period $N_{th}^{i}$ and $N_{th}^{Au}$ were

$$N_{th}^{i}=n_{nu}^{i}n_{\gamma}^{i}\varepsilon_{\gamma}^{i}\alpha^{i}\bar{\sigma}_{th}^{i}\Phi_{th}=k^{i}\sigma_{th}^{i}\Phi_{th}; \quad (5)$$

$$N_{th}^{Au}=n_{nu}^{Au}n_{\gamma}^{Au}\varepsilon_{\gamma}^{Au}\alpha^{Au}\bar{\sigma}_{th}^{Au}\Phi_{th}=k^{Au}\bar{\sigma}_{th}^{Au}\Phi_{th}. \quad (6)$$

Here $n_{nu}$ is the number of nuclei in the indicator $n_{\gamma}$ is the number of $\gamma$ quanta per decay $\varepsilon_{\gamma}$ is the recording efficiency; $\alpha$ is the isotopic composition.

From Eqs. (5) and (6) we have

$$K^i = \frac{N_{th}^i \bar{\sigma}_{th}^{Au}}{N_{th}^{Au} \bar{\sigma}_{th}^i} K^{Au}. \quad (7)$$

During the calibration of the indicators we determined the values of $k^i$ for each of these. The measured and calculated values of $k^i$ agreed closely.

In the relative measurements we compared the numbers of reactions (the indicators being irradiated in a cadmium filter) due to resonance in the cross section of the indicator. The contribution from the 1/v part of the cross section for each resonance indicator was determined from the $^{164}Dy(n, \gamma)$ reaction in the cadmium filter and was subtracted from the total number of reactions, i.e., for all the resonance indicators we obtained the quantities

$$A_{(65\,cm)}^i = N_{Cd}^i - N_{Cd}^{Dy} \frac{k^i \bar{\sigma}_{th}^i}{k^{Dy} \bar{\sigma}_{th}^{Dy}}.$$

The unknown spectra at a distance x from the front face of the cube were determined from the equation

$$\varphi_x(E_i) = \varphi_{(65\,cm)}(E_i) \frac{A_{(x)}^i}{A_{(65\,cm)}^i}.$$

When measuring the $1/E^\alpha$ spectrum by reference to resonance indicators calibrated in a 1/E spectrum, in order to calculate the corrections for the side resonances we only have to allow for the changes in the values of these corrections in the $1/E^\alpha$ spectrum as compared with the 1/E distribution, since by calibration in the 1/E spectrum these corrections will already have been automatically introduced. The contributions of the side resonances in the 1/E spectrum were calculated in [11] for thin indicators. The form of the unknown spectral distributions was finally determined by introducing these corrections on the successive-approximation principle. In reconstructing the spectra no corrections were introduced for the side resonances associated with the $^{23}Na(n, \gamma)$ and $^{37}Cl(n, \gamma)$ reactions, since the contribution of side resonances was unknown.

The measured resonance neutron spectra (Fig. 1) have the form $1/E^\alpha$ for energies between 1 eV and 1 keV. For energies above 1 keV the form of the spectrum may differ from that indicated in Fig. 1, since no allowance was made for the contribution of side resonances in the reactions involving the $^{23}Na$ and $^{37}Cl$ isotopes (Table 2).

The neutron characteristics here studied justify us in using the graphite cube in question as a calibrated source of thermal and resonance neutrons with different spectral characteristics.

## LITERATURE CITED


1. R. D. Vasil'ev, At. Énerg., 34, No. 4, 277 (1973).
2. I. A. Yaritsyna et al., Neutron Measurements [in Russian], Standarty, Moscow (1973).
3. B. G. Arabei et al., in: Nuclear Instrument-Making [in Russian], Vol. 17, Atomizdat, Moscow (1972), p. 3.
4. E. Axton, React. Sci. and Technol., 17, No. 17, 125 (1963).
5. C. Hargrove and K. Geiger, Canad. J. Phys., 42, 1593 (1964).
6. T. Ryves and E. Paul, J. Nucl. Energy, 22, No. 12, 759 (1968).
7. V. I. Golubev et al., At. Énerg., 23, No. 2, 138 (1967).
8. T. S. Mordovskaya and V. I. Petrov, in: Nuclear Instrument-Making [in Russian], Vol. 13, Atomizdat, Moscow (1970), p. 59.
9. K. Bekurz and K. Wirtz, Neutron Physics [Russian translation], Atomizdat, Moscow (1968).
10. Neutron Fluence Measurements, Technical Reports, Series No. 107, IAEA, Vienna (1970).
11. V. N. Avaev and Yu. A. Egorov, in: Problems of Dosimetry and Radiation Shielding [in Russian], Vol. 4, Atomizdat, Moscow (1965), p. 15.

# USE OF FEW-GROUP METHODS FOR CALCULATING THE PHYSICAL CHARACTERISTICS OF FAST REACTORS

V. A. Karpov, V. I. Matveev,
N. E. Gorbatov, L. V. Averin,
V. A. Chernyi, and V. G. Samsonov

UDC 621.039.526

One leading characteristic of fast reactors is the wide range of energies (1 keV-10 MeV) within which the basic nuclear-physical processes take place. In order to calculate these reactions many-group (multigroup) approximations are usually employed. To this end it is important to have a detailed knowledge of both the upper part of the neutron energy spectrum (involving $^{238}U$ fission and inelastic scattering) and also the lower part (Doppler effect).

A fast power reactor is a fairly complicated system with a large number of inhomogeneities. In the active zone some 10% of the cells are occupied by control and emergency devices (rods). In order to equalize the heat-evolution field over the reactor radius, zones of different degrees of enrichment are provided. In the axial direction asymmetry occurs because of the gas phase.

For a correct description of a reactor with these characteristics we require a three-dimensional model with a fairly large number of computing zones and also a detailed energy analysis. The computing model is too cumbersome even for a computer of the BÉSM-6 type. The creation of approximate but fairly accurate methods is therefore an important and pressing problem.

In its initial stages, the development of computing methods followed the principle of adopting a geometrical idealization of the reactor, since the accuracy of calculating the principal reactor functionals (the critical mass and the conversion ratio) is determined more by the accuracy of calculating the neutron spectrum than by a detailed analysis of the geometry.

The development of fast high-powered reactors required a detailed study of the heat-evolution field; the accuracy with which this may be calculated depends very considerably on the reactor geometry. For calculating the heat-evolution field and the quantities associated therewith (such as the interference corrections encountered when determining the efficiency of the control and emergency rods), few-group methods have proved very efficient. Problems arising in this connection include that of deciding upon an adequate number of groups and choosing the manner in which energy ranges should be divided up, as well as that of the method to be used in averaging the few-group cross sections. Another important point is the accuracy of calculating the integrated reactor characteristics (the critical mass and conversion ratio), and also the efficiency of the control and emergency rods.

In this paper we shall consider experience which has been gained in the use of few-group methods for calculating reactors of the BN-600 type and the corresponding model assemblies [1, 2]. For these calculations we used programs based on the diffusion approximation with two-dimensional hexagonal geometry, as developed in the Physical Power Institute and the I. V. Kurchatov Institute of Atomic Energy.

## Computing Methods and Programs

Few-group methods are already used for calculating systems involving fast neutrons, especially assemblies simulating the BN-350 reactor. A one group approximation in two-dimensional (r, $\varphi$) geometry gave satisfactory results in describing the heat-evolution fields for assemblies incorporating absorbing rods [3].

Translated from Atomnaya Énergiya, Vol. 38, No. 4, pp. 213-216, April, 1975. Original article submitted August 9, 1974.

TABLE 1. Principal Physical Characteristics of the Reactor Obtained by Means of the Programs Devised for the BÉSM-6 Computer

| State of the reactor | Number of groups | $K_{eff}$ | Radial nonuniformity coefficient of heat evolution in the active zone | Conversion ratio | | Efficiency of the rod system, %Δk/k | |
|---|---|---|---|---|---|---|---|
| | | | | active zone | lateral screen † | compensating rods | emergency rods |
| After fuel recharging | 2 * | 1,0024 | 1,25 | 0,320 | 0,222 | 5,83 | 3,40 |
| | 2 | 1,0048 | 1,25 | 0,320 | 0,223 | 5,85 | 3,42 |
| | 4 | 1,0053 | 1,24 | 0,317 | 0,221 | 5,83 | 3,49 |
| | 6 | 1,0019 | 1,26 | 0,322 | 0,225 | 5,78 | 3,47 |
| | 9 | 1,0029 | 1,25 | 0,321 | 0,224 | 5,78 | 3,55 |
| Before fuel recharging | 2 | 1,0028 | 1,25 | 0,374 | 0,222 | 6,29 | 4,22 |
| | 2 * | 1,0050 | 1,25 | 0,375 | 0,222 | 6,40 | 4,32 |
| | 6 | 1,0040 | 1,24 | 0,374 | 0,223 | 6,43 | 4,36 |
| | 9 | 0,9992 | 1,26 | 0,373 | 0,226 | 6,20 | 4,28 |

* The boundary between the groups is equal to 0.2 MeV; in the other two-group calculations it equals 0.8 MeV.
† Without allowing for the end sections.

Subsequently few-group methods were developed for a hexagonal geometry, in view of the fact that this gave a better description of reactors comprising hexahedral cassettes. The first hopeful result of using a two-group diffusion approximation in hexagonal geometry for calculating the model of the BN-600 reactor was obtained on using the program developed by I. S. Akimov in the Physical Power Institute for calculating thermal reactors [2].

This program was then considerably modified from the point of view of increasing the number of computing points (2560) and automating the calculation of a number of functionals; it was then used for calculating fast reactors. The program was designed for the M-220 computer. In addition to this, analogous programs were developed for the BÉSM-6 computer in the Kurchatov Institute of Atomic Energy; these had a larger number of computing points (1200-2000) and two to nine energy groups. The programs for the BÉSM-6 and M-220 computers are based on an adequate finite-difference approximation to the differential diffusion equation, but differ in their methods of solving the systems of linear algebraic equations. The finite-difference approximation is based on representing the reactor in the form of a model consisting of hexagonal cells with computing points at the corners. The methods of obtaining the system of finite-difference equations and the iteration methods for their solution are set out in [4-6].

For solving the finite-difference problem a double iteration process is employed in the M-220 computer program. The outer (source) iterations are followed by inner iterations, as required for calculating fluxes with a specified distribution of neutron sources. The inner iterations are accelerated by the Yang – Frankel method, with preliminary calculation of the group-relaxation coefficients. The number of inner iterations depends directly on the accuracy of the outer iterations. The total number of iterations is determined by the accuracy specified both for $K_{eff}$ ($\varepsilon_1$) and for the source distribution over the reactor volume ($\varepsilon_2$).

In the program for the BÉSM-6 computer the interaction procedure for calculating many-group neutron fluxes and sources no longer comprises the traditional combination of outer and inner iterations. The calculation comprises a sequence of calculations relating to the neutron source and flux distributions, without any internal iterations.

These programs calculate $K_{eff}$, the group fluxes, the heat-evolution field, the heat-evolution nonuniformity factor, and the power. The program for the M-220 also determines the position (nodal point number) of maximum heat evolution in the cassette, while the BÉSM-6 programs calculate the isotopic composition, the conversion ratio, and the doubling time.

The computing time for a reactor of the BN-600 type (with the complete printing of the results) using the M-220 program is ~50 min for $\varepsilon_1 = 5 \cdot 10^{-5}$ and $\varepsilon_2 = 5 \cdot 10^{-3}$. An analogous calculation using the BÉSM-6 computer program requires ~10 min for a $K_{eff}$ accuracy of $10^{-7}$ and a neutron-flux accuracy of $10^{-4}$. The calculation of the same reactor in nine groups requires ~45 min.

TABLE 2. Characteristics of the One-Zone Model of the BN-600 Reactor

| No. of groups | Boundary, MeV | $K_{eff}$ | Rod efficiency, % Δk/k |
|---|---|---|---|
| 2 | 0,4 | 0,9939 | 1,67 |
| | 0,2 | 0,9933 | |
| | 0,1 | 0,9940 | |
| | 0,0465 | 0,9955 | |
| | 0,01 | 0,9967 | 1,64 |
| 26 | | 0,9877 | 1,66 |

## Few-Group Cross Sections

The determination of the few-group cross sections has a considerable effect on the accuracy of the calculation. Experience shows that it is impossible to find a single system of few-group cross sections for reactors of different sizes and compositions giving an adequate accuracy for the calculations. Few-group cross sections, like those of the many-group type, have to be found with due allowance for the resonance blockings and for the special characteristics of the neutron spectrum in the reactor under consideration. We may realize this approach by using the programs of [7, 8] in the following way:

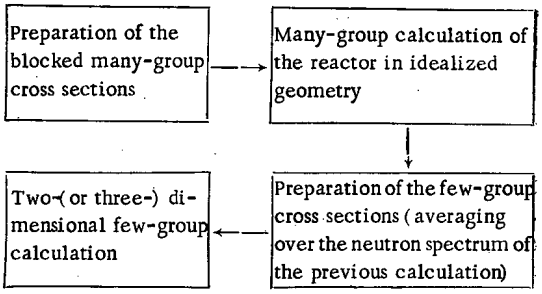


The reactor is thus calculated twice: first in the many-group approximation (in idealized geometry) and then in the few-group approximation, with detailed allowance for the geometrical singularities. This approach is extremely effective when calculating practically all the main reactor characteristics.

For the few-group programs the following macroscopic constants are averaged: the diffusion coefficient $\langle D \rangle$; the total cross section for the passage of neutrons out of the group (including absorption) $\langle \Sigma_0 \rangle$; the neutron breeding factor $\langle \nu_f \Sigma_f \rangle$; the cross section for the transition of neutrons from group to group by virtue of elastic and inelastic neutron scattering $\langle \Sigma \rangle^{i \to j}$.

The original system of many-group constants is the BNAB-70 twenty-six-group system [9].

Averaging introduces a certain error, associated with the assumption that the few-group cross sections remain constant over the averaging zones. Since the neutron spectrum in the active zone of a fast reactor varies little from point to point it may well be expected that this error will only be slight.

Another important aspect is that of obtaining the few-group cross sections for heterogeneous zones (for example, absorbing rods) forming part of the reactor. In this case the few-group cross sections may be calculated for the regions under consideration by arbitrarily placing them in the center of the one-dimensional model.

## Results of the Calculations

For purposes of calculation we chose the BN-600 reactor, the composition of which was described in [1]. In order to equalize the heat-evolution zone, the reactor is provided with a central zone of low enrichment and another zone of high enrichment. The low-enrichment zone contains nineteen compensating rods incorporating natural boron carbide, six emergency rods containing enriched boron carbide, and two automatic control rods containing natural boron carbide. The active zone is surrounded by the five rows of cassettes of the lateral screen, containing uranium oxide.

The calculations were carried out for two characteristic states of the reactor: that immediately after fuel recharging, when the packs which have achieved maximum burn-up are replaced by fresh ones and all the compensating rods have been introduced into the active zone, and that immediately before fuel recharging when all the compensating rods have been withdrawn from the active zone.

For these calculations we prepared two-, four-, six-, and nine-group cross sections, respectively having the following boundaries between the energy groups: 0.8 and 0.2 MeV; 0.2 MeV, 46.5 and 10 keV; 0.8 and 0.2 MeV 46.5, 10 and 2.15 keV; 0.8, 0.4, 0.2 and 0.1 MeV, 46.5, 21.5, 10 and 2.15 keV. In choosing the boundaries we remembered the following points. In reactors of the BN-600 type the proportion of $^{238}U$

TABLE 3. Efficiency of Boron Compensating Rods for the BFS-24-16 Assembly, % $\Delta K/k$

| Position of compensating rod | Calculation | | Experiment, [2] |
|---|---|---|---|
| | 2 group | 4 group | |
| Inner ring | 0,75 | 0,72 | 0,748±0,007 |
| Outer ring | 0,34 | 0,32 | 0,283±0,004 |

fissions is very considerable (~15% of the total number of fissions); hence one of the boundaries was taken as 0.8 MeV. The greater proportion of the neutrons in the active zone of reactors of this kind lies in the energy range 0.01-1 MeV. This region was described in as much detail as possible in the system of few-group constants. In the system of two-group constants, apart from the 0.8 MeV boundary we also made use of the 0.2 MeV boundary, corresponding to approximately equal numbers of fissions in both groups. A more detailed investigation into the choice of boundaries in the two-group constants will be presented below.

Table 1 shows the results of the calculations; these indicate that the principal physical characteristics of a fast power reactor of the BN-600 type do not depend on changes in the number of energy groups between two and nine, at any rate to an accuracy sufficient for design purposes (the changes in $K_{eff}$ are no greater than 0.5%, in the conversion ratio and the heat-evolution nonuniformity factor 2%, and in the efficiency of the compensating and emergency rod systems 5%).

Since we would not be absolutely sure that the group constants satisfied these accuracy requirements (on the basis of experience with the use of the twenty-six-group constants), we made some additional calculations using the M-220 program. We studied the accuracy of our determination of $K_{eff}$, the heat-evolution field, and the efficiency of the boron rods in the two-group calculation by comparison with the one-dimensional twenty-six-group calculation in the same $P_1$ approximation. At the same time we studied the influence of the choice of boundary for the two-group constants on the same characteristics.

The calculations leading to the results indicated in Table 2 were carried out for a one zone model (low-enrichment-zone composition) of the BN-600 reactor with a compensating rod in the center.

The comparison between the twenty-six-group and two-group calculations showed that the values of $K_{eff}$ differed by less than 1%, while the difference in the heat-evolution field (even close to the boron rod) was no greater than 5%; the same applied to the efficiency of the compensating rod. The results depended very little on the choice of boundary in the case of the two-group constants. However, a two-group-constant boundary of 0.2 MeV appeared to be the best for determining these characteristics of the BN-600 type of fast reactor (after comparing with the twenty-six-group calculation).

Thus our calculations for the BN-600 reactor have confirmed the permissibility of using few-group approximations in determining the main characteristics of fast power reactors of this type.

## Comparison with Experiment

The validity of the use of the few-group $P_1$ approximation for hexagonal geometry was also verified when calculating the critical assemblies of the BFS-2 test-bed simulating the BN-600 reactor. Calculations carried out on the M-220 computer using a two-group program agreed closely with the calculated and experimental efficiencies of the boron rods and heat-evolution fields indicated in [2].

In addition to this, we also carried out some calculations for one of the critical assemblies simulating the BN-600 reactor (assembly BFS-24-16) by means of the two- and four-group programs designed for the BÉSM-6 computer (Table 3). We see from Table 3 that the calculated efficiencies of the boron rods inside the low-enrichment zone agree satisfactorily with experimental data (the difference is 5%). The calculated efficiencies of the boron rods close to the boundary between the zones of low and high enrichment are 15-20% higher than the experimental values; this is evidently due to errors in calculating the neutron fluxes by the diffusion approximation close to the boundaries of zones with different diffusion properties, and also possible inaccuracies in the many- and few-group constants. It should be noted that the results of the calculations agree satisfactorily with the results of many-group diffusion calculations.

Thus few-group diffusion methods in two-dimensional hexagonal geometry yield satisfactorily accurate results in calculating the main physical characteristics of fast power reactors. The efficiency of such methods is achieved by combining them with the many-group, one-dimensional calculations used for averaging the few-group cross sections. A comparative analysis of the methods employed (in which the numbers of energy groups varied from two to nine) has shown that even the two-group approximation is adequate for calculating the physical characteristics of a fast reactor.

## LITERATURE CITED


1. A. I. Leipunski et al., The BN-600 Fast Reactor, Nuclex-69, Basel, Switzerland (1969).
2. V. V. Orlov et al., Symposium on the Physics of Fast Reactors, October 16-19, 1973, Tokyo, Paper A-25.
3. V. V. Bondarenko et al., Proc. IAEA Symp. on Fast Reactor Physics, October 30-November 3, 1967, Karlsruhe, Vol. 2, p. 305.
4. W. Wasow and J. Forsyte, Difference Methods of Solving Differential Equations in Partial Derivatives [Russian translation], IL, Moscow (1963).
5. R. Richtmeyer, Difference Methods of Solving Boundary Problems [Russian translation], IL, Moscow (1960).
6. A. Hassit, in: Computing Methods in Reactor Physics [Russian translation], Atomizdat, Moscow (1972), p. 50.
7. Sh. S. Nikolaishvili et al., in: Transactions of the Tripartite Soviet–Belgian–Dutch Symposium on Certain Problems of Fast-Reactor Physics [in Russian], Vol. 1, Izd. TsNIIAtominform, Moscow (1970).
8. V. V. Khromov et al., in: Physics of Nuclear Reactors [in Russian], Vol. 1, Atomizdat, Moscow (1968), p. 159.
9. L. P. Abagyan et al., Group Constants for Calculating Nuclear Reactors [in Russian], Atomizdat, Moscow (1964).

# REMOVAL OF TRITIUM FROM THE GASEOUS WASTES FROM NUCLEAR POWER STATIONS

L. F. Belovodskii, V. K. Gaevoi, V. I. Grishmanovskii, V. V. Andramanov, V. N. Demenyuk, and V. V. Migunov

UDC 66.074.7:546.11.02.3

The expanding network of nuclear power stations and fuel element reprocessing plants is causing an increase in the global environmental distribution of the radioactive isotopes of Ar, Kr, Xe, and I, as well as $^{14}C$ and T due to emission of these gases into the atmosphere. This results in additional irradiation of the population [1, 2]. The main contribution to this global irradiation of the population is from $^{85}Kr$ and T [2; 3]. It has been conjectured that by the year 2000 there will have been up to $5 \cdot 10^8$ curies of tritium released to the environment [2]. Electric power production by thermonuclear reactors may also lead to a significant buildup of tritium in the biosphere, since it is assumed that a thermonuclear reactor will release $10^4$–$10^5$ times more tritium than a nuclear power station of equivalent power [4-5].

At present, methods and equipment for collecting Kr, Xe, and I have been developed [6-8]. Reducing the emission of tritium, whose potential danger is associated with its possible absorption into genetic material, is a serious problem which is practically unsolved at this time [9-11].

T is formed in nuclear reactors directly in the fuel elements, and in the coolant ($H_2O$, $D_2O$), moderator (graphite, $D_2O$), and boron control rods. The average emission of tritium depends on the type of nuclear power plant and ranges from 2 curies/year to 10 curies/day, with a maximum of more than 100 curies/day [5, 11]. The principal source of atmospheric T is fuel reprocessing plants which release 50-432 curies/day [5, 12]. During accidents up to $2.9 \cdot 10^5$ curies/hour may be released [13]. Up to 25% gaseous tritium and 75% HTO reaches the atmosphere [9]. The tritium at effluent stacks comes with waste gases (air, inert gases) from the active zone or the primary loop of reactors, or from the processing rooms (canyons) of fuel reprocessing plants. The concentration of T in the gases entering the ventilation stacks varies from $10^{-5}$ to 20 curies/liter [11, 13].

Thus, the problem of cutting down emissions reduces to removal of T and HTO from the gases which enter the ventilation system from relatively small localized volumes, i.e., to removal of hydrogen and water vapor from air and inert gases. Highly effective adsorption gas drying methods are extensively used in industry; hence, removal of HTO is comparatively easy by means of adsorption columns [14, 15]. It is more difficult to trap tritium since it constitutes $4 \cdot 10^{-7}$ to $8 \cdot 10^{-1}$% by volume of the effluent gases. In practice, it is necessary to obtain gases of high purity (with respect to T) from the cleaned gases [16]. Of the known means of removing hydrogen from gaseous mixtures (sorption by certain metals and activated carbon, deep freezing, chemical transformation, selective diffusion through palladium), the most widely used in laboratory and industrial practice is chemical transformation. In this scheme oxidation of hydrogen on solid heterogeneous catalysts is most often used in continuously operating systems [14, 16]. Catalytic oxidation permits reduction of the amount of hydrogen in inert gases from 1 or 2 to $10^{-4}$% with strict conservation of the stoichiometric ratio of $H_2$ and $O_2$ [17]. The efficiency of catalytic removal of hydrogen impurities ($10^{-7}$–$10^{-2}$%) from inert gases and multicomponent mixtures (air) is not sufficiently known and does not yield to theoretical estimates. This is because the kinetics of the reaction $H_2 + O_2$ are complicated due to the dependence of the properties of the catalyst on the composition of the gas mixture and cannot be expressed in terms of a single equation over a wide range of concentrations of the components. Thus, industrial installations are based on experimental devices with analogous catalysts and gaseous mixtures [14, 18].

Translated from Atomnaya Énergiya, Vol. 38, No. 4, pp. 217-221, April, 1975. Original article submitted August 9, 1974.

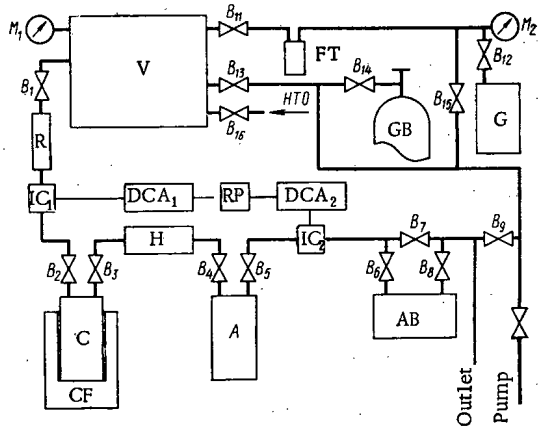


Fig. 1

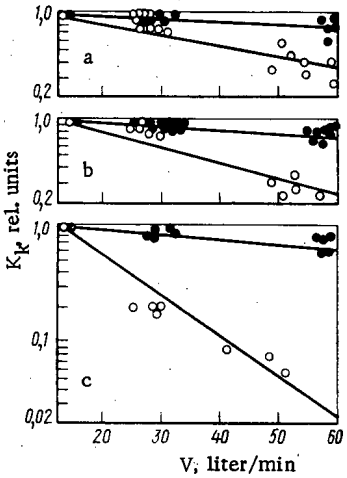


Fig. 2

Fig. 1. Diagram of the apparatus for testing the efficiency of removal of $^3H$ from gases: C) converter; A) adsorber; CF) electric crucible furnace, type TG-1m; H) heat exchanger; AB) air blower, type VL-1; R) rotameter, type RS-5; $IC_1$, $IC_2$) ionization chambers; $DCA_1$, $DCA_2$) direct current amplifiers, type SP-1m; RP) recording potentiometer, type PS-1-10; V) vacuum-tight volume; G) tritium container; FT) freezing trap; GT) gas bottle; $M_1$, $M_2$) vacuum manometers; $B_1$–$B_{16}$) valves.

Fig. 2. Dependence of the conversion coefficient of the catalyst for tritium on the flow rate for various catalyst volumes and gas compositions: (a) 2.2 liters; (b) 1.4 liters; (c) 0.7 liters; ○) air; ●) argon.

In order to obtain initial data for calculations on industrial apparatus, in the present paper we describe a study of the efficiency of catalytic removal of slight additions of tritium ($10^{-7}$–$10^{-20}$%) from gases (air, argon, and their combination) followed by adsorption of the resulting tritium oxide.

This method also permits collection of HTO present in the gases being cleaned.

This cleanup system consists of two main parts: catalytic (converter) and adsorption (adsorber). The decontamination coefficient (K) is defined by the efficiency of these parts. In general, K over the time period $(t_2-t_1)$ is given by the ratio

$$K=\frac{\int_{t_1}^{t_2} C_{\text{H}} v_{\text{H}}\, dt}{\int_{t_1}^{t_2} C_{\text{K}} v_{\text{K}}\, dt}=\frac{A_{\text{H}}}{A_{\text{K}}}, \qquad (1)$$

where $C_H$, $C_K$, and $A_H$, $A_K$ are the concentration and activity of tritium at the input and output of the system, respectively; $v_H$ and $v_K$ are the gas flow rates (in systems without suction and dilution, $v_H = v_K = v$). At nuclear power stations and fuel reprocessing plants $A_H$ is composed of the activity of T ($A_{G.H}$) and of HTO ($A_{O.H}$) at the inlet, i.e., $A_H = A_{G.H} + A_{O.H}$. Analogously, at the outlet, $A_K = A_{G.K.} + A_{O.K}$. The degree of decontamination is determined by the conversion coefficient of tritium into the oxide ($K_K$) and by the coefficient of adsorption of HTO ($K_a$), i.e., $K = f(K_K, K_a)$. Expressing $A_K$ in terms of $A_{G.H}$, $A_{O.H}$, $K_K$, and $K_a$, we obtain

$$A_{G\,\text{к}}=A_{G.\,\text{H}}/K_{\text{к}};\ A_{\text{o.к}}=\frac{A_{G.\text{H}}-A_{G.\text{H}}/K_{\text{к}}}{K_{\text{a}}}+\frac{A_{\text{o.н}}}{A_{G.\,\text{H}}}. \qquad (2)$$

Substituting the expressions for $A_H$ and $A_K$ in Eq. (1) and writing $A_{O.H}/A_{G.H} \doteq \xi$, we find

$$K=\frac{K_{\text{к}}K_{\text{a}}(1+\xi)}{K_{\text{a}}+K_{\text{к}}(1+\xi)-1}.$$

The number 1 in the denominator may be neglected if $K_a$ and $K_k \gg 1$. From Eq. (2) it is clear that for constants $K_K$ and $K_a$, K increases with $\xi$, i.e., as $A_{O.H}$ increases. For $A_{O.H} = 0$ ($\xi = 0$),

$$K=K_{\text{a}}K_{\text{к}}/(K_{\text{к}}+K_{\text{a}}). \qquad (3)$$

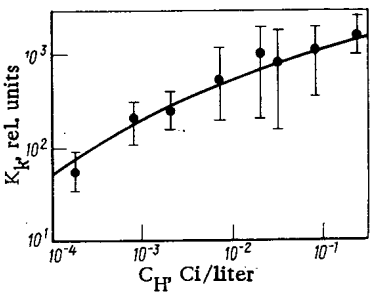


Fig. 3

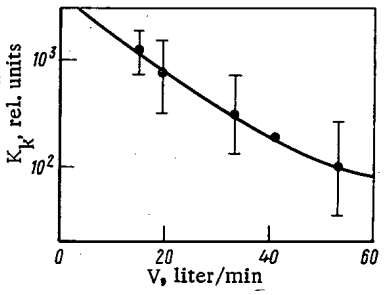


Fig. 4

Fig. 3. Tritium conversion coefficient of the catalyst as a function of the tritium concentration in the mixture being decontaminated.

Fig. 4. Dependence of the tritium conversion coefficient of the catalyst on the flow velocity in the second series of experiments.

$K_a$ depends on the type of adsorbent, the humidity of the gas being cleaned, and other factors. If synthetic zeolites are used as an adsorbent (drying to the dew point, 85°C), then, for a moisture content in the gas of about 0.1 g/m$^3$, $K_a > 10^2$ may be obtained [19]. $K_K$ depends on the type of catalyst, the volume rate of gas flow, the presence of contaminants that poison the catalyst, the composition of the gas being cleaned, etc. For these reasons, it is impossible to estimate the order of magnitude of $K_K$ for the conditions under consideration. Thus it is determined experimentally.

Metals of group VIII serve as catalysts for the $H_2 + O_2$ reaction, with Pt and Pd being the most active. In order to increase the working surface and the stability, adsorption catalysts were used in this work. These consist of a thin layer of metal (0.1-3.0 wt.%) on a substrate (silicagel, alumogel, etc.). A preliminary estimate of the necessary amount of adsorption catalyst may be made using the relation given in [18]; the volume of catalyst, $V_K$, increases with the amount of separated component and the decontamination coefficient. Thus, $V_K$ was estimated for a maximum concentration of tritium of 20 curies/liter (emergency case). The required decontamination coefficient was taken to be 1000, based on a comparison of the emergency ($2.9 \cdot 10^5$ curies/hour) and maximum allowed ($8 \cdot 10^2$ curies/hour from a stack of height 80 m [20]) emission including a factor of three reserve [11]. For these parameters, the estimated amount of catalyst is 0.7 liters for v = 100 liters/min and a catalyst working temperature of 200°C.

This cleanup system was experimentally tested during an apparatus (Fig. 1) consisting of a converter and an adsorber. The converter is heated in a temperature regulated crucible furnace. A heat exchanger is used to cool the gaseous mixture which passes from the converter to the adsorber. The gas mixture is pumped through by an air blower, whose flow rate is controlled by a rotameter. The concentration of tritium is measured using flow-through ionization chambers of volume 0.5 and 5.0 liters with two dc amplifiers. The readouts are recorded on a recording potentiometer. The gas mixture which is to be decontaminated is prepared in a vacuumtight volume of 1.3 m$^3$. The required amount of T is fed into this volume by passing tritium through a liquid air trap to remove HTO. The gas (argon, dry air) is fed into the volume from a bottle. The vacuum manometers control the pressure in the container. The elements of the system are interconnected by 20 mm diameter stainless steel tubing through type Du-15 valves.

The converter and adsorber were made of Kh18N10T steel in the shape of a cylinder 117 mm in diameter and 280 mm high (volume 2.2 liters). The inlet and outlet of these components are separated by a coaxial inner cylinder, whose cross sectional area (38 cm$^2$) is equal to the area of the annulus between the outer and inner cylinders. The converter was filled with a platinum catalyst in silicagel (KSK brand) to 1.3 wt.% Pt. The catalyst was prepared by impregnating silicagel (grain size 4 mm) with a solution of platinum in hydrochloric acid and then recovering the platinum in a flow of hydrogen [21]. The adsorber was filled with the zeolite NaA (MRTU 6-01-906-60). The zeolite could be reactivated by heating in a vacuum of about $10^{-3}$ torr at 500°C for 4 hours.

In the experiments we studied the activity of the catalyst as a function of the flow rate and the concentration of T for various volumes of catalyst (from 0.7, the calculated volume, to 2.2 liters). The efficiency of the adsorber was also determined. Two series of experiments were conducted. In the first, the

concentration of T in the mixture to be cleaned was varied from $10^{-5}$ to $10^{-3}$ curies/liter while the concentration of HTO did not exceed 0.1%. The moisture content was up to 0.05 and 0.3 g/mm$^3$ in argon and air with oxygen contents of 0.03 and 20% respectively.

In the second series of experiments, the T concentration was $10^{-4}$ to $2.6 \cdot 10^{-1}$ curies/liter with an HTO content of 1 to 90%. In this case actual conditions were being simulated, i.e., the presence of HTO in the effluent gases. HTO was fed into the volume by evaporation of tritiated water of known specific activity. The moisture content was 0.1-0.4%, and the oxygen content 0.2-2% in argon and 20% in air. The humidity of the gases was measured by the dew point and the oxygen in argon was measured using an Orsat apparatus. The gas flow rate was varied from 10 to 60 liters/min.

K was calculated using Eq. (1) by means of graphical integration of $C_H$ and $C_K$ over time. In the first series of experiments, $K_K$ was found using Eq. (3), since $\xi = 0$; in the second, by using Eq. (2) including the HTO.

The amount of HTO was periodically monitored by sampling the gas at three points: the volume V, and before and after A (Fig. 1). The gas was sampled with evacuated glass samplers (volume 0.1-0.2 liters). The HTO in them was isolated by distilled water placed in the sampler. The activity of the HTO was determined by a liquid scintillation counter (type URB-1).

The efficiency of the adsorber was estimated by the coefficient $K_a$ which was determined from the ratio of the concentrations of HTO at the inlet and outlet of A (Fig. 1). $K_a$ was found to be $10^2$-$2 \cdot 10^3$, where $K_a$ increases as the humidity and T concentration in the mixture increase.

Curves showing the dependence of $K_K$ on the flow rate v for various catalyst volumes, based on the data from the first series of experiments, are shown in Fig. 2. The value of $K_K$ at $v \approx 15$ liters/min is taken as unity, since in this case $K_K$ is independent of $V_K$ and the gas composition (air, argon). The absolute value of $K_K$ was $100 \pm 50$, which corresponds to at least 98% conversion of tritium into oxide.

Evidently (Fig. 2), K decreases as v increases, with a much smaller drop in argon than in air. As $V_K$ is increased, the dependence of $K_K$ on v is less noticeable. Thus, for $V_K = 0.7$ liters $K_K$ decreases by a factor of 30 in air when v is increased from 15 to 60 liters/min, while for $V_K = 2.2$ liters, $K_K$ falls by only a factor of 3. In argon, the decrease in $K_K$ as v increases for various values of $V_K$ is insignificant (20-30%). These data indicate a complicated dependence of $K_K$ on v, $V_K$, and the composition of the gas. $K_K$ also depends on the T concentration. This dependence was investigated in the second series of experiments, where $V_K = 2.2$ liters. The curve $K_K = f(C_H)$ is shown in Fig. 3, where the mean values of $K_K$ from 3-7 measurements at a given concentration of T (in the gaseous phase) are given as well as the maximum deviation from the mean value.

$K_K$ as a function of $C_H$ was obtained at v = 15-20 liters/min. When v is increased to 60 liters/min, the nature of this dependence is conserved, with a decrease in the absolute values. This is clear from Fig. 4, where the function $K_K = f(v)$ is shown for the second series of experiments for similar values of $C_H$. As opposed to the first series (Fig. 2), the function $K_K = f(v)$ was general for argon, air, and their mixtures, since no significant difference in the conversion coefficient for air and argon was recorded. It is possible that this was due to an increased oxygen content in the argon compared to the first series.

During the tests 98.6 m$^3$ of gaseous mixture with a total tritium content of ~1540 curies were sent through the system; 6.5 curies were measured at the output, i.e., the integrated decontamination coefficient was 240. The maximum and minimum values of K were $2.3 \cdot 10^3$ and 20 for v = 19 and 60 liters/min and $C_H = 2.6 \cdot 10^{-1}$ and $3 \cdot 10^{-3}$ curies/liter, respectively; i.e., 95.0-99.9% of the tritium was collected.

After the tests the zeolite from A (Fig. 1) underwent desorption in vacuum with freezing out of the water released: 200 cm$^3$ of water were released with a tritium concentration of $7.5 \cdot 10^3$ curies/liter, corresponding to 1500 curies of tritium.

A good agreement in the amount of T measured by two different methods (ionization in the gaseous phase and scintillation in water) indicates that these results are fairly reliable. Some divergence (5-7 times) is observed between the amount of moisture desorbed from the zeolite and that entering A during operation. This is explained by periodic decontamination of the apparatus (Fig. 1) by blowing atmospheric air, which has a much higher moisture content than the gaseous mixtures used in the experiments, through it.

Thus, it is possible in principle to effectively remove tritium from the gaseous wastes in nuclear power generation by catalytic oxidation and later desorption of the resulting HTO. Based on our data it is

possible to estimate the amount of catalyst needed for real gas flow rates, tritium concentrations, and decontamination coefficients.

The tritium which is collected may be buried along with the zeolite in a sealed container, for example, in the adsorber [22]. It is also possible to remove the HTO from the zeolites and to use it in scientific research or to decompose the HTO to obtain gaseous tritium [23].

## LITERATURE CITED


1. Yu. A. Izrael, Atomnaya Énergiya, 32, No. 4, 273 (1972)
2. A. M. Kuzin, Atomnaya Énergiya, 33, No. 4, 870 (1972).
3. L. I. Gedeonov and A. G. Trusov, Atomnaya Tekhnika za Rubezhom, No. 12, 22 (1973).
4. F. Parker, Science, 159, No. 3810, 83 (1968).
5. H. Peterson, et al., in: Environmental Contamination by Radioactive Materials, IAEA, Vienna, (1969), p. 35.
6. A. S. Oveshkov, Atomnaya Tekhnika za Rubezhom, No. 7, 3 (1972).
7. E. K. Yakshin, et al., Atomnaya Énergiya, 34, No. 4, 285 (1973).
8. I. E. Nakhutin, et al., Atomnaya Énergiya, 35, No. 4, 245 (1973).
9. V. S. Yuzgin and B. E. Yavelov, Atomnaya Tekhnika za Rubezhom, No. 10, 24 (1973).
10. N. V. Krylova and A. N. Kondrat'ev, Atomnaya Énergiya, 34, No. 4, 316 (1973).
11. A. D. Turkin, Dosimetry of Radioactive Gases [in Russian], Atomizdat, Moscow (1973).
12. N. Sax, J. Daly, and J. Gabay, Nucl. Appl. Technol., 7, No. 1, 106 (1969).
13. I. Nikolich, Express-Information [in Russian], No. 38 (817), Izd. TsNII-atominform (1972), p. 14.
14. A. L. Koul' and F. S. Rizenfel'd, Cleaning of Gases [in Russian] Gosoptekhizdat, Moscow (1962).
15. Cleaning of Ventilated Effluents in Foreign Industrial Plants [in Russian], No. 18 (318), Izd. TsNII-élektronika, Moscow (1971).
16. G. Muller and G. Gnauk, High Purity Gases [Russian translation], Mir, Moscow (1968).
17. V. G. Fastovskii, A. E. Rovinskii, and Yu. V. Petrovskii, Inert Gases [in Russian], Atomizdat, Moscow (1972).
18. G. K. Boreskov and M. G. Slin'ko, Khim. Prom-st', No. 2, 69 (1956).
19. Z. A. Zhukova, et al., ibid., No. 2, 24 (1962).
20. Maximum Allowable Release of Gas from Reactor Stacks [in Russian], Atomnaya Tekhnika za Rubezhom, No. 4, 32 (1966).
21. V. S. Chesalova and G. K. Boreskov, Dokl. AN SSSR, 85, No. 2, 377 (1952).
22. E. Evans, Tritium and Its Compounds [Russian translation], Atomizdat, Moscow (1970).
23. D. Jacobs, TID-24635, USAEC (1968).

# PURIFICATION OF LIQUID RADIOACTIVE EFFLUENTS BY CONTINUOUS ION EXCHANGE

B. E. Ryabchikov, D. I. Trofimov,*
E. I. Zakharov, A. S. Dudin,
and L. K. Mikheev

UDC 621.039.73

Experience of the use of pulsation sorption columns (PSC) to purify liquid radioactive effluents with a low level of activity has revealed [1] that this type of apparatus has a number of advantages over the traditional type of sorption filters (higher relative productivity, small amount of sorbent loaded at a time, low pressure loss, etc.). However, the volume of a PSC operating with free sorbent settlement is larger than that of filters. The volume can be reduced by using fluidization conditions and slightly increasing the load of resin. As a result of later investigations, it became possible to use the principles described in [2, 3] to design an improved column specially for processing low-concentration solutions – a column with transport pulsation (PSC-T) [4].

*Deceased.

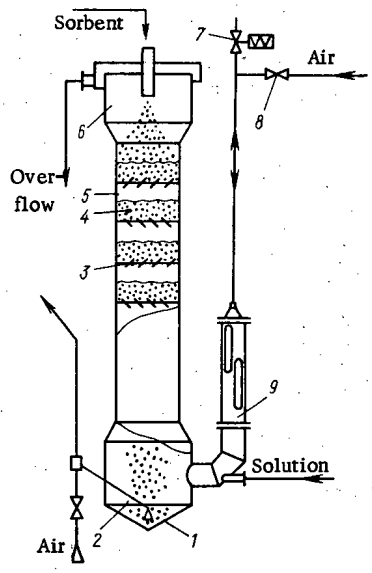


Fig. 1

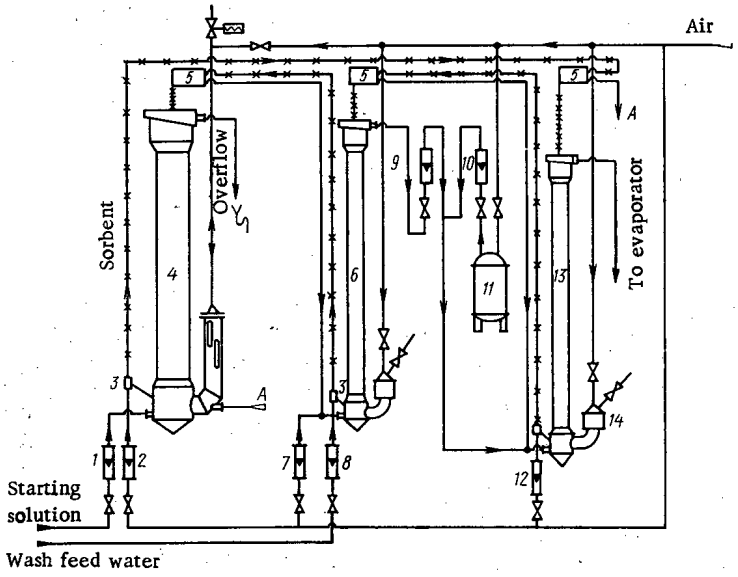


Fig. 2

Fig. 1. Diagram of sorption column. 1) Bottom settlement zone; 2) air-lift; 3) distribution plate; 4) sorbent bed; 5) casing; 6) top settlement zone; 7) electromagnetic valve; 8) air supply valve; 9) pulsation chamber.

Fig. 2. Diagram of experimental apparatus. 1) Rotameter for input solution; 2), 8), 12) air rotameters; 3) air-lift; 4) sorption column; 5) separators; 6) washing column; 7) rotameter for washing feed water; 9) rotameter for wash water; 10) acid rotameter; 11) reservoir with concentrated nitric acid; 13) regeneration column; 14) pulsator.

Translated from Atomnaya Énergiya, Vol. 38, No. 4, pp. 222-225, April, 1975. Original article submitted April 9, 1974.

TABLE 1. Average Indices of Purification Process

| Item | pH | Concentration, mg-eq/liter | | β-Activity, Ci/liter | | | | | | | |
|---|---|---|---|---|---|---|---|---|---|---|---|
| | | Na | Ca + Mg | total β-activity | $^{90}Sr$ | $^{131}I$ | $^{137}Cs$ | $^{60}Co$ | $^{144}Ce$ | $^{106}Ru$ | $^{95}Zr + ^{95}Nb$ |
| Original solution | 8,3 | 3,2 | 2,5 | $2,2 \cdot 10^{-7}$ | $4,8 \cdot 10^{-9}$ | $1,7 \cdot 10^{-8}$ | $1,7 \cdot 10^{-8}$ | $2,0 \cdot 10^{-8}$ | $2,0 \cdot 10^{-8}$ | $5,6 \cdot 10^{-8}$ | $8,2 \cdot 10^{-9}$ |
| Waste solution | 2,5 | $\leqslant 0,1$ | $< 0,01$ | $1,9 \cdot 10^{-8}$ | $3,1 \cdot 10^{-11}$ | $4,5 \cdot 10^{-9}$ | $3,1 \cdot 10^{-9}$ | $3,4 \cdot 10^{-9}$ | $\leqslant 4,2 \cdot 10^{-11}$ | $\leqslant 2,4 \cdot 10^{-11}$ | $\leqslant 9,2 \cdot 10^{-12}$ |
| MPC | — | — | — | — | $4,0 \cdot 10^{-10}$ | $2,0 \cdot 10^{-9}$ | $1,5 \cdot 10^{-8}$ | $3,5 \cdot 10^{-8}$ | $1,2 \cdot 10^{-8}$ | $1,2 \cdot 10^{-8}$ | $6,2 \cdot 10^{-8}$ |
| Purification factor | — | $\geqslant 32$ | $> 250$ | 12 | 153 | 3,8 | 15,9 | 6,0 | $> 475$ | $> 2230$ | $> 8900$ |

The column casing (Fig. 1), in which there are grid plates with small clear cross section, has a pulse chamber, and is fitted with top and bottom settling zones. When the column is operating, solution is fed in continuously from below, and sorbent is fed from above and falls to the top plate. Since the clear cross section of the latter is small ($F_{cl}$ = 5-15%), the velocity of the solution in the holes in the plate is much higher than the drift velocity of the resin particles, and as a result they cannot get through the holes and accumulate above the plate. During the operational period (sorption), air is fed slowly through a valve into the pulse chamber. The sorbent moves downward when air is suddenly released through an electromagnetic valve. Then the solution moves upward in the pulse chamber, and correspondingly downward in the column, carrying resin from one plate to the next. By varying the frequency and amplitude of these transport pulses, we can regulate the flow of resin and its residence time in the apparatus, i.e., we can set up optimal conditions for purification of the solution and saturation of the resin.

Hydraulic and technological tests of these columns in a number of systems have enabled us to devise a method of design calculation, and have shown that they are highly efficient in the treatment of effluent water. It was found that if other conditions are equal, PSC-T columns give a sorbent residence time 10-20 times longer than that of PSC columns, and consequently that they can be shorter and smaller in approximately the same ratio.

Since PSC columns [4-7] give their greatest efficiency when working with concentrated solutions [5], it is advisable to compose a continuous-action plant for processing liquid effluent from PSC-T columns acting by sorption and PSC columns acting by regeneration and washing of resin. Using this scheme, at the Moscow Purification Station (MPS) we built a plant with a throughput of 1 $m^3/h$ for purifying wastes with a KU-2-8 cation exchanger. Sorption was effected in a PSC-T column 200 mm in diameter and 10 m long, and regeneration and washing in PSC columns 76 mm in diameter and 9 m long. The columns occupy an area of 0.5 $m^2$, and the whole plant with its storage tanks occupies 5 $m^2$. The load of resin is 30 kg.

The apparatus (Fig. 2) operates as follows. The solution to be purified is fed to the bottom of the sorption column through a rotameter. In the column it comes into contact with a counterflow containing separate layers of cation exchanger. The purified solution overflows from the column into the special drains. Regenerated and washed resin is continuously fed from a separator to the upper zone of the sorption column. As it moves downward it becomes saturated and is pumped from the bottom zone of this column by an air-lift to the regenerator. The action of the air-lift is monitored by an air rotameter. Since the air-lift pumps solution over together with the resin, over each column there is a separator consisting of a stationary cylindrical grid containing a revolving worm screw. The filtered solution is returned to the column from which it was pumped, while the worm screw feeds the resin to the top zone of the next column. In the regeneration column the sorbent is regenerated by nitric acid, and in the washing column it is washed free of traces of acid by mains water which is fed to the bottom of this column via a rotameter. Emerging from the wash column, the wash solution contains up to 0.8 M $HNO_3$. It flows by gravity through the rotameter to a line connected to the regeneration column. Concentrated 12 M $HNO_3$ is fed via a rotameter to the same line. The concentration of the resulting regeneration solution is calculated from the ratio of the wash solution and acid flows and is checked by analyzing samples. The regenerate is passed to the concentration unit.

Pulsation of the solution in columns 6 and 11 at 50-100 vibrations per minute with an amplitude of 5-10 mm is effected by special autopulsators.

TABLE 2. Composition of Regenerated Nitric Acid

| Index | Concentration | | | | β-Activity, Ci /liter | Concentration ratio | | | Regenerate flow, liters /h |
|---|---|---|---|---|---|---|---|---|---|
| | regenerating $HNO_3$ soln., M | regenerating $HNO_3$ solution, M | Na, mg-eq /liter | Ca + Mg, mg-eq /liter | | Na | Ca + Mg | Σβ | |
| Range | 1,8—2,2 | 0,35—0,64 | 160—520 | 180—480 | $9,5 \cdot 10^{-6}$—$2,0 \cdot 10^{-5}$ | 50—165 | 70—180 | 50—100 | 9—12 |
| Mean | 2,0 | 0,51 | 335 | 330 | $1,7 \cdot 10^{-5}$ | 105 | 130 | 85 | 10 |
| Range | 4—5 | 0,54—0,92 | 400—860 | 430—680 | $(2,25—3,75) \cdot 10^{-5}$ | 125—270 | 175—265 | 110—180 | 4—6 |
| Mean | 4,5 | 0,72 | 540 | 535 | $3,0 \cdot 10^{-5}$ | 170 | 215 | 150 | 5 |

The apparatus successfully passed hydraulic operational tests with a throughput of 1.0-1.2 $m^3/h$ (relative productivity 30-40 $m^3/m^2 \cdot h$) with a resin flow of 3-20 liters/h (the ratio of the resin to the solution flow was 1 : 50 to 1 : 300) with wash water and regenerate flows of 5-20 liters/h. The residence time of the resin in the sorption operation is 1-10 h, and that in washing and regeneration is 20-30 min.

Laboratory investigations of the purification of liquid radioactive effluent by the KU-2-8 cation exchanger in the $H^+$ form revealed that equilibrium of the resin—solution system is established in 30-60 min, and the maximum purification factor with respect to the total beta activity for a given radioisotope composition (Table 1) is 10-15.

In our technological experiments we purified liquid radioactive effluents (total beta activity $5 \cdot 10^7$ Ci/liter) processed by the MPS, after blending, coagulation, and conventional filtration. During our experiments we processed over 100 $m^3$ of solution. The throughput of solution was 0.9-1.0 $m^3/h$, and the current of resin through the system was 3-10 liters/h. The current of 2 M $HNO_3$ to the regenerator was 10-12 liters/h, or 4-5 liters/h in the experiments with 4-5 M $HNO_3$. A residence time of 3 h of the resin in the sorption process was effected by transport pulsations at 0.5 vibrations/min with an amplitude of 50 mm.

Table 1 lists the average compositions of the original solution and the waste filtrate, the purification factors, and the mean permitted concentrations (MPC). The data on the microcomponents were obtained by analyzing samples. From Table 1 we see that the solution is freed from radioisotopes in cation form (Cs, Sr, Ru, Zr, Nb) down to the MPC. The purification factor for total beta activity was 10-15. The residual activity is evidently due to the presence of radioisotopes present as anions, complexes, or compounds (I, Co). Further purification of this solution on an anion exchanger in the laboratory reduced its activity by another order of magnitude. These data agree with those obtained from ion-exchange filters.

It was also found that fluctuations of the Na content of the waste solution between 0.02 and 0.5 mg-eq /liter (purification factor 10-100) had practically no effect on the purification factor for the total beta activity, because heavier elements, which are mainly responsible for the total activity, are nearly completely removed. The content of macrocomponents in the waste solution is close to that in filtrates after passing through the cation exchange filters of desalination plants.

Since the treatment of liquid radioactive effluents includes not only purification but also concentration of the activity into the minimum possible volume, it is interesting to consider the results of regeneration of the resin (Table 2).

The results show that when 2M $HNO_3$ is used for regeneration (the same as in the basic MPS scheme), the content of Na salts and hardness salts (Ca + Mg) in the regenerate averages 330 mg-eq/liter, which is 1.5 times greater than the mean results for the basic MPS scheme during the period of the tests [8]. The use of a smaller amount of more concentrated acid (4-5 M $HNO_3$) gave regenerates with concentrations of these ions ranging from 400 to 850 mg-eq/liter (average 530 mg-eq/liter), i.e., 2.5 times greater than that obtained at present at the MPS. Consequently, continuous ion exchange can increase the concentration of the regenerates and reduce their volume. If these regenerates are additionally treated or buried, there will be economic savings on the process as a whole.

TABLE 3. Analysis of KU-2 Resin*

| Item | Saturation of resin, mg-eq/g | | | β-Activity, Ci/liter |
|---|---|---|---|---|
| | Na | Ca + Mg | total | |
| Saturated resin | 2,0 | 2,9 | 4,9 | $9{,}2 \cdot 10^{-8}$ |
| Regenerated resin | 0,18 | 1,37 | 1,45 | $1{,}0 \cdot 10^{-8}$ |
| Coefficient of regeneration | 11 | 2,1 | 3,5 | 9,2 |

* The resin was analysed by regenerating it with excess of 4 M $HNO_3$ and detemining the components in the regenerate.

These concentrated regenerates are obtained as a result of increasing the ratio of the currents, the concentration of the regenerated solution, and the saturation of the resin. If the resin is in contact with the solution for 3 h during sorption, the saturation of the resin averages 4.9 mg-eq/g (Table 3), which is practically equal to its total exchange capacity (rated value 4.8 mg-eq/g).

The degree of regeneration of the resin with respect to the macrocomponents was 70%; the Na ions were practically completely removed, but the heavier Ca and Mg ions partly remained on the resin. For more complete regeneration we can alter the conditions of operation of the column, creating a fluidized bed, or increasing the flow of regenerating solution. However, additional experiments with completely regenerated resin revealed that this residual content of cations has practically no influence on the purification factor. Therefore it is expedient to work in the cheaper conditions with a residual saturation of 1.0-1.5 mg-eq/g.

## LITERATURE CITED


1. F. V. Rauzen et al., At. Énerg., 36, No. 1, 27 (1974).
2. F. Cloete and M. Streat, Nature, 200, No. 4912, 1199 (1963).
3. F. Cloete and M. Streat, British Patent No. 1,070,251 (1963).
4. B. E. Ryabchikov and E. I. Zakharov, Equipment for Ion Exchange [in Russian], Izd. NII Tsvetmetinformatsiya, Moscow (1974).
5. S. M. Karpacheva, E. I. Zakharov, and V. N. Koshkin, in: Development and Use of Pulsation Apparatus [in Russian], Atomizdat, Moscow (1974), p. 184.
6. E. I. Zakharov et al., ibid., p. 170.
7. S. M. Karpacheva et al., Chemical and Petroleum Refining Engineering: Pulsation Apparatus [in Russian], Izd. Tsintikhimneftemash, Moscow (1971).
8. D. Trofimov et al., in: Proc. Symp. IAEA "Practices in the Treatment of Low and Intermediate Level Radioactive Wastes," Vienna, 6-10 Dec. 1965, SM-71/59.

# CALCULATION OF DOSE COMPOSITION OUTSIDE SHIELDING OF HIGH-ENERGY ACCELERATORS BY THE MONTE-CARLO METHOD

N. V. Mokhov and V. V. Frolov

UDC 621.039.78

The hadron contribution to the dose outside homogeneous shielding of an accelerator has been investigated [1]. The calculation was performed for a one-dimensional geometry using the HAMLET program [2, 3]. This paper describes the MARS program which was written for the Monte-Carlo calculation of the nuclear cascade in a heterogeneous accelerator shield. A method is presented for estimating particle fluxes in an arbitrary geometry and results are presented for maximum dose and dose composition outside the shielding of accelerators of energies $E_0 = 1$-$1000$ GeV. The contribution of kaons, muons, and $\gamma$ rays to the dose is taken into account. A knowledge of the radiation dose composition makes it possible to determine the magnitude of the total dose outside shielding from the magnitude of a partial dose obtained either by calculation or from experiment.

The MARS program uses the Monte-Carlo method to determine the energies and scattering angles for particles at selected points in a three-dimensional block of material irradiated by a beam of protons, neutrons, or pions having an arbitrary angular and spectral distribution. The shielding block may be heterogeneous and may have arbitrary cavities. The fluxes of protons, neutrons, and charged pions with $E \geq 15$ MeV, and their energy spectra, are computed for four hundred given elementary regions in the block. The primary hadron energies are 0.05-1500 GeV. The maximum transverse and longitudinal dimensions of the shield block are 2500 g/cm$^2$. The program employs both standard methods for the reduction of variance and also modifications developed for this energy range which, together with the use of a system of semi-empirical formulas for the description of inclusive distributions, make it possible to go beyond the parameters of existing programs [4, 5].

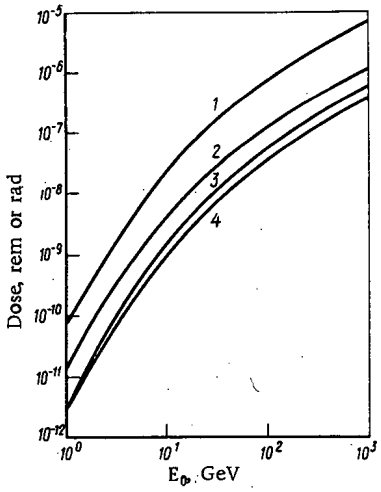


Fig. 1. Dependence on primary proton energy of maximum dose equivalent (1, 3) and absorbed dose (2, 4) outside a shield; 1, 2) iron (1500 g/cm$^2$); 3, 4) iron and concrete (1500 and 115 g/cm$^2$ respectively).

The MARS program includes six basic subprograms written in FORTRAN.

BEGI – preparation of input data; selection of energy, direction cosines, and coordinates of incident primary particle.

TRACE – calculation of mean free path including ionization loss for charged particles; calculation of statistical weight for exponential transformation.

GEOM – calculation of coordinates of point of interaction; recording of events involving escape of particles from the block of material or the crossing of planes bounding cavities or assigned regions for various materials. If a particle arrives in an assigned element of the block, the preliminary analysis program FINI is initiated and the result and its variance are stored.

TREE – treatment of the "trajectory tree." The tree is scanned in accordance with a lexico-graphical scheme [6]. Selection of the energy E, scattering angle $\theta$, and azimuthal angle $\varphi$ occurs in the program SELECT by means of sampling functions for each type of particle (j = p, n, $\pi$) and each energy range. Depending on the type of

Translated from Atomnaya Énergiya, Vol. 38, No. 4, pp. 226-228, April, 1975. Original article submitted July 10, 1974.

TABLE 1. Dependence on Primary Proton Energy of Contribution to Maximum Dose Equivalent from Radiation Components outside Various Shields (%)

| $E_0$, GeV | Shield H, g/cm² | Shield material | p+π+K >10 MeV | n >15 MeV | n <15 MeV | γ >1 MeV | μ >10 MeV |
|---|---|---|---|---|---|---|---|
| 1 | 1500 | Iron | 0,01 | 0,19 | 97,3 | 2,5 | — |
| | 1500 | Iron | | | | | |
| | 115 | Concrete | 0,7 | 7,8 | 56,3 | 35,2 | — |
| 10 | 1500 | Iron | 2,2 | 2,0 | 93,8 | 2,0 | 0,03 |
| | 1500 | Iron | | | | | |
| | 115 | Concrete | 32,6 | 26,6 | 28,0 | 12,4 | 0,4 |
| | 1440 | Iron | | | | | |
| | 60 | Lead | 2,3 | 2,2 | 95,2 | 0,2 | 0,1 |
| | 1440 | Iron | | | | | |
| | 115 | Concrete | 34,0 | 32,3 | 31,5 | 1,5 | 0,7 |
| | 60 | Lead | | | | | |
| 50 | 1500 | Iron | 3,2 | 2,3 | 93,0 | 1,4 | 0,1 |
| | 1500 | Iron | | | | | |
| | 115 | Concrete | 40,5 | 27,5 | 22,2 | 9,3 | 0,5 |
| | 2500 | Iron | 1,5 | 1,6 | 93,8 | 2,1 | 1,0 |
| | 2500 | Iron | | | | | |
| | 115 | Concrete | 20,5 | 22,3 | 26,5 | 15,0 | 15,7 |
| 500 | 2500 | Iron | 2,0 | 1,7 | 93,1 | 1,9 | 1,3 |
| | 2500 | Iron | | | | | |
| | 115 | Concrete | 24,0 | 19,5 | 21,8 | 12,0 | 22,7 |

problem to be solved (deep penetration, lateral shielding, calculation of energy deposition, etc.) biased sampling of angle and energy is performed from the necessary functions $f_j(E, \theta)$ normalized to unity. For example, in a deep-penetration problem, preference is given to high energies and small angles, i.e., energy is selected from functions such as AE or $AE^2$ and angles from functions $\sim \exp(-BE^2 \cdot \Theta^2)$, where A and B are certain constants. Bias is eliminated by a statistical weight which is included in the total statistical weight.

FANG – calculation of spectral and angular distributions of secondary particles from nuclear interactions. The same system of semi-empirical formulas that is used in the HAMLET program [2, 3] is used for the description of inclusive spectra.

SERV – final analysis; calculation of functionals and errors, printout of results, and plotting of curves.

At high primary energies, the "trajectory tree" becomes highly branched and the following procedure is employed in order to reduce computing time. For each particle type j, a maximum weight $W_j^{max}(K)$ for the K-th interaction is selected in preceding histories. A number $P \ll 1$ is chosen and events having a weight $W_j(K) < W_j^{max}(K)\alpha$, where $\alpha \ll 1$, are neglected with a probability $1-P$. These events are included with a probability P but with a weight $W_j(K)/P$. For values $P = 0.01$, $\alpha = 0.0001$ and primary energies $E_0 \gtrsim 30$ GeV, the required computing time is reduced by factors of 10-15. Significant sampling with respect to space and biased sampling from well-chosen functions $f_j(E, \theta)$ reduce the statistical error by an order of magnitude. The time required for the calculation of particle fluxes having 10% error is 10-20 min on a BÉSM-6. Spectra having the same statistical error are calculated in 30-45 min.

The program SYNHET, which synthesizes calculated results from the programs MARS and HAMLET, was written to estimate fluxes of neutrons with $E < 15$ MeV and fluxes of $\gamma$ rays, charged kaons, and muons in an arbitrary geometry. Let there be known functions of flux density for particles of type j with energies above some value $\Gamma_i$ which are calculated for identical initial conditions from the programs HAMLET $[\Phi_j(z, \Gamma_j)]$ and MARS $[F_j(\mathbf{r}, \Gamma_i)]$. We use the fact that the flux density of the particles at some depth Z for a broad beam is numerically the same as the flux from a point monodirectional source integrated over the transverse plane at the same depth. Then the following relations will be approximately satisfied:

$$\left.\begin{aligned} F_m(Z,\Gamma_i) &= F_j(Z,\Gamma_i)\,\Phi_m(Z,\Gamma_i)/\Phi_j(Z,\Gamma_i) \\ F_n(Z,\Gamma_k) &= F_n(Z,\Gamma_l)\,\Phi_n(Z,\Gamma_k)/\Phi_n(Z,\Gamma_l) \end{aligned}\right\}; \tag{1}$$

$$\left.\begin{aligned} &F_m(\mathbf{r},\Gamma_i)/_{|\mathbf{r}|=Z} \\ &= F_j(\mathbf{r},\Gamma_i)/_{|\mathbf{r}|=Z}\Phi_m(Z,\Gamma_i)/\Phi_j(Z,\Gamma_i) \\ &F_n(\mathbf{r},\Gamma_k)/_{|\mathbf{r}|=Z} \\ &= F_n(\mathbf{r},\Gamma_l)/_{|\mathbf{r}|=Z}\Phi_n(Z,\Gamma_k)/\Phi_n(Z,\Gamma_l) \end{aligned}\right\}. \tag{2}$$

Here, $F_j(Z, \Gamma_i) = \int_{-\infty}^{\infty} dx \int_{-\infty}^{\infty} dy F_j(\mathbf{r}, \Gamma_i)$, $\Gamma_k < \Gamma_l = 15$ MeV; $j = p, n, \pi^{\pm}$; $m = K^{\pm}, \mu^{\pm}, \gamma$. The Eqs. (1), which reflect the proportionality of the fluxes in a plane perpendicular to the axis of the beam are, of course, satisfied more rigorously than Eqs. (2), which are valid sufficiently far from boundaries.

Using Eqs. (1), we calculated the maximum dose equivalent and the absorbed dose outside shielding consisting of a block of iron having the transverse dimensions 150 × 150 cm and thicknesses of 1500 and 2500 g/cm² and having shields of ordinary concrete and lead on the outside (H = 115 and 60 g/cm², $\rho$ = 2.3 and 11.35 g/cm³, respectively). The energy of the beam of primary protons normally incident in the center of the iron block varied from 1 to 1000 GeV. The spectral distributions outside the shield were integrated over a plane perpendicular to the axis of the beam and were normalized to a single incident proton.

Flux-to-dose conversion coefficients for energies E > 10 MeV were calculated by the method of [7] and were taken from [8, 9] for neutron and $\gamma$-ray energies E $\leq$ 10 MeV.

The dependence of maximum dose equivalent and absorbed dose on primary proton energy outside shields of iron and of iron and concrete is shown in Fig. 1. The addition of a layer of concrete 50 cm thick reduces the dose equivalent by an order of magnitude and lowers the quality factor from 5.5 to 2. This is related to the fact that fast and intermediate neutrons make the main contribution to the dose outside iron; concrete attenuates precisely these neutrons groups leading to a reduction in the quality factor.

The radiation dose composition outside homogeneous and heterogeneous shielding is given in Table 1 for primary energies $E_0$ = 1, 10, 50, and 500 GeV. Given in the table is the maximum dose equivalent for protons, charged $\pi$ and K mesons (E > 10 MeV), neutrons (E > 15 MeV), low-energy neutrons (E $\lesssim$ 15 MeV), muons from pion and kaon decay (E > 10 MeV), and $\gamma$ rays (E > 0.1 MeV). Included is $\gamma$ radiation produced as the result of radiative capture of neutrons, inelastic scattering of fast and intermediate neutrons, release of residual excitation of a nucleus following the cascade-evaporative stage of an interaction, and $\pi^0$ decay. Outside an iron shield, the dose at all energies is determined by the low-energy neutrons. The addition of concrete when $E_0 \gtrsim 10$ GeV equalizes the contributions from hadrons and from high- and low-energy neutrons and the dose is 60-70% determined by the high-energy hadrons. The $\gamma$-ray contribution to the dose at low energies is significant (35%) and decreases to 10-15% for $E_0 \geq 10$ GeV (shield of iron and concrete). The introduction of a layer of lead 60 g/cm$^2$ thick (while maintaining the overall thickness) reduces the $\gamma$-ray dose by an order of magnitude. The muon dose, which is negligibly small at low and medium energies, rises with increasing energy and shield thickness becoming a decisive factor at high energies outside shield thicknesses H $\gtrsim$ 3000-3500 g/cm$^2$.

The results obtained for doses from hadrons agree with previous data [1]. Using data such as that given in Fig. 1 and Table 1, it is easy to calculate the total dose from the dose for any of the components.

## LITERATURE CITED


1. L. R. Kimel' and N. V. Mokhov, in: Problems in Dosimetry and Radiation Protection [in Russian], Vol. 14, V. K. Sakharov (editor), Atomizdat, Moscow (1974), p. 27.
2. L. R. Kimel' and N. V. Mokhov, Izv. VUZ, Fiz., No. 10, 101 (1974).
3. G. I. Britvich et al., IHEP Preprint 74-86, Serpukhov (1974).
4. K. Chandler and T. Armstrong, Operating Instructions for the High-Energy Nucleon-Meson Transport Code HETC, ORNL-4744 (1972).
5. V. S. Barashenkov, N. M. Sobolevskii, and V. D. Toneev, JINR Preprint R2-5719 (1974).
6. N. P. Buslenko et al., Method of Statistical Trials [in Russian], Fizmatgiz, Moscow (1962).
7. V. T. Golovachik et al., IHEP Preprint 73-29, Serpukhov (1973).
8. K. Shaw, G. Stevenson, and R. Thomas, Depth Dose and Depth Dose Equivalent Data as Functions of Neutron Energy, RHEL/M 149 (1968).
9. L. R. Kimel' and V. P. Mashkovich, Protection against Ionizing Radiations. A Handbook [in Russian], Atomizdat, Moscow (1972).

# WAVE ABSORPTION DURING MAGNETOACOUSTIC HEATING IN THE TO-1 TOKAMAK

N. V. Ivanov and I. A. Kovan

UDC 621.039.643

It has been shown in experiments on the TO-1 tokamak [1, 2], that when magnetoacoustic oscillations are excited in the plasma column effective heating is observed, accompanied by an increase in the plasma diamagnetism, an outward shift of the plasma loop, and an increased current in the equilibrium regulators. An increase in the ion temperature of the plasma is observed as recorded by the Doppler broadening of a highly ionized impurity line (CV) and by changes in the energy spectrum of charge exchanged atoms. RF power is fed to the plasma by a loop exciter which surrounds the plasma column and is connected by a coaxial cable to a fixed frequency oscillator. The current flowing in the loop produces a longitudinal RF magnetic field near the walls of the tokamak. The oscillations produced in the plasma were recorded by a magnetic probe located 90° away from the exciter (with respect to the principal axis of the torus) in the shadow of the diaphragm. The signals from this probe indicate successive excitation of spatial harmonics of the natural modes of the plasma column as the density of the plasma changes in time. From the form of the individual resonance peaks it is possible to determine the Q-factor of the plasma resonator, which is a measure of the plasma dissipation. Measurement of the Q-factor and discussion of a possible mechanism for absorption of the oscillations are the topics of the present paper.

## Measurement of the Q-factor

It is known that when a resonator with varying parameters is excited by an oscillator at a fixed frequency, the variation in time of the corresponding frequency, $\omega$, and Q has the form of a resonance curve. For slow variation of the frequency, i.e., $d\omega/dt \ll \omega^2/2Q^2$, the resonance curve is symmetric and the Q-factor may be determined from the width of the curve. As noted in [3], when the only variable parameter

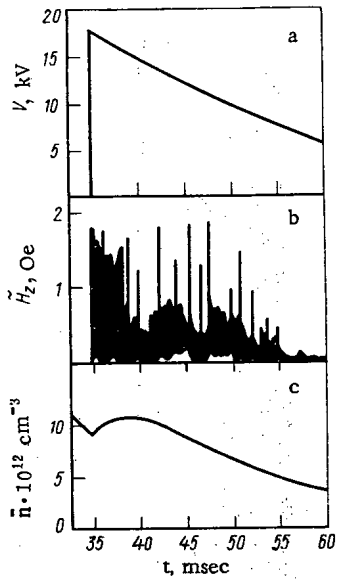


Fig. 1. Time variation of the voltage on the exciter loop (a), and envelope of the signal from the magnetic probe (b), and the plasma density averaged over the diameter of the diaphragm (c).

Translated from Atomnaya Énergiya, Vol. 38, No. 4, pp. 229-233, April, 1975. Original article submitted June 17, 1974.

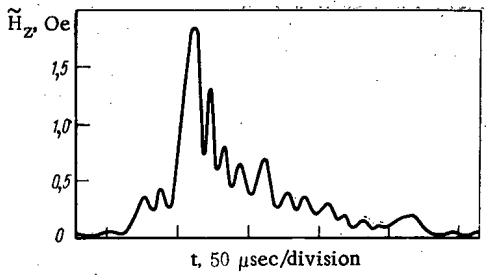


Fig. 2. Rapid scan of the envelope of the signal from the magnetic probe.

determining the natural frequency of a plasma resonator is the plasma density, the Q may be evaluated by the formula $Q = 2n/\Delta n$, where $\Delta n$ is the change in the plasma density over the half width of the resonance curve. This formula is valid for weakly oblique magnetoacoustic oscillations in a dense plasma at frequencies small compared to the lower hybrid frequency, since in this region the square of the refractive index is proportional to the plasma density and is independent of the frequency. In the case of strongly oblique oscillations the expression for Q is reduced by a factor of 2.

When the natural frequency is changed rapidly the resonance curve loses its symmetry. At the moment the natural frequency and the oscillator frequency coincide, the amplitude of the oscillations in the resonator increases steeply and then falls slowly with a characteristic time given by $\tau = 2Q/\omega$. On the falling part of the curve beating occurs with a period depending on the rate of change of the natural frequency.

In the experiments [1, 2] the spectrum of the oscillations has a typical dynamic character. Figure 1 shows an oscilloscope trace of the signal from the probe used to record the longitudinal component of the RF magnetic field. A typical scan of a single resonance peak, obtained in the 36-th millisecond of the discharge, is given in Fig. 2.

The dynamic resonance curve may be described by the equation for forced oscillations. If, as pointed out above, the square of the refractive index is proportional to the plasma density, n, then, as n changes in time, the product $\omega^2 n$ must remain constant for each spatial harmonic. Using this condition and assuming that the plasma density is linearly dependent on time, we may relate the natural frequency to the excitation frequency, $\Omega$, by

$$\omega^2=\Omega^2/\left(1+\frac{1}{n}\frac{dn}{dt}t\right). \tag{1}$$

For weak absorption, taking Eq. (1) into account, the equation for forced oscillations takes the form

$$\ddot{x}+\frac{\Omega}{Q}\dot{x}+\frac{\Omega^2}{1+\frac{1}{n}\frac{dn}{dt}t}=\cos\Omega t. \tag{2}$$

The envelope of the rapidly oscillating function x was isolated by use of a detector circuit whose operation is roughly described by the equation

$$\dot{X}=\frac{x-X}{r_1C}\theta(x-X)-\frac{X}{r_2C}, \tag{3}$$

where X is the signal at the output of the detector circuit; $\theta(x) = \begin{cases} 1, & x\geqslant 0; \\ 0, & x<0; \end{cases}$ $r_1$, $r_2$, and C are the forward resistance, the resistance of the load, and the capacitance of the detector, respectively. The reverse conductivity of the detector was assumed equal to zero.

Solutions of the system of Eqs. (2) and (3) for various values of Q are given in Fig. 3. The following experimental parameters were used in the calculations:

$$1/n\cdot dn/dt=100\ \text{sec}^{-1};\ r_2C=5\cdot10^{-7}\ \text{sec};\ r_1C=5\cdot10^{-8}\ \text{sec};\ \Omega=3\cdot10^8\ \text{sec}^{-1}.$$

On comparing Figs. 2 and 3, we conclude that the unknown value of the Q-factor lies near $Q = 5\cdot10^3$. Some difference between the experimental and computed curves is apparently explained by the nonlinear time variation of the plasma density and by the influence of nearby modes.

Besides the simple resonance peaks shown in Fig. 2, the excited spectrum also contained more complicated curves due to interference between two nearby modes. Such curves are described by two oscillation equations in which the resonance points, $\omega = \Omega$, do not coincide in time and are shifted by an interval $\Delta t$. An example of a comparison between the experimental and computed curves of this type is shown in Fig. 4.

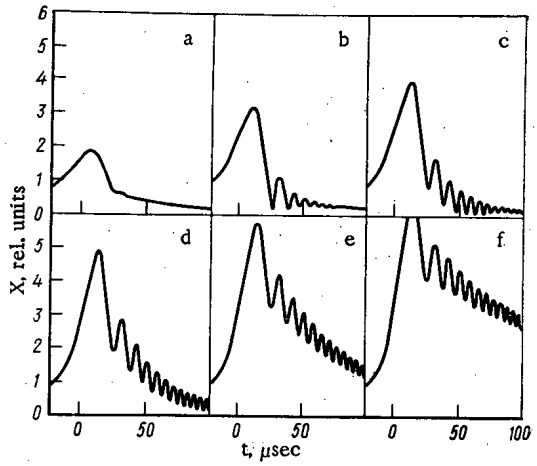


Fig. 3

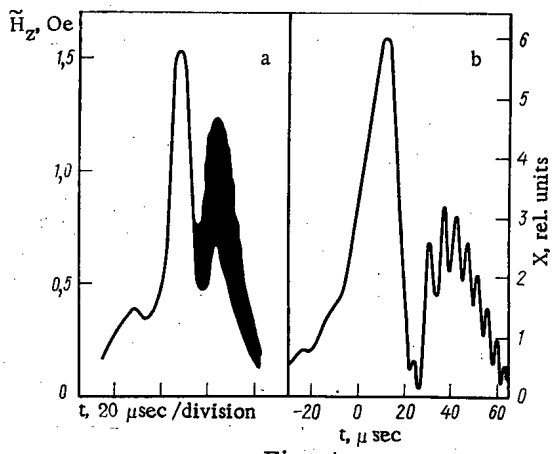


Fig. 4

Fig. 3. The change in the form of the dynamic resonance curve for various values of Q: Q = 1000 (a); 2000 (b); 3000 (c); 5000 (d); 10,000 (e); and 15,000 (f).

Fig. 4. Comparison of complex resonance curves: (a) experiment, (b) computation ($Q = 5 \cdot 10^3$; $n^{-1} \cdot dn/dt = 200\ sec^{-1}$; $\Delta t = 5\ \mu sec$).

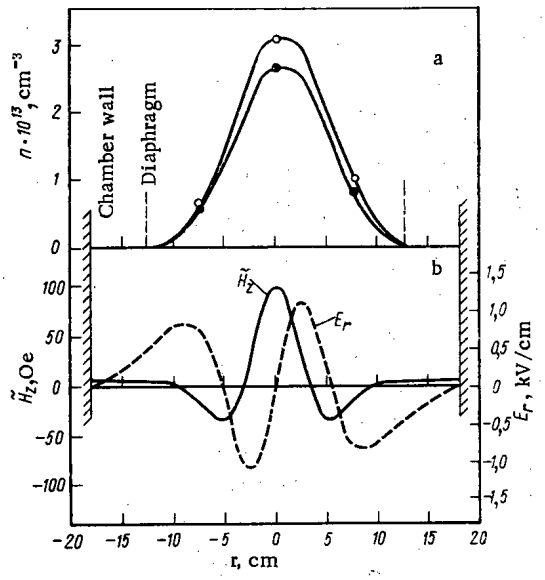


Fig. 5. Radial distribution of the plasma density for t = 35 (●), 40 (○) msec (a) and of the amplitude of the RF fields in the plasma (b).

## Structure of the Natural Mode Fields

In these experiments the geometry of the exciter placed certain limitations on the spectrum of the excited oscillations; the predominant modes excited in the plasma were axially symmetric magnetoacoustic oscillations with relatively low longitudinal wave numbers $k_z = l/R < 0.3\ cm^{-1}$ (here $l = 0, 1, 2, \ldots$ is the number of waves in a circuit of the torus and R = 60 cm is the major radius of the torus). At the same time, during the interval 35-45 msec into the discharge, the radial wave number, $k_r \approx 1\ cm^{-1}$; thus, it is possible to speak of almost radial oscillations of the plasma column. In this case, to find the spatial structure of the natural mode fields it is convenient to use the approximation of a long plasma cylinder ($k_z = 0$) surrounded by a coaxial conducting screen of radius b. If the transverse dimension of the screen is small compared to the vacuum wavelength of the wave, then the radial distribution of the azimuthal component of the electric field can be found by solving the following boundary value problem

$$\begin{cases} \frac{d}{dr}\left(\frac{1}{r}\frac{d}{dr} rE_\varphi\right) + \frac{\omega^2}{c^2} N_A^2 \frac{n(r)}{n(0)} E_\varphi = 0; & (4) \\ E_\varphi(0) = E_\varphi(b) = 0, & (5) \end{cases}$$

where $N_A$ is the Alfven index of refraction on the cylinder axis and n(r) is the plasma density.

Solution of Eqs. (4) and (5) enables us to find the set of characteristic frequencies, $\omega$, which determine the spectrum of the radial oscillations of the cylinder. A harmonic with a frequency close to the excitation frequency was taken as an unknown frequency. It should be noted that the singular point at which the $\varepsilon_{11}$ component of the plasma dielectric tensor goes to zero drops out of Eq. (4). In our case, the condition $\varepsilon_{11} = 0$ is satisfied when $n = 5 \cdot 10^{10}\ cm^{-3}$, which corresponds to the far periphery of the plasma column, where the fields of the natural modes are small. Thus, the influence of the singular point may be neglected, as follows from [4]. In the numerical integration of Eq. (4), a radial density distribution of the form

$$n(r) = n(0)\left[1 - \frac{r^2}{b^2}\right]^6,$$

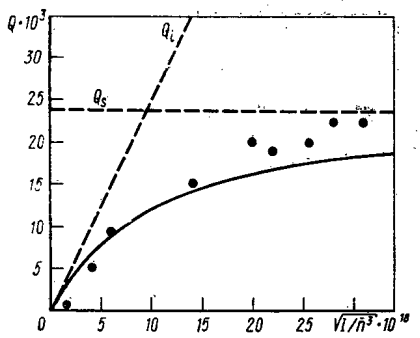


Fig. 6. Q of the plasma resonator as a function of the discharge parameters.

was used as an approximation to the experimental n(r) obtained using microwave probing in the vertical direction along the diameter and two chords. The function n(r) and the corresponding radial electric field distribution of the wave,

$$E_r(r) = -i\frac{\omega}{\omega_i}E_\varphi(r)$$

(in our case $\omega/\omega_i = 4$) as well as the longitudinal component of the RF magnetic field,

$$\tilde{H}_z(r) = -i\frac{c}{\omega r}\frac{d}{dr}rE_\varphi(r)$$

are shown in Fig. 5.

Absolute calibration of the $E_r(r)$ and $\tilde{H}_z(r)$ distributions were made using the known relation

$$Q = \omega\int_v \tilde{H}_z^2\,dV/8\pi\tilde{P}$$

with a measured resonator Q of $5\cdot10^3$ and an absorbed power $\tilde{P} = 25$ kW. The amplitude of the magnetic field at the chamber wall shown in Fig. 5 corresponds to a directly measured value on the order of $\tilde{H}_z(b) \approx 1$ Oe. The difference is explained by a weakening of the RF field near the port of the chamber through which the magnetic probe is inserted.

It follows from the curves of Fig. 5 that for a bell shaped radial density distribution the natural mode fields concentrate at the axis of the plasma column. This leads, on one hand, to a reduction in the coupling of the resonator with the exciter, and on the other, to a reduction in the losses to the chamber walls and in the periphery of the plasma.

The resonator Q, assuming wall losses, has the form

$$Q_S = \frac{2b}{\delta}\alpha,$$

where $\delta = c/\sqrt{2\pi\sigma\omega}$ is the skin thickness and $\alpha = \int_0^b \tilde{H}_z^2(r)rdr/b^2\tilde{H}_z^2(b)$ is a coefficient accounting for the form of the radial distribution in $\tilde{H}_z$ and equal to 4 in our case. A computation for stainless steel ($\sigma = 10^{16}$ CGSE) gives $Q_S = 2.4\cdot10^4$. Thus, under the RF heating conditions of [1, 2], the power lost at the walls was 20% of the total power absorbed in the resonator.

## Dissipation Mechanism

Measurements at various levels of RF power (varied from several watts to tens of kilowatts) showed that the Q of the plasma resonator is independent of the amplitude of the fields excited in the plasma. This allows us to limit ourselves to consideration of linear mechanisms alone for the dissipation of the energy of these oscillations. Estimates show that the known absorption mechanisms (Joule losses, finite ion and electron Larmor radius damping, Cherenkov and cyclotron damping, linear wave transformation, and classical viscosity) give negligibly small contributions to dissipation under these conditions and cannot explain the experimentally observed plasma Q. At the same, it is precisely ion viscosity which is a possible mechanism for dissipation of the magnetoacoustic oscillations of the plasma column since the energy of the oscillations is mainly concentrated in radial motion of the ions and the transverse transport coefficients in a tokamak plasma are large (and exceed the classical values by several orders of magnitude).

The plasma Q, assuming ion viscosity, is given by

$$Q = \omega/k^2D_i, \qquad (6)$$

where k is the transverse wave number and $D_i$ is the transverse ion diffusion coefficient. In the classical case, where $D_i \approx \rho_i^2\nu_i$ ($\rho_i$ is the ion cyclotron radius; $\nu_i$ is the ion–ion collision frequency), Eq. (6) remains valid regardless of the ratio of the frequency of the oscillations to the ion cyclotron frequency [5]. Supposing that the transverse viscosity and thermal conductivity in a tokamak are determined by one and the same transport mechanism, and taking into account the localization of the wave energy near the axis of the plasma column, we may write $k \sim \omega/V_A$ and $D_i \sim a^2/\tau_{E_i}$, where $V_A$ is the Alfven velocity on the axis of the column, $\tau_{E_i}$ is the ion energy lifetime, and $a$ is the radius of the diaphragm.

$\tau_{E_i}$ can be determined from the ion energy balance during Ohmic heating of the plasma [6],

$$\tau_{E_i}=50\frac{T^{3/2}}{n}$$

and expressed in terms of the discharge parameters using the known formula [7]

$$T_i=7\cdot10^{-3}\sqrt[3]{IH_zR^2\bar{n}},$$

where $T_i$ is the ion temperature (°K); I is the discharge current (A); $H_z$ is the toroidal magnetic field strength (Oe); R is the major radius of the torus (cm); and $\bar{n}$ is the density averaged over the diaphragm diameter ($cm^{-3}$). Using these relations and assuming that $n = 2\bar{n}$, we obtain the following approximate formula for the plasma Q:

$$Q_i=3\cdot10^{20}\frac{H_z^{5/2}R}{\omega a^2}\sqrt{\frac{I}{\bar{n}^3}}. \qquad (7)$$

The Q of the plasma resonator as a function of $\sqrt{I/\bar{n}^3}$, including absorption at the walls $Q = Q_iQ_s/(Q_i + Q_s)$, for various discharge regimes with $H_z = 8.5$ kOe, R = 60 cm, and $a = 12.5$ cm is shown in Fig. 6. Measured values of Q, obtained either for low RF power levels or immediately after switching on of the RF oscillator, when the ion temperature has not yet changed significantly as a result of RF heating, are also given. It follows from Fig. 6 that the measurements agree well with the dependence given above.

It should be noted that Eq. (7) is semiempirical since to establish the accuracy of Eq. (6) requires an investigation of the specific transport mechanism, which at present is an open question.

## LITERATURE CITED


1. N. V. Ivanov, et al., Pis'ma v ZhÉTF, 16, 88 (1972).
2. N. V. Ivanov, et al., Atomnaya Énergiya, 36, No. 5, 374 (1974).
3. N. V. Ivanov, I. A. Kovan, and E. V. Dos', Atomnaya Énergiya, 32, No. 5, 389 (1972).
4. Yu. N. Dnestroviskii, D. N. Kostomarov, and G. V. Pereverzev, ZhTF, 42, 10 (1972).
5. V. L. Yakimenko, Dissertation [in Russian], Moscow (1965).
6. L. A. Artsimovich, E. P. Gorbunov, and M. P. Petrov, Pis'ma v ZhÉTF, 12, 89 (1970).
7. L. A. Artsimovich, A. V. Glukhikh, and M. P. Petrov, ibid., 11, 449.

# QUASI-CONTINUOUSLY OPERATING INDUCTIVE ACCELERATORS

V. N. Kanunnikov, A. A. Kolomenskii, P. S. Mikhalev, and A. P. Fateev

UDC 621.384.612

## Introduction

Betatrons are widely employed in scientific research and in industrial applications. Though betatrons are simple, inexpensive accelerators, they have a smaller average beam intensity than, say, linear accelerators.

The beam intensity of a betatron can be increased basically in two ways: 1) by increasing the repetition frequency of the accelerating cycles; and 2) by using a controlling field which is constant in the course of time and a long-lasting injection (betatrons with a constant controlling field). The present article is concerned with the second method though several results obtained in calculations of the particle dynamics and in the development of the magnetic system can be applied to betatrons with a variable controlling field and a high repetition frequency of the accelerating cycles.

The average beam intensity of a betatron with a constant controlling field is given by the ratio of the duration of the injection process to the period of variation of the rotational accelerating field. In a betatron with a constant controlling field, the ratio can exceed the corresponding ratio in a betatron with a variable controlling field by several orders of magnitude [1]. It is possible to determine the range of electron energies for which it is even now convenient and promising to use a betatron with a constant controlling field. Firstly, there is the region of low ($\lesssim$ 10 MeV) energies at which betatrons with a constant controlling field are often employed in applied physics work (defectoscopy, radiation chemistry, etc.). Secondly, there is the energy of ~100 MeV and more, which is of interest in photonuclear and electron-nuclear research. Mainly linear accelerators are now used in this energy range whereas betatrons and synchrotrons are used at energies $\lesssim$50 MeV. Linear accelerators are characterized by a high beam intensity ($10^{14}$-$10^{15}$ electrons /sec) and are distinguished by the simple extraction of the electrons; the low duty factor ($\lesssim 10^{-3}$), the high cost of the equipment and the operation of these accelerators, and the relatively large energy spread of the accelerated particles are the shortcomings of the linear accelerators. At energies $\lesssim$50 MeV microtrons can compete with linear accelerators. Conventional betatrons are in certain respects better and simpler than linear accelerators and microtrons, but the beam intensity of betatrons is low ($\lesssim 10^{11}$ electrons/sec) owing to their pulsed operation. Betatrons with a constant controlling field advantageously combine high average beam intensity with a good beam quality (low output impedance and small energy spread) and even require lower capital investments and costs of operation than, say, linear accelerators. A high beam intensity in betatrons with a constant controlling field is obtained mainly because the duty cycle can be substantially increased (i.e., the pulse duty factor) is reduced.

Several strongly focusing accelerators with a constant controlling field have been developed and put into operation [2-5]. However, when these accelerators were used as inductive accelerators, they were operated at low energies (up to 2 MeV) and with a high pulse duty factor. To date no high-current betatron with a constant field has been built. There is a good reason for that: betatrons with a constant controlling field resemble the usual betatrons only as far as an inductive acceleration system is employed; as far as all the other aspects are concerned (constant field, strong focusing, long-lasting or repeated injections, beam extraction, etc.), betatrons with constant controlling fields are a special type of accelerator without an analog. The development of betatrons with a constant controlling field was preceded by research on the

Translated from Atomnaya Énergiya, Vol. 38, No. 4, pp. 234-239, April, 1975. Original article submitted October 11, 1974.

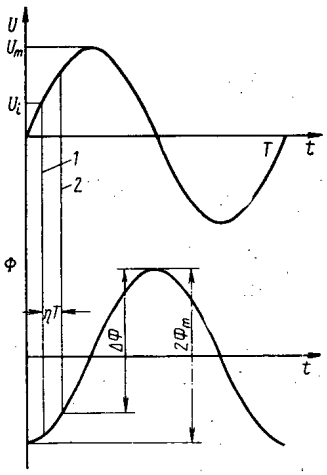


Fig. 1

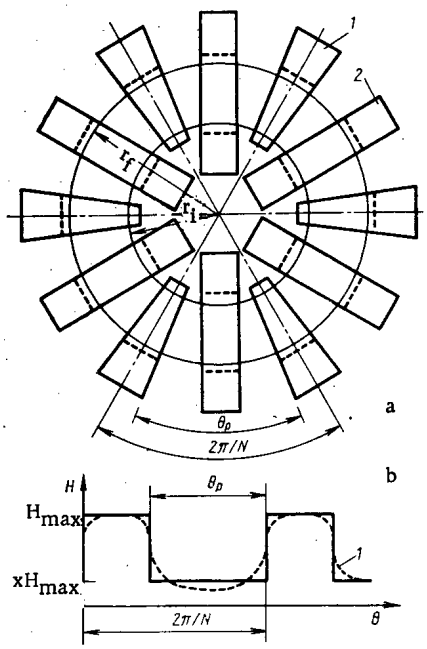


Fig. 2

Fig. 1. Time dependence of the accelerating voltage and the magnetic flux in a betatron with a constant controlling field: 1) beginning of the injection process; 2) end of the injection process.

Fig. 2. Scheme of the magnetic system. a) Top view: 1) sector of the electromagnet generating the controlling field; 2) magnetic core of the accelerating flux; $r_i$ and $r_f$ denote the initial radius and the final radius in the accelerating area, respectively; b) azimuthal form of the field: 1) real field.

usual betatron and phasotron conditions in small models [2, 3] and, afterwards, in the existing electron accelerators for the maximum energy of 40 MeV [4, 5]. The difficulties encountered in the generation of the controlling field of a betatron with a constant controlling field were overcome in the course of those investigations and a simplified method of calculating and generating the field [6] was developed. Experiments [9] were made and proved that it is possible to increase the controlling field at least up to 13 kOe without a substantial distortion of the field. The Laboratory of Problems of Novel Accelerators of the Physics Institute of the Academy of Sciences of the USSR used an electron ring phasotron with a maximum energy of 40 MeV in a series of experimental investigations and modeled systems and operating conditions of betatrons with a constant controlling field [7-9]. In particular, electron acceleration experiments were made with two injection methods: single, long-lasting injection and multiple injection of a group of short pulses with a high duty factor. The lower limit of the average beam intensity ($\sim 10^{14}$ electrons/sec) was determined from the average current obtained.

The extraction of the beam from the magnetic system of a betatron with a constant controlling field was accomplished in the American ring phasotron [5]. One usually employs a beam of hard bremsstrahlung emitted from a target located in the actual accelerator area in photonuclear research work. The bremsstrahlung beam of the electron ring phasotron was extracted through a channel in the yokes of the magnet so that the upper limit of the bremsstrahlung could be adjusted.

Small scattering fields which distort the orbits, reduce the aperture, and decrease the maximum amplitude of the free electron oscillations, are one of the requirements which the accelerating system of a betatron with a constant controlling field must satisfy. The azimuthal resonance harmonic of the scattering field normally must not exceed 0.1% of the basic harmonic of the oscillations. Experience gathered in the operation of the electron ring phasotron has shown that the problem of reducing the scattering field to the above value has been fully solved in the betatron area.

Thus, the main difficulties in the development of betatrons with a constant controlling field can be overcome and it is now possible to consider the planning of an accelerator of this type. We describe below the basic concepts in the selection of the parameters of betatrons with a constant controlling field designed

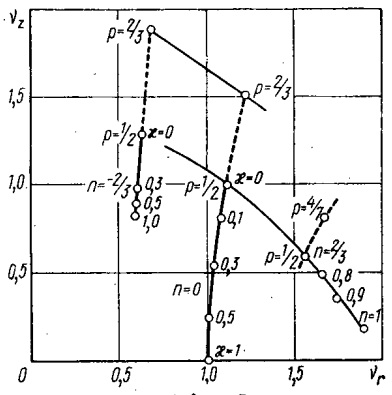


Fig. 3

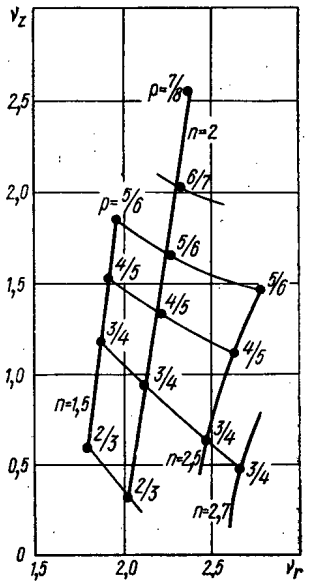


Fig. 4

Fig. 3. Stability diagram for a magnet system without sectors of negative field at N = 4. The lines drawn from the top downward join the points of operation with identical field exponent n; the lines drawn from the left downward to the right connect the points of identical field variation in azimuthal directions, with the same relative width p of the gap and with the same relative field strength $\varkappa$ in the gap (the dashed lines indicate the variation of p at $\varkappa = 0$; the solid lines refer to the variation of $\varkappa$ at p = 1/2).

Fig. 4. Stability diagram of a six-vector magnet system for various p and n values at $\varkappa = 0$.

for low energies and an energy of 100 MeV.* The latter value must be considered a reference value which makes it possible to estimate the advantages offered by a betatron with a constant controlling field at high energies. In general, the energy must be selected with proper consideration of the specific requirements which are given by, say, the program of experiments to be performed.

Parameters of the Accelerating System. At a given pulse duty cycle factor $\eta$ of the beam and an accelerating injection voltage $U_i$, the formula for the flux $\Phi_m$ required for accelerating electrons to the energy $E_m$ (Fig. 1) has the form

$$\Phi_m = \Delta\Phi / \left[1 + \cos\left(2\pi\eta + \arcsin\frac{U_i}{U_m}\right)\right],$$

where $U_m$ denotes the accelerating voltage which depends upon the flux $\Phi_m$ and the frequency of the flux variations; $\Delta\Phi$ denotes the smallest current increment required:

$$\Delta\Phi = \frac{\Pi_i}{c} \cdot \frac{1+n}{2+n} \left(\frac{E_i^2 - E_0^2}{e^2}\right)^{1/2} \left[\left(\frac{E_m^2 - E_0^2}{E_i^2 - E_0^2}\right)^{\frac{2+n}{2(1+n)}} - 1\right].$$

where $\Pi_i$ denotes the perimeter of the orbit of injection; n denotes the field exponent; $E_i$ denotes the energy of injection; and $E_0$ denotes the rest energy.

Though in a betatron with a constant controlling field, the betatron condition which establishes a relationship between the controlling field and the accelerating field is not applicable and though the magnetic systems generating the fields are distributed systems, restrictions exist. The fact that the accelerating inductive core is shifted inside the ring of the controlling magnetic system can be used to derive an inequality which imposes restrictions upon the radius $r_i$ of the injection orbit and the magnitude of the controlling field $H_m$ effective on the maximum orbit $r_m$. At a given maximum energy $E_m$, a lower limit for

*A projected betratron with a constant controlling field and a maximum energy of 150 MeV and an average beam current of 1 mA was discussed in the USA [10], but it is not known how far the project has progressed.

TABLE 1. Approximate Parameters of Small Betatrons with Constant Controlling Field

| Parameters | Number N of sectors | | | |
|---|---|---|---|---|
| | 4 | 6 | | 8 |
| Field exponent | 0,8 | 2,7 | 2,7 | 5,0 |
| Flutter | 1,0 | 3,0 | 3,0 | 6,0 |
| Radius (cm) of the injection orbit | 8 | 18 | 18 | 32 |
| Radius (cm) of the final orbit | 14 | 33 | 45 | 60 |
| Maximum strength (kOe) of the controlling field | 0,6 | 1,3 | 2,8 | 5,0 |
| Frequency of the betatron oscillations | | | | |
| in radial direction | 1,8 | 2,7 | 2,7 | 3,2 |
| in vertical direction | 0,7 | 0,75 | 0,75 | 0,7 |
| Induction (kG) of the accelerating field | 1,5 | 1,5 | 7 | 6 |
| Total flux (mWb) in the cores | 0,75 | 6 | 30 | 90 |
| Frequency (kHz) of flux variation at $U_m$ = 300 kHz | 60 | 8 | 1,6 | 0,6 |
| Maximum kinetic energy (MeV) of the electrons | 0,3 | 1,5 | 5 | 10 |

the quantity $r_i$ results from the condition that the flux $\Phi_m$ must penetrate into the ring of the magnetic system, since the induction in the accelerating magnetic core cannot exceed a certain value which depends upon the material and the frequency of magnetic reversal.

Betatrons with a constant controlling field are distinguished from conventional betatrons also insofar as the injection system must be more powerful. In order to make the system sufficiently economic, the efficiency of the injection must be increased by selecting a sufficiently high accelerating voltage $U_i$ which is given by the amplitude and the variation rate of the flux $\Phi_m$. The flux depends upon the maximum energy and the radius of the betatron. Hence, in the case of betatrons with a constant controlling field for low energies, one must employ an increased repetition rate [11]. In the case of a 100 MeV betatron with a constant controlling field, the required accelerating voltage can be obtained in operation with the line frequency of 50 Hz. Furthermore, the injection energy influences the efficiency of operation of a betatron with a constant controlling field and its maximum beam intensity. The space charge problem in a betatron with a constant controlling field cannot be complicated because the instantaneous (pulsed) beam current does not exceed the corresponding current in conventional betatrons.

Magnetic System and Particle Dynamics. In order to reduce the width of the magnetic ring system, one must select the greatest possible exponent n of the increase in the magnetic field strength in the radial direction: $H(r) = H_m(r/r_m)^n$; in order to ensure vertical focusing in a radial sector system, a sufficiently large flutter $F = 4\sum_{k=1}^{\infty}|f_k|^2/f_0^2$, is required, where $f_0$ and $f_k$ denote the azimuthal harmonics of the field $H(\theta) = H_{max}[f_0 + \sum_{k=1}^{\infty} f_k e^{ikN\theta}]$. A large flutter can be obtained with a conventional magnetic system having a field polarity alternating from sector to sector. This system is characterized by several shortcomings when it is applied to a betatron with a constant controlling field, particularly in the case of a low-energy betatron ($\lesssim$ 10 MeV) of this type.

In contrast to the previously considered versions [1-10], a unipolar radial sector system of the controlling field was analyzed [11]. Figure 2a shows the scheme of a unipolar magnetic system (particular case of a 6-sector electromagnet). Sectors with negative fields are missing. The large gap between the sectors can accommodate accelerating magnetic cores and ensure the required azimuthal field variation. The field variation in this system is almost rectangular. In an ideal steplike field, the flutter can be written in the form

$$F = \frac{p(1-p)(1-\varkappa)^2}{[1-p(1-\varkappa)]^2},$$

where $\varkappa$ denotes the relative field strength in the equivalent gap; $p = N\theta_p/2\pi$ denotes the relative width of the gap; and N denotes the number of sectors (see Fig. 2b).

The price for a large F is a small average azimuthal field

$$f_0 = \frac{\langle H\rangle}{H_{max}} = 1 - p(1-\varkappa)$$

and, accordingly, a relatively large average radius of the accelerator. However, the increase in the radius at a given maximum electron energy makes it possible to reduce the induction of both the controlling field and the accelerating field and to decrease the losses in the magnetic system. On the other hand, the required strong azimuthal field variation (large p and small $\varkappa$) can be obtained only with a sufficiently large radius at which the width of the magnetic sector in the azimuthal direction is greater than the vertical accelerating gap.

TABLE 2. Approximate Parameters of a 100 MeV Betatron with Constant Controlling Field

| Parameters | Electron ring phasotron | Symmetric magnetic system | Unipolar sector system |
|---|---|---|---|
| Controlling field | | | |
| Number of sectors | 40 | 44 | 15 |
| Field exponent | 16 | 12 | 6 |
| Average radius (m) of the final orbit | 1,6 | 2,5 | 2,8 |
| Average radius (m) of the orbit of injection | 1,25 | 1,7 | 1,4 |
| Maximum field strength (kOe) on the final orbit | 12 | 12 | 9,6 |
| Maximum field strength (kOe) on the orbit of injection | 0,1 | 0,12 | 0,13 |
| Frequency of the betatron oscillations | | | |
| In radial directions | 5,6 | 6,2 | 2,7 |
| In vertical directions | 1,8 | 6,7 | 0,7 |
| Accelerating field | | | |
| Total flux (Wb) | 2,6 | 3,5 | 3,6 |
| Accelerating voltage (kV) | 0,8 | 1,0 | 1,1 |
| Induction (kG) in the iron | 15 | 15 | 13 |
| Total weight (ton) of the active iron | 135 | 160 | 105 |
| Number of accelerating cores | 3 | 4 | 15 |

When the dynamics of the particles was analyzed, the basic calculations were made with the number N = 4, 6 or 8 of sectors. The field exponent n and the flutter F were varied. The azimuthal dependence of the field was represented by a step function (see Fig. 2b) which was expanded in a Fourier series; the harmonics $f_k$ determined in this fashion were inserted into the accurate equations of motion. This made it possible to analyze any real field by selecting the two parameters p and $\varkappa$. The magnitude of the flutter was the criterion for the selection of p and $\varkappa$, because both the step-like field and the real field are equivalent (as far as the frequencies of the betatron oscillations are concerned), provided that the flutters of the fields coincide. In practice, it often suffices that the sum of the squares of the two first harmonics coincide. The reason is that the harmonics with $k > 2$ contribute very little to the frequency of the betatron oscillations.

It follows from the stability diagram for a four-sector magnet (Fig. 3) that the frequency $\nu_r$ of the radial oscillations depends only slightly upon the parameters p and $\varkappa$ which characterize the azimuthal form of the field. The case $n > 0.5$ can be of interest in practice. Stability can be obtained in this case only for $n \lesssim 1$ (stability limit $\nu_r = N/2$) and for a sufficiently strong ($\varkappa \lesssim 0.1$) variation, i.e., at large flutter values. The stability diagram (Fig. 4) shows that a six-sector magnet system is more promising than a four-sector system. In the six-reactor system, the admissible value is $n \approx 2.8$. This means that, under otherwise equal conditions, both the width of the ring and the weight of the magnet are reduced in the case of the six-sector magnet.

A similar analysis of an eight-sector magnet system has shown that relatively large n can be used with $n \approx 5$. Therefore, a multi-sector magnet system must be used in a betatron with constant controlling for high energies.

Additional nonlinear resonances are one of the shortcomings of a sector system. The results of special calculations have shown that, though the nonlinearity limits the amplitude of the oscillations in the injection process, the limitation is not so severe as to affect the high intensity which can be obtained with a betatron with a constant controlling field. This conclusion is corroborated by the successful operation of the ring phasotron of the Physics Institute of the Academy of Sciences of the USSR [4, 8] in which the maximum amplitudes amount to ~1 cm.

Selection of Parameters. When the parameters of a betatron with a constant controlling field are selected, one can start from an N value which determines the geomtry of the system and most of the other accelerator characteristics. Three versions with N = 4, 6, or 8 are listed in Table 1. The energy of injection and the amplitude of the accelerating voltage are assumed to be given and to be equal in the three versions: $W_i = 0.05$ MeV, $U_m = 300$ V, duty cycle factor $\eta \approx 0.1$, $U_i/U_m \approx 0.6$.

The figures listed in Table 1 are tentative figures, because the accurate parameter values depend upon several technological details in the solution of the problem. In particular, the selection of both the induction used for the operation and the frequency is substantially affected by the material selected, the design of the cores, the heat transfer conditions, etc. A detailed technological evaluation is required for a definite determination of the parameters of the accelerator.

100 MeV Betatron. The magnetic system of the electron ring phasotron which is now operating in the Physics Institute of the Academy of Sciences of the USSR [4] can be considered a first version of the magnetic system for a 100 MeV betatron with a constant controlling field. The energy of 40 MeV in the electron ring phasotron corresponds to a maximum field strength of 4.7 kOe on the radius 160 cm. This means that when this maximum radius is conserved, $H_m \approx 12$ kOe must correspond to the energy 100 MeV. This value

can be adopted as a tentative value. In view of the experience in the operation of the electron ring phasotron, it is safe to say that no technological difficulties will be encountered when this magnetic system is built.

The symmetric magnetic system of [12] which has several advantages when applied to a betatron with a constant controlling field can be considered a second version. The symmetric magnetic system makes it possible to use both half-periods of the rotational field for the acceleration and, as in a conventional betatron without magnetic biasing, to obtain two beams of accelerated electrons. The efficiency of the accelerator is almost doubled, because the duty cycle coefficient and the average beam current are doubled while the same power losses occur in the accelerating system. In addition, a symmetric controlling field facilitates increased vertical focusing and improves the design of the magnet system (horizontal yokes can be used; free access to the vacuum chamber is possible from the outside of the ring [13]; the maximum induction in the iron is increased; extensive adjustments of the field strength are possible; and a unified supply circuit of equal coils in all sectors can be employed, etc.).

A third version of a 100 MeV betatron with a constant controlling field is based upon the above-described unipolar magnetic sector system. The approximate parameters of the magnetic system of the 100 MeV betatron are listed in Table 2. We assumed in the calculations $\eta \approx 0.1$, $U_i/U_m \approx 0.5$, a kinetic energy of 0.3 MeV for the injection, and a repetition frequency of ~50 Hz.

The versions differ mainly by the width of the magnetic path and the extent of focusing. In the third version, the magnetic system is more advantageous than in the two other versions inasmuch as the weight and the power consumption are concerned at an injection radius of 1.4 m (which is given by the above-specified conditions for the azimuthal field variation) and at a large width of the magnetic path (because the field exponent is small). As far as the weight of the accelerating system (105-160 ton) is concerned, we recall for comparison that a conventional betatron (without magnetic biasing) for 100 MeV has a weight of 130 ton. The final selection of the parameters of a betatron with a constant controlling field must be made when the plan for an accelerator project is worked out so that the system as a whole can be considered.

The authors thank L. N. Kazanskii, V. A. Papadichev, and B. N. Yablokov who participated in the various development stages of several systems for betatrons with a constant controlling field, and G. I. Kharlamova for her help in the numerical calculations.

## LITERATURE CITED

1. L. N. Kazanskii et al., in: Proc. of the All-Union Conference on Accelerators [in Russian], Vol. 2, Izd. VINITI, Moscow, p. 351.
2. F. Cole et al., Rev. Sci. Instr., 28, 403 (1957).
3. V. A. Petukhov et al., Atomnaya Énergiya, 9, No. 6, 491 (1960); A. A. Zhuravlev et al., Zh. Tekh. Fiz., 41, 905 (1962).
4. V. N. Kanunnikov et al., Pribory i Tekh. Éksperim., No. 5, 71 (1967).
5. F. Cole et al., Rev. Sci. Instr., 35, 1393 (1964).
6. V. N. Kanunnikov, A. A. Kolomenskii, and V. A. Papadichev, in: Proc. of the Second All-Union Conference on Accelerators [in Russian], Vol. 2, Nauka, Moscow (1970), p. 12.
7. L. Kazansky et al., in: Proc. Sixth Intern. Conference on High Energy Accelerators, Cambridge (1967), p. 419.
8. V. N. Kanunnikov and P. S. Mikhalev, Kratkie Soobshcheniya po Fizike, Izd. FIAN, Moscow, No. 1, 38 (1974).
9. V. N. Kanunnikov, P. S. Mikhalev, and V. A. Papadichev, Kratkie Soobshcheniya po Fizike, Izd. FIAN, Moscow, No. 5, 39 (1972).
10. R. Haxby et al., Progress Report IS-FFAG-3, Iowa State University (1968).
11. V. N. Kanunnikov et al., Preprint FIAN, No. 58 (1974).
12. A. A. Kolomenskii, ZhÉTF, 33, 298 (1957).
13. M. Barbier et al., in: Proc. Intern. Conference on High Energy Accelerators, CERN (1959), p. 100.

# ADVANCES IN METROLOGY OF NEUTRON RADIATION IN REACTORS AND ACCELERATORS

R. D. Vasil'ev

UDC 539.1.08

Advances in nuclear engineering place ever stricter demands on the reliability of results of measurements of the properties of neutron radiation fields and sources. This stimulates interest in metrology, one of the branches of engineering whose task is to provide researchers with standard measures, reference instruments, standard samples of materials, standard measuring techniques, etc.

To sum up the results of metrological activity in the Soviet Union, the 1st All-Union Conference on the Metrology of Neutron Radiation in Reactors and Accelerators was held in Moscow on October 18-22, 1971 [1]. The Conference proved that many research groups are engaged in metrology. Their task is to develop standards, reference sources, standard samples of materials, counters, instruments, and calibration devices, typical measuring techniques, etc. Of special importance in nuclear engineering is the development of a set of monoenergetic neutron sources based on accelerators. In the late sixties metrologists began to seek a solution to an entirely new metrological problem: the creation of an All-Union system of metrological instrumentation for neutron measurements in nuclear facilities. Fundamental problems have been solved concerning the scientific foundations of the system, and the design of a comprehensive set of standard reference measuring instruments has been started.

The 2nd All-Union Conference on Metrology of Neutron Radiation in Reactors and Accelerators, held in Moscow on October 14-17, 1974 [2], has summed up the metrological research carried out during the three intervening years.*

## Structure of Metrological Approach to Nuclear Facilities

The structure was realized in a scheme for calibrating instruments measuring the characteristics of neutron fields, and legalized as a State Standard [3]. The scheme covers measurements of neutron energy from thermal to 20 MeV and flux density from $10^5$ to $10^{14}$ neutr./cm$^2$ sec, and guarantees an accuracy of 2 to 20% with a confidence level of 95%. The scheme is based on a special State Standard Unit of neutron flux density, preserved at the All-Union Scientific-Research Institute of Physical and Electronic Measurements, and measuring reference devices in the form of standard samples of neutron-activation and fissionable materials and reference neutron sources based on nuclear physics facilities.

For the first time the calibration scheme includes, besides direct measurements, also indirect and composite measurements which make it possible to determine any physical quantities and relationships characterizing neutron radiation fields and sources.

The created neutron measurements structure is in fact a program of metrological activities whose purpose is the solution of various measuring problems encountered in nuclear physics facilities.

## Standard and Reference Neutron Sources (Fields)

In 1973, the State Committee of Standards of the Council of Ministers of the USSR approved a special State Standard of the unity of neutron flux density [3]. This standard includes two sources based on a neutron generator providing a thermal neutron flux whose density can be varied between $10^2$ to $10^7$ neutr./cm$^2$ sec, and a flux of 14.5 MeV neutrons with a density variable between $10^4$ and $10^7$ neutr./cm$^2$ sec. The following two new standard sources are being developed now: a) sources of 2.5 MeV neutrons with a 1/E

*For information on the results of this Conference see At. Énerg., 38, No. 1, 58 (1975) (editor's note).

Translated from Atomnaya Énergiya, Vol. 38, No. 4, pp. 240-244, April, 1975. Original article submitted August 19, 1974.

spectrum covering the $^{235}U$ fission neutron spectrum, based on the same neutron generator, and b) sources of monoenergetic neutrons in the energy range from 0.001 to 5 MeV, based on the ÉG-2M electrostatic accelerator.*

Basic principles have been developed for metrological certification of reference neutron sources based on nuclear physics facilities in which the neutron field is only reproduced but not preserved. The first reference neutron sources (fields) based on static and pulse reactors have been developed in 1974. The sources have been certified for various quantities and relationships necessary for solution of specific problems.

One of the sources is the vertical channel of the MR material-research reactor of the I. V. Kurchatov Institute of Atomic Energy. The source is used for calibrating direct-charge detectors which are regularly used for reactor monitoring. The source has been certified for the following characteristics:

the effective thermal neutron flux density per unit reading of the monitor used in the calibration channel (the error of this quantity did not exceed 5% for a confidence limit of 95%);

the relative distribution of the effective thermal neutron flux density along the channel at the location of the calibrated detectors;

the epithermal parameter, which characterizes the relation between the epithermal and thermal components of the neutron field, in the reactor channel.

In the course of detector calibration the effective thermal neutron flux density was determined from the first mentioned characteristic multiplied by the monitor reading.

The second reference source is based on a pulsed reactor with an open core and is used for solving certain applied problems in solid state physics. The object of certification was the neutron field in a small volume around a given point in space. The quantities determined were the integral flux density and fluence of neutrons with an energy in excess of 0.1 MeV as referred to the integral flux density (and fluence) of neutrons with an energy higher than 3 MeV measured by the monitor; the accuracy was 15% for a confidence level of 95%. This characteristic is a spectral coefficient. In subsequent reactor operation, the integral flux density (and fluence) of neutrons with an energy in excess of 0.1 MeV at the given point was found from the spectral coefficient multiplied by the monitor readings. The neutron field around the chosen point was called the reference field. Other points of space around the reactor, called the operating points, were certified relative to the reference field with an accuracy only slightly less than the accuracy of the reference point.

Besides reactor certification, work proceeds on the development of reference sources based on neutron generators and electrostatic accelerators.

## Standard Samples, Counters, and Instruments

Reference measuring devices such as sets of standard neutron activation and fissionable samples, AKN and NDS [1], used for field measurements in fast neutron reactors, have been produced since 1973. The AKN set includes "detector and $\gamma$ or $\beta$ source" activation pairs: $^{103}Rh$ – $^{241}Am$ in a cadmium filter, $^{115}In$ – $^{51}Cr$, $^{199}Hg$ – $^{139}Ce$, $^{58}Ni$ – $^{58}Co$, $^{32}S$ – $^{32}P$, and a "detector and fission fragment recorder" fission pair $^{237}Np$ – mica. The NDS set includes an $^{32}S$ – $^{32}P$ activation pair. The AKN(t) set now being prepared for production has been developed for measuring the characteristics of thermal neutron fields in reactors and for estimating the portion of epithermal neutrons. The set will include $^{197}Au$ – $^{113}Sn$, $^{59}Co$ – $^{60}Co$, $^{55}Mn$ – $^{54}Mn$, and $^{54}Fe$ – $^{54}Mn$ activation pairs, and a pair of "thermal" activation detectors $^{175}Lu$ – $^{63}Cu$ with a calibration $\gamma$ source of $^{109}Cd$. All sets are certified in standard and reference facilities.

*It should be noted here that the D. I. Mendeleev Institute of Metrology has a State Standard for the neutron flux density unit which can produce a thermal neutron field of the order $10^4$ neutr./cm$^2$ sec. This standard is used as a metrological tool in measurements at thermal neutron energies. The difficulties associated with the creation of similar standards over the entire range of reactor neutrons was the reason for developing the special State Standard. This standard has been extended to the reactor neutron range by including in it sources of both thermal and fast neutrons, and by expanding the range of reproduced neutron flux densities by several orders of magnitude. Both sources serve as fundamental means for the certification of standard samples which are used in measurements. The comparison of both these standards at thermal neutron energies is now being prepared.

Work is continued on the development of standard neutron activation detectors made of alloys and phenolformaldehyde resin for measurements at high ambient temperatures. Unlike in earlier studies, main emphasis is now placed on sample certification. Work has begun on the development of standard fissionable sets DKN for measurements in neutron fields with relatively low neutron field densities such as, for example, in critical test stands. This work has been preceded by a detailed study of detectors and various recorders of fission fragments.

Much attention is recently devoted to the preparation of standard targets of fissionable materials and to their certification as to isotopic composition and number of nuclei. This is a natural response to need of experimenters engaged in the measurement of nuclear physics constants and to the demand for ever more reliable nuclear data. New certification possibilities are afforded by the MKh-3301 double-focusing mass spectrometer now available at the V. I. Lenin Institute of Atomic Reactors.

Many experiments have analyzed detectors consisting of a combination of activation or fissionable samples in spherical boron filters. The feasibility of filters based on phenolformaldehyde resin allows to expect the appearance of standard "composition" detectors of this type in the near future.

The industrial development of gas-filled neutron recording counters continues. The most important of such counters are the SNM-50, -52, -53, and 57 spectrometric proportional counters, and SNM-51, -55, and -56 corona counters. The "Narva" set of measuring devices, consisting of a facility for measuring the induced activity of neutron detectors and of a kit of standard detector and calibration sources, has been prepared for production.

Since 1974, many counters, ionization chambers, and measuring instruments used for nuclear physics measurements, are being certified with the aid of the special State Standard of neutron flux density and the reference neutron source (field) based on the MR reactor. This has greatly improved the reliability of the certification.

Obviously, not all experimental problems can be solved with the aid of standard measuring devices. As a result, individual researchers continue to develop and certify special devices such as slow neutron detectors using x-ray films, probe detectors for fast neutrons, proportional counters for exact measurements in monoenergetic neutron fields, calorimetric detectors of thermal and fast neutrons, fission fragment recorders, etc.

## Nuclear Physics Constants

The attention of neutron radiation metrologists is attracted principally to two groups of physical constants: in the first place, to reference cross sections and, secondly, to constants used in the measurement of neutron fields and sources such as neutron activation cross sections, decay scheme parameters, etc.

Several collectives are engaged in the study of physical constants. One of the most fruitful is the activity of the Nuclear Data Center of the Obninsk Physics and Power Institute. The Center collects practically all available neutron data with the purpose of their coordination and evaluation.

Coordination Groups for the measurement of nuclear physics constants and for the application of nuclear data in reactors, organized at the Committee of Nuclear Data at the State Committee on the Application of Atomic Energy of the USSR, help to coordinate the analysis of nuclear data. These Coordination Groups have recently organized Topical Subgroups dealing with specific types of constants. One of these Subgroups related to metrology is the Topical Subgroup on Standards and Reference Quantities. In the beginning of 1974, the Subgroup worked out recommendations on the basic reference constants including $\sigma_{total}(^{1}H)$, $\sigma_{n,p}(^{3}He)$, $\sigma_{n,t}(^{6}Li)$, $\sigma_{n,\alpha}(^{10}B)$, $\sigma_{total}(^{12}C)$, $\sigma_{n,\gamma}(^{197}Au)$, and $\bar{\nu}(^{252}Cf)$. Recommendations on $\sigma_{n,f}(^{235}U)$, on the neutron spectrum of spontaneous fission of $^{252}Cf$, and certain other constants, are to be published in 1975.

The Center of Atomic and Nuclear Data at the L. V. Kurchatov Atomic Energy Institute has existed since 1972. The range of topics covered by this Data Center is extremely wide as it is called upon to fill gaps in all non-neutron data used in neutron measurements.

## Standard Measuring, Certification, and Calibration Techniques

The development of certain measuring, certification, and calibration techniques are concluded with their standization. The standardards Publishing Press has recently prepared for publication several standard methods of composite indirect measurements:

TABLE 1. Information on Reactor Comparisons

| Reactor | Mode | Energy range, MeV | Compared quantities and relationships |
|---|---|---|---|
| VVR-50 | Static | $0{,}0253 \cdot 10^{-6}$—20 | Effective flux density and temperature of thermal electrons, fluence, spectral coefficient, differential and integral spectra, etc. |
| IRT-2000 | Static | 0,1—20 | Spectral coefficient |
| IIN | Pulse | 0,1—20 | Spectral coefficient |
| GODIVA-IV type reactor [4] | Pulse | $0{,}0253 \cdot 10^{-6}$—20 | Neutron fluence, kerma |
| HRPP type reactor [4] | Pulse | $0{,}0253 \cdot 10^{-6}$—20 | Neutron fluence, kerma |
| HRPP type reactor( Yugoslavia) | Pulse | $0{,}0253 \cdot 10^{-6}$—20 | Neutron fluence, kerma |
| Test spectrum | | 0,1—8 | Differential neutron flux density spectrum |

determination of the characteristics of thermal neutron fields by activation methods (effective flux density and temperature of thermal neutrons, the epithermal parameter, etc.);

recovery of fast neutron spectra by an express method based on activation measuring devices;

monitoring of characteristic fast neutron fields;

determination of the spectral coefficient by extrapolation methods.

Several additional standard techniques are now being developed including methods for recovery of epithermal neutron spectra using the cadmium-relation method for a resonant detector which was quite recently developed; recovery of neutron spectra over the entire energy range from thermal to 20 MeV using a program similar to SAND-II; certification of reference thermal neutron sources based on reactors with the aid of the AKN(t) set and their application to instrument calibration; direct precision measurements with the aid of direct-charge detectors.

Experimenters have proposed programs for processing the photopeaks of $\gamma$ radiation emitted by neutron activation detectors, for processing the results of measuring fast-neutron spectra with proportional counters, etc.

Studies are continued on precision measuring techniques for monoenergetic neutron fluxes in electrostatic accelerators based on hydrogen counters of target activation, and physical integration using manganese and vanadium. These studies are being carried out primarily in connection with measurements of nuclear physics constants and calibration of equipment designed for this purpose. A refined technique for calibrating the energy scale of electrostatic accelerators again p, n reaction thresholds has been proposed recently.

## Comparisons

This kind of metrological activity becomes increasingly popular. Following the 1st All-Union Conference on the Metrology of Neutron Radiation in Reactors and Accelerators, many Soviet organizations participated in seven comparisons, including one on an international scale (see Table 1). Their purpose has been to find promising measuring means and techniques, to detect unknown systematic errors, and to establish the most reliable magnitudes of the compared quantities and relationships. Experience indicates that the results of such comparisons can be sometimes profitably used for certification of reactors as reference sources.

## Determination of Errors and Design of Experiments

These are the fundamental problems of metrology.

The 1st All-Union Conference was followed by the development of general methods of processing the results of direct and indirect measurements. Recommendations have been proposed for the summations of random and systematic errors [5]. Standard methods have been suggested for establishing the character of various trends as applied to specific problems. Valid methods of establishing errors in nuclear data obtained by estimation have been established.

Apart from the solution of general theoretical problems, standard methods have been created for normalizing the accuracy properties of measuring means [6], for presenting the measured results [7], for error estimation, etc.

It must be stressed that in recent years experimenters have taken a more careful approach to the description of the accuracy of their results, in particular, of the results of combined measurements. Publications in which the error in neutron spectra recovery is stated to be less than 10-15% are now quite infrequent. Many authors carefully analyze the sources of systematic errors and state the confidence limits of their results.

### Terminology

The basic terminology of neutron radiation has been discussed for more than three years. Tens of organizations participated in these discussions. The discussion took place within the limits of the recently approved GOST [8]. Most difficulties have been associated with the English term "neutron fluence," neutr./cm$^2$. Eleven Russian versions of this term used in Soviet literature have been mentioned: neutron flux, total neutron flux, effective neutron flux, integral neutron flux, neutron flux integral in time, integral neutron flux density, neutron flux density integrated over time, time integral of neutron flux density, neutron exposure, neutron transport, and neutron fluence. The original form "neutron fluence" has been preserved in the GOST.

## CONCLUSIONS

Certain conclusions can be drawn from a generalization of the materials of the 2nd All-Union Conference on Metrology of Nuclear Radiation in Reactors and Accelerators.

1. For the first time in the USSR, the foundations have been established for a State system of metrological principles for neutron measurements (direct, indirect, and composite) in nuclear physics facilities. An experimental basis of this system is provided by the Special State Standard of neutron flux density, standard neutron activation and fissionable material samples, and reference neutron sources (fields) based on reactors and accelerators. The production of the first sets of standard samples has been started, and the first reference sources using static and pulsed reactors have been created.

2. Great activity is observed in studies of nuclear constants, especially of their compilation and evaluation.

3. A trend can be noted towards the standardization of neutron measuring techniques in nuclear physics facilities, of the certification of reference sources based on reactors and accelerators, and of the calibration of measuring equipment with the aid of these sources.

4. Special progress has been made in the comparison of the results of neutron measurements in nuclear reactors. This kind of metrological activity should be further developed as a method of selecting the most promising and advanced measuring means and techniques and of improving the reliability of results. The method should be extended to accelerators and, in particular, to neutron generators.

5. There are certain advances in the establishment of unified methods for error estimation, especially in the case of systematic errors.

## LITERATURE CITED

1. Metrology of Neutron Radiation in Reactors and Accelerators, Proceedings of the 1st Conference [in Russian], Vol. 1 and 2, Izd. Standartov, Moscow (1972).
2. Metrology of Neutron Radiation in Reactors and Accelerators, Proceedings of the 2nd Conference [in Russian], Vol. 1 and 2, Izd. TsNIIatominform-VNIIFTRI, Moscow (1974).
3. GOST 8.105-74. "Special State standard and All-Union calibration scheme for neutron flux density measuring devices in nuclear physics facilities" [in Russian], Izd. Standartov, Moscow (1974).
4. T. F. Wimett, R. H. White, and R. G. Wagner, "Fast burst reactors," Proc. of National Topical Meetings on Fast Burst Reactors, University of New Mexico, Albuquerque, Jan. 28-30, 1969.
5. Zh. F. Kudryashova, S. G. Rabinovich, and K. A. Reznik, "Methods of processing the results of measurements," Proc. of Metrological Institutes of the USSR [in Russian], Vol. 134 (194), Izd. Standartov, Moscow–Leningrad (1972).
6. GOST 8.009-72, "Normalizing metrological characteristics of measuring means" [in Russian], Izd. Standartov, Moscow (1972).
7. GOST 8.011-72, "Indicators of the accuracy of measurement and representation of measured results" [in Russian], Izd. Standartov, Moscow (1972).
8. GOST 19.849-74, "Neutron radiation. Terminology and definitions" [in Russian], Izd. Standartov, Moscow (1974).

ABSTRACTS

# EXPERIMENTAL INVESTIGATION OF RESONANCE ABSORPTION OF NEUTRONS IN A URANIUM–GRAPHITE LATTICE

L. N. Yurova, A. V. Bushuev,
V. I. Naumov, V. M. Duvanov,
and V. N. Zubarev

UDC 539.125.5.162.3

The effective resonance absorption integral for $^{238}U$, $I_T^{28}$, in a uranium–graphite lattice, described in [1] was measured. The value $I_T^{28} = (10.3 \pm 0.3)$b was obtained. The dependences of $I_T^{28}$, $\rho_{28}$ and $\langle\sigma_c^{28}\rangle/\langle\sigma_f^{25}\rangle$ on the ratio of the volumes of graphite and uranium, $V_C/V_U = 38; 76; 152$ and on the thickness of the water space around the uranium rods for $V_C/V_U \approx 38$ were investigated. The measurements were made by means of an activation procedure with the utilization of a Ge(Li) – spectrometer for recording $\gamma$-radiation from $^{239}Np$ with an energy of 277 keV and the fission product $^{143}Ce$ with an energy of 293 keV. The results of the measurements are presented in Tables 1 and 2. For convenience, the values of the parameters are normalized to the corresponding values in a "dry" lattice for $V_C/V_U = 38$. Their analysis allow one to draw the following conclusions.

1. The observed dependence of $I_T^{28}$ on the ratio $V_C/V_U$ agrees well with the theoretical data and is explained by the departure of the spectrum of epicadmium neutrons incident on a uranium rod from a $1/E$ distribution.

2. The introduction of a water space around the uranium rods with a thickness up to 6 mm does not affect the quantity $I_T^{28}$.

3. The values of the quantities $\langle\sigma_c^{28}\rangle/\langle\sigma_f^{25}\rangle$ and $\rho_{28}$ are not reduced with an increase in the ratio $V_C/V_U$ in the lattice and the thickness of the water space around the uranium rods, which is explained by moderation of the neutron spectrum.

4. With an increase in the thickness of the water space around the uranium rods, the ratio $\langle\sigma_c^{28}\rangle/\langle\sigma_f^{25}\rangle$ and the parameter $\rho_{28}$ are reduced most rapidly for small space thicknesses.

TABLE 1. Dependences of $I_T^{28}$, $\rho_{28}$ and $\langle\sigma_c^{28}\rangle/\langle\sigma_f^{25}\rangle$ on the Ratio $V_C/V_U$ in the Lattice

| $V_C/V_U$ | $I_T^{28}$ | | $\rho^{28}$ | $\langle\sigma_c^{28}\rangle/\langle\sigma_f^{25}\rangle$ |
|---|---|---|---|---|
| | experiment | theory | | |
| 38 | 1 | 1 | 1 | 1 |
| 76 | 1,12±0,01 | 1,10 | 0,56±0,02 | 0,808±0,010 |
| 152 | 1,31±0,02 | 1,29 | 0,37±0,02 | 0,736±0,007 |

TABLE 2. Effect of the Thickness of the Water Space about the Uranium Units on the Quantities $I_T^{28}$, $\rho_{28}$ and $\langle\sigma_c^{28}\rangle/\langle\sigma_f^{25}\rangle$ for $V_C/V_U = 38$

| Space, mm | $I_T^{28}$ | $\rho^{28}$ | $\langle\sigma_c^{28}\rangle/\langle\sigma_f^{25}\rangle$ |
|---|---|---|---|
| 0 | 1 | 1 | 0 |
| 2 | 1,00±0,02 | 0,886±0,017 | 0,928±0,005 |
| 4 | 0,97±0,03 | 0,841±0,027 | 0,921±0,008 |
| 6 | 0,98±0,02 | 0,763±0,023 | 0,887±0,009 |

Translated from Atomnaya Énergiya, Vol. 38, No. 4, pp. 245–248, April, 1975.

LITERATURE CITED

1. T. V. Golashvili, At. Énerg., 13, No. 5, 435 (1962).

# THE HYDRODYNAMICS OF FISSIONABLE MATERIALS

## II. NONLINEAR SOLUTIONS OF THE SIMPLE WAVE TYPE

V. M. Novikov

UDC 621.039.51

In a previous paper [1], the author showed that for sufficiently high neutron fluxes the dispersion of the acoustical oscillations in fissionable materials can be changed substantially. This is manifested by a change in the effective velocity of sound and the occurrence of acoustical instability, resulting in a pronounced increase in the amplitude of the oscillations. Consideration of the subsequent evolution of such a wave results in a nonlinear problem. In this paper, the nonlinear solution of the simple wave type (Riemannian solution) is generalized for the case of the hydrodynamics of fissionable materials in constant neutron fluxes. The solution is constructed on the assumption that the dissipation of the heat from the fission is completely determined by the thermodynamic quantities themselves and not by their derivatives. This assumption is fulfilled well for a gas occupying a sufficiently long duct with heat removal through the lateral surface.

Analyzing the solutions obtained, one can make the following conclusion regarding the difference of the nonlinear solutions of the simple wave type in the hydrodynamics of an ideal liquid (gas) and in a fissionable liquid (gas).

The simple wave adjusts to propagate in only one direction and a wave trail disturbance arises behind it, moving in the opposite direction. With heat removal occurring according to Newton's law or by means of radiant thermal conduction from an optically thick layer, the density of matter increases (decreases) in the vicinity of the wave if the initial density is greater (lesser) than the equilibrium value. For an initial disturbance of the "hump" type, the density of matter in the vicinity of the trail is lower than the equilibrium value. Near the characteristic curve $x = -c_0 t$ (Fig. 1), one can distinguish an "echo" region of the wave, where the density is almost constant and different from equilibrium. In the vicinity of the wave, the $C_+$-characteristic curves adjust to be straight lines, which results in a faster transition of the simple wave into a shock wave. For initial disturbances of density $\Delta\rho/\rho_0 \approx 10^{-2}$ and wave extent $\Lambda \approx 10$ cm, the time of this transition can be shortened by ten-fold for neutron fluxes $N \approx 10^{16}$ cm$^{-2}\cdot$sec$^{-1}$. The diagram shown in the figure illustrates the evolution of an initial disturbance of the "hump" type in a fissionable gas up to the formation of a dislocation.

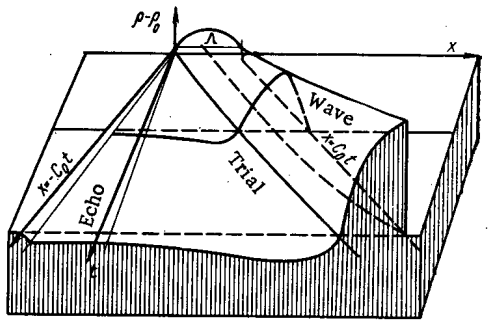


Fig. 1. Evolution of the initial disturbance of the "hump" type in a vissionable gas.

LITERATURE CITED

1. V. M. Novikov, At. Énerg., 30, No. 4, 446 (1971); Preprint IAÉ-2007 (1970).

Original article submitted May 20, 1974.

# ELECTRON SPECTRA BEHIND BARRIERS HAVING A THICKNESS COMPARABLE TO THE EXTRAPOLATED RANGE OF THE ELECTRONS

V. V. Evstigneev and V. I. Boiko

UDC 539.121.72

The article reports on investigations of the energies in a beam of electrons which passed through aluminum, copper or lead barriers having a thickness of $(0.1-0.9)R_e$, where $R_e$ denotes the extrapolated range of the electrons. The initial energies amounted to 3-8 MeV.

An ironless magnetic spectrometer with a homogeneous magnetic field was used as the analyzer of the electron energy.

The basic characteristics of the spectra (most probable energy losses $\Delta E_p$, the average energy loss, and the half-width of the energy distributions) are listed in a table (see full text of the article). The results were compared with the characteristics of spectra measured behind barriers having a thickness of up to $0.6R_e$; the spectra had been previously obtained by van Camp [1], Lonergan [2], and Gusev [3]. A selective comparative calculation in the model of catastrophic collisions was made for several spectra with the aid of the Monte-Carlo method using the program described in [4].

The dependencies of the basic spectral characteristics upon the initial energy, the atomic number, and the thickness of the absorber were analyzed for great depths of penetration. It was shown that the most probable energy losses are not sharp in these distributions and that the nonlinearity of the thickness dependence of the characteristics is rather strong. The average energy loss exceeds the most likely energy losses, but the difference decreases in proportion to the increase in barrier thickness. At sample thicknesses of $(0.8-0.9)R_e$, the spectra are smeared so that the half-width of the spectral distributions cannot be considered an objective parameter of fluctuations of energy losses.

A detailed investigation of the experimental energy distributions behind thick ($(0.6-0.9)R_e$) absorbers led to the detection of a maximum in the low-energy parts of the energy distributions, with the maximum resulting from the accumulation of electrons with energies of about 1 MeV. The accumulation of electrons is more intense when the initial energy of the electrons and the atomic number of the absorber are increased. The accumulation reaches its maximum at thicknesses of $(0.7-0.8)R_e$. The additional maximum which was recorded coincides to some extent with the experimental results of Bumiller et al., [5] and with the calculations of Baranov et al., [6]. The maximum at low energies in the electron spectra observed behind barriers results from multiple processes and the strong dependence of the total energy losses of electrons upon their initial energy.

## LITERATURE CITED

1. K. I. van Camp and V. I. Vanhuyse, Z. Physik, 211, 152-164 (1968).
2. I. A. Lonergan, C. P. Jupiter, and G. Merkel, J. Appl. Phys., 41, 2 (1970).
3. E. A. Gusev and B. A. Kononov, Izv. Vuzov, Ser. Fizika, 6, 12-16 (1969).
4. A. V. Plyasheshnikov et al., in: Monte-Carlo Methods in Computational Mathematics and Mathematical Physics [in Russian], Izd-vo Vychislitel'nogo Tsentra SOAN, Novosibirsk (1974), p. 285.
5. F. A. Bumiller, E. R. Buskirk, and I. M. Dyer, Z. Physik, 224, 182-192 (1970).
6. V. F. Baranov et al., Atomnaya Énergiya, 32, No. 2, 156 (1972).

Original article submitted July 1, 1974.

# TRANSPORT EQUATION FOR GAMMA RADIATION IN THE SMALL-ANGLE SCATTERING APPROXIMATION

L. D. Pleshakov

UDC 539.171.015

The propagation of gamma radiation in matter is described by the Boltzmann kinetic equation, whose solutions are generally obtained by numerical methods. In the development of apparatus which uses gamma radiation, shielding design problems occur for which it is desirable to have an analytic solution, thus eliminating the need for an electronic computer to do the calculation. An analytic solution of the kinetic equation has been given [1, 2] for the case of plane-parallel geometry, using the approximation of "direct forward scattering." In this case, however, the distribution function of the gamma photons gives a satisfactory description of their propagation for source energies of at least 5-6 MeV.

In this communication, we solve the kinetic equation in the small-angle scattering approximation in the the case of plane-parallel geometry. For this case the equation contains an additional term which is neglected in the "direct forward scattering" approximation. The spatial, energy, and angular distribution functions of the gamma photons give a satisfactory description of their propagation for the case of both light and heavy elements for source energies of at least 1 MeV.

The function describing the propagation of those photons which have traveled more than four mean free path lengths must be calculated by an electronic computer because of the large increase in the amount of calculation.

The distribution function is obtained under the assumption that the attenuation coefficient can be approximated by linear and quadratic functions. When the attenuation coefficient is approximated by a linear function, the distribution function for the flux of energy density has the form

$$I(x, \lambda-\lambda_0)=\frac{\lambda_0^2}{\lambda}e^{-\mu_0 x}\left\{\delta(\lambda-\lambda_0)+\left[b\frac{1-e^{-(\mu_0+\mu_1)(\lambda-\lambda_0)x}}{(\mu_0+\mu_1)(\lambda-\lambda_0)}\right]+\frac{(bx)^2}{2!}(\lambda-\lambda_0)\left[1-\frac{x(\lambda-\lambda_0)}{3}\left(\frac{3}{2}\mu_0+\frac{3}{2}\mu_1\right)+\frac{x^2(\lambda-\lambda_0)^2}{4\cdot3}\right.\right.$$

$$\left.\left.\times\left(\frac{13}{6}\mu_0^2+\frac{11}{3}\mu_0\mu_1+\mu_1^2\frac{11}{6}\right)-\ldots\right]+\frac{(bx)^3}{3!}(\lambda-\lambda_0)^2\left[1-\frac{x(\lambda-\lambda_0)}{4}(\mu_0+\mu_1)+\frac{x^2(\lambda-\lambda_0)^2}{5\cdot4}\left(\frac{15}{8}\mu_0^2+\frac{35}{12}\mu_0\mu_1+\frac{35}{24}\mu_1^2\right)-\ldots\right]+\ldots,$$

where $b = 2\pi n_0 r_0^2$, $n_0$ is the electronic density of the matter, and $r_0$ is the classical radius of the electron. The terms within the square brackets give the contribution of individual scatterings to the distribution function.

The present study shows that within the small-angle scattering approximation, the distribution function of the density of energy flux from a point isotropic source is accurately described to within a factor $1/4\pi r^2$ by the same expression as the distribution function of the density of energy flux for a plane perpendicular source.

These results have been compared with the experimental data and also with the results obtained by the method of moments.

## LITERATURE CITED

1. V. I. Ognevitskii, Zh. Éksperim. i Teor. Fiz., 29, 454 (1955).
2. L. I. Foldy, Phys. Rev., 82, 927 (1951).

Original article submitted August 14, 1974.

# SPATIAL DISTRIBUTION OF SCATTERED ENERGY FROM A UNIDIRECTIONAL POINT SOURCE OF HIGH-ENERGY ELECTRONS IN AN INFINITE TISSUE-EQUIVALENT MEDIUM

A. K. Savinskii and O. N. Chernova

UDC 539.12.08:539.124

Both theoretical and experimental data pertaining to the geometry of the source under consideration are virtually nonexistent in the literature. An exception is the paper [1], in which the authors, solving the

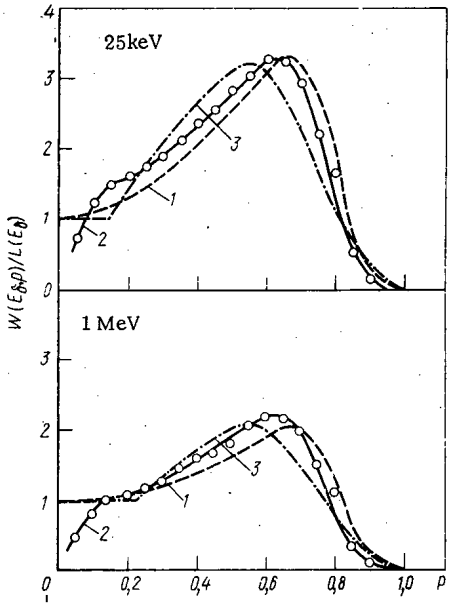


Fig. 1. Spatial distribution of scattered energy from an isotropic, point source of electrons with energies of 25 keV and 1 MeV in a tissue-equivalent medium: 1) results of the calculations of Narkevich and collaborators [1]; 2) results of the calculations of Spenser [2]; 3) experimental results of Bochkarev and collaborators [3].

kinetic equation for electrons in the continuous deceleration approximation, obtained a series of spatial distributions of the scattering energy, $(dE/dv)(E_\delta p, \alpha)$, for a "narrow beam" of electrons in polystyrene over the range from 25 keV to 10 MeV. Here, dE/dv is the energy, scattered into a volume element dv by a "narrow beam" of electrons with energy $E_\delta$; p is the distance from the source to the volume element under consideration as a fraction of the mean free path of the electrons; $\alpha$ is the angle between the normal to the surface of the scatterer and the orientation of their source in the volume element under consideration.

It is difficult to estimate the accuracy of the results obtained at the present time in view of the absence of experiments with sources of this type. In connection with this, an independent method of calculating the distribution dE/dv was developed, based on the method of statistical sampling, having a number of advantages over the kinetic equation approach. In particular, the method allows one to investigate the fluctuation in the energy loss of the electrons and to obtain information on the energy and angular distributions of the electrons at an arbitrary point of the medium being studied.

The method was executed on an electronic computer for a uniform, infinite tissue-equivalent medium over a range of initial energies for the source electrons from 25 keV-1 MeV. It was shown that, for $p \gtrsim 0.2$, one can describe the distribution of the scattered energy with an accuracy not worse than 10-15% by a general (independent of the energy of the source electrons) function $n(p, \alpha)$, which one can represent as a dosage function of a unidirectional, point source of electrons with unit initial energy and mean free path.

In order to estimate the accuracy of the results obtained, an indirect comparison of them was made with the theoretical and experimental data on a source with a different geometry, i.e., for an isotropic point source of monoenergetic electrons $W(E_\delta, p)$; here

$$W(E_\delta, p)/L(E_\delta) = \frac{2\pi E_\delta}{L(E_\delta)\cdot R_\delta^2} p^2 \int_0^\pi n(p, \alpha) \sin\alpha \, d\alpha, \qquad (1)$$

where $E_\delta$ is the initial energy of the source electrons; $R_\delta$ is the mean free path of the electrons with energy $E_\delta$; $W(E_\delta, p)$ is the energy scattered into a spherical layer of unit thickness at a distance p from the source; $L(E_\delta)$ is the mean energy loss per unit length of the path of the electrons in the medium being studied.

In Fig. 1, the values of $W(E_\delta, p)$ from the present work are compared with the calculations in [1] (curve 2) and [2] (curve 1) obtained in the continuous deceleration approximation (kinetic equation method) and with the experimental data in [3] (curve 3).

From the figure, it is seen that the results of the calculations agree satisfactorily with the "experimental" data in [3]. One can consider this as a verification of the calculational algorithms obtained and of the accuracy of the analysis of the experimental data, on the basis of which the values of $W(E_\delta, p)$ are also calculated. The disagreements with the theoretical data in [1, 2] are caused mainly by the approximation,

which does not take into account the effect of a fluctuation in the ionization loss in energy by the electrons during their deceleration in matter.

## LITERATURE CITED

1. B. Ya. Narkevich, V. S. Endovtskii, and I. E. Konstantinov, At. Énerg., 26, No. 5, 473 (1969).
2. L. Spenser, NBS, Washington, GPO (1959).
3. V. V. Bochkarev et al., Int. J. Applied Radiation and Isotopes, 23, 493 (1972).

Original article submitted September 9, 1974.

## LETTERS TO THE EDITOR

# THE DISCHARGE OF GASEOUS FISSION PRODUCTS FROM FUEL ELEMENTS OF NONHERMETIC CONSTRUCTION

V. M. Gryazev, V. V. Konyashov,
V. N. Polyakov, and Yu. V. Chechetkin

UDC 621.039.548

The utilization of fuel elements with discharge of gaseous fission products from under the jacket enables one to reduce the volume of the gas cavity, which results in the saving of neutrons in the active zone, an increase in the specific heat release, and the improvement of the hydraulic characteristics of the active zone. Moreover, the discharge of gases from fuel elements and the reduction of pressure in them ought to prolong the period of nondefective operation and, consequently, to reduce contamination of the loop by radioactive fission products.

In order to investigate the efficiency of such fuel elements and to determine the fractional discharge of gaseous fission products (GFP) in a BOR-60 reactor, tests were conducted on two assemblies of 37 fuel elements with special, nonhermetic subassemblies. The conditions for the irradiation of the fuel elements were similar to the usual ones.

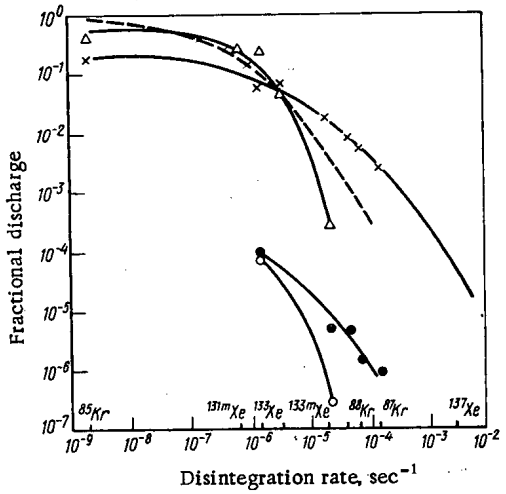


Fig. 1. Fractional discharge of GFP's from nonhermetic and defective fuel elements: O and ● refer to the stationary level and maximum emission of gases, respectively, for an assembly of fuel elements of nonhermetic construction; x refers to a defective fuel element; - - - -) refers to the theoretical values for an assembly of fuel elements of nonhermetic construction [1]; Δ refers to a fuel element with a subassembly of the "bell jar" type [2].

The radioactivity of the GFPs in the gas cavities of the assembly was measured daily in gas spectrometric loops equipped with NaI(Tl) crystal detectors. The mean error in the relative measurements was ~10%, while the mean error in the absolute measurements of the radioactivity was ~25%.

The level of radioactivity of $^{133}$Xe and $^{135}$Xe in the gas cavity of a reactor prior to the installation of an assembly of fuel elements with nonhermetic subassemblies was $4 \cdot 10^{-6}$ and $2.7 \cdot 10^{-6}$ Ci/liter, respectively. A rapid increase in the specific activities of $^{133}$Xe and $^{135}$Xe in the gas cavities was observed with attainment of ~0.8-1.1% burn-up in the assembly being studied. Subsequently, with an increase in the burn-up to 3.7%, the radioactivity of the GFPs was again increased 2-4 times and reached $(1\text{-}2) \cdot 10^{-3}$ and $(1\text{-}10) \cdot 10^{5}$ Ci/liter for $^{133}$Xe and $^{135}$Xe, respectively. The level of radioactivity of short-lived GFPs ($^{85}$Kr, $^{88}$Kr, $^{87}$Kr) did not increase in comparison with that observed in the case of a completely hermetic active zone.

Changes in the radioactivity of the GFPs are characterized by the presence of stationary levels of $(0.8\text{-}1) \cdot 10^{-3}$ and $(0.8\text{-}2) \cdot 10^{-5}$ for $^{133}$Xe and $^{135}$Xe with emissions. The ratio of the specific activities of the isotopes $^{133}$Xe and $^{135}$Xe varies from 50-80 at the stationary level up to 10 at the time of emission.

Translated from Atomnaya Énergiya, Vol. 38, No. 4, pp. 249-250, April, 1975. Original article submitted July 1, 1974.

As subsequent measurements showed, the variation in the radioactivity is connected with the behavior of an assembly of fuel elements of nonhermetic construction, and not with defects in the regular fuel elements. As regards this, the small amount of radioactivity, for a single emission (< 3 Ci for $^{133}Xe$, and 40 Ci for a defective fuel element) indicates a significantly higher emission of $^{133}Xe$ than $^{135}Xe$ (the mean ratio is 5, while for a defective fuel element, it is 3) and a low level of radioactivity in the stationary region.

Utilizing the experimental results, we calculated the fractional discharge of GFPs from assemblies of fuel elements of nonhermetic construction during the stationary period and during emissions (Fig. 1). These fractional discharges are significantly lower than those determined experimentally for defective fuel elements and also lower than the theoretical [1] and experimental values for nonhermetic fuel elements with a subassembly of the "bell jar" type [2].

Comparing the level of radioactivity in the gas cavity of a reactor during operation of an installation with nonhermetic and defective fuel elements, one can conclude that a significantly large fractional discharge of GFPs from fuel elements of nonhermetic construction is permissible. With safe containment of the stable fission products and taking into account that the fractional discharge of $^{137}Xe$ is $\sim 10^{-5}$ even from defective fuel elements, one can reduce the retention time of the GFPs under the jacket.

Furthermore, during operation of the reactor with two assemblies of nonhermetic construction (5-8% burn-up) and defective fuel elements, the stationary level of radioactivity for $^{133}Xe$ was $\sim 1 \cdot 10^{-2}$ Ci/liter or $\sim 20$ Ci in the gas cavities. If one assumes that this radioactivity is caused only by fuel elements of nonhermetic construction, then the most expected amount of radioactivity with complete loading of a BOR-60 with these assemblies was ~2000 Ci. Such levels of radioactivity actually occurred in the BOR-60 and did not cause complications during operation.

The discharge of stable fission products from fuel elements of nonhermetic construction can be safely estimated from measurements of the radioactivity in the loop only for a fuel burn-up in them of 2.7%. The specific activity of $^{137}Cs$, $^{131}I$, and $^{95}Nb$ in sodium was less than $1 \cdot 10^{-7}$, $4 \cdot 10^{-7}$, and $2 \cdot 10^{-6}$ Ci/kg of sodium, respectively. Calculations indicate that during this period the discharge of stable fission from fuel elements of nonhermetic construction did not exceed $10^{-5}$. With the maintenance of this discharge in the case of high burn-ups, the level of radioactivity of the sodium coolant in a BOR reactor completely loaded with nonhermetic fuel elements will be significantly lower than normally.

Thus, the loading of the active zone of a BOR-60 reactor with assemblies of nonhermetic construction does not result in an intolerable increase in the level of radioactivity in the sodium coolant and gas cavities. When stable fission products are retained under the jacket, a reduction in the detention time of the GFPs and an increase in their fractional discharge from fuel elements of nonhermetic construction is permissible.

## LITERATURE CITED

1. A. I. Leipunskii et al., Preprint FÉI-187, Obninsk (1969).
2. G. Keilholtz and G. Battle, Nucl. Safety, 9, No. 6, 494 (1968).

# QUANTITATIVE ESTIMATE OF THE EFFECT OF CHLORIDE CONCENTRATION ON THE STABILITY OF AUSTENITIC STAINLESS STEELS UNDER THE OPERATING CONDITIONS OF A BOILING REACTOR

V. V. Gerasimov and G. V. Andreeva

UDC 621.039.53

In the boiling reactors of seacoast atomic power stations, owing to the presence of oxygen and chlorides in the medium, there may arise conditions which facilitate the development of corrosion in austenitic stainless steels under stress. Dangerous $Cl^-$ concentrations can be evaluated quantitatively on the basis of present-day ideas about the mechanism of corrosion under stress and of the electrochemical reactions leading to the breakdown of the passive state.

The value of the stationary potential of the steel is given by the concentration of oxygen in the reactor water. Therefore, in accordance with [1], the time elapsed before the development of corrosion under stress ($\log\tau$) will be related to the equilibrium potential of the reaction which causes the breakdown of the passive state of the steel in solutions of chlorides ($\varphi_{br}$ = steel breakdown potential, the potential at which the steel comes out of the passive state) by the following relation:

$$\lg\tau = K + \frac{\beta_n F}{RT}\varphi_{br} \quad (1)$$

In this reaction the $Cl^-$ interacts with the passivating layer which was formed on the austenitic stainless steel as a result of its chromium content.

Hence it is necessary to determine the composition and thermodynamic characteristics of the passivating layer. The chromium passivation reaction takes place with the participation of water [2]. This fact and the fact that the passivation potential $\varphi_p$ depends on the pH value ($\Delta\varphi/\Delta$ pH) $=-0.118$) [3] make it possible to write the passivation reaction in the form

$$Cr + H_2O_{ads} = Cr^{+1}O^{-2} + 2H^+ + e. \quad (2)$$

Therefore

$$\varphi_p = \frac{Z_{Cr^{+1}O^{-2}}}{F} - \frac{Z_{H_2O_{ads}}}{F} - 0.118\,\text{pH} = 0.043 - 0.118\,\text{pH}, \quad (3)$$

where F is the Faraday number and the Z are thermodynamic potentials: $Z_{H_2O\,ads} = -42.4$ kcal/mole [4]; $Z_{Cr^{+1}O^{-2}} = Z_{Cr_2O_3}/6 = 41.4$ kcal/g-eq of metal [5].

The values of the passivation potential for chromium at pH = 0 and pH = 7 have been calculated by means of Eq. (3) and found to be 0.043 V and $-0.78$ V, respectively, which is in satisfactory agreement with the experimentally determined values of 0.05 V and $-0.7$ V [6, 7].

The reaction responsible for the breakdown of the passive state can be written in the form

$$Cr^{+1}O^{-2} + 3Cl' = CrCl_3 + 1/2O_2 + 4e, \quad (4)$$

and the potential of this reaction can be written as

$$\varphi_{br} = \varphi^0 + \frac{RT}{4_nF}\lg C_{O_2} - \frac{RT}{4_nF}3\lg C_{Cl'}. \quad (5)$$

Translated from Atomnaya Énergiya Vol. 38, No. 4, pp. 250-251, April, 1975. Original article submitted August 23, 1974.

It follows from the data given below that the values calculated from Eq. (5) and the values determined experimentally are in satisfactory agreement:

| | Calculated | Experimental |
|---|---|---|
| $\varphi_b^0$, nhe * | 0,16 | 0,25—0,35 |
| $\Delta\varphi_p/\Delta\lg C_{Cl^-}$ | —0,075 | —0,04 — —0,15 |
| $\Delta\varphi_p/\Delta C_{O_2}$ | 0,008 | 0,015 |

From Eqs. (1) and (5) we find:

$$\lg \tau = K' - 0.75 \lg C_{Cl^-}. \quad (6)$$

An experimentally determined relation [8] for water containing 8 mg/kg of oxygen at 260°C correlates satisfactorily with the theoretical relation:

$$\lg \tau_h = 2.6 - 0.9 \lg C_{Cl^-}. \quad (7)$$

For an oxygen concentration of 8-10 mg/kg the $Cl^-$ concentrations which are dangerous from the standpoint of the development of corrosion under stress are equal to 0.5 mg/kg [9]. For such a $Cl^-$ concentration, in accordance with (7), destruction of the austenitic stainless steel, under conditions of operation of a loop with multiple circulation in a boiling reactor, may take place after 1,000 h.

## LITERATURE CITED


1. V. V. Gerasimov, Dokl. AN SSSR, 212, No. 6 1404 (1973).
2. Ya. M. Kolotyrkin, Vestn. AN SSSR, No. 6, 46 (1973).
3. K. Fetter, Electrochemical Kinetics [in Russian], Khimiya, Moscow (1967), p. 800.
4. W. Latimer, Oxidation States of the Elements and Their Potentials in Aqueous Solutions [Russian translation], IL, Moscow (1954), p. 254.
5. I. P. Zhuk Corrosion and Protection of Metals (Calculations) [in Russian], Mashgiz, Moscow (1967), p. 259.
6. V. M. Knyazheva and Ya. M. Kolotyrkin, Dokl. AN SSSR, 114, No. 6, 1267 (1957).
7. Ya. M. Kolotyrkin and V. M. Knyazheva, Zh. Fiz. Khim., 30, No. 9, 1990 (1956).
8. R. Latanisen, in: Proc. National Association of Corrosion Engineers, Houston (1962), p. 304.
9. V. P. Pogodin, V. L. Bogoyavlenskii, and V. P. Sentyurev, Intercrystallitic Corrosion and Corrosion Cracking of Stainless Steels in Aqueous Media [in Russian], Atomizdat, Moscow (1970), p. 194.


*Standard electrode potential of the reaction, expressed in volts, with respect to a normal hydrogen electrode.

# SCALE EFFECT IN THE EXPLOSIVE DESTRUCTION OF WATER-FILLED VESSELS

V. I. Tsypkin, O. A. Kleshchevnikov, A. T. Shitov, V. N. Mineev, and A. G. Ivanov

UDC 620.178.7

This article describes the investigation of the destruction of two types of water-filled vessels (Fig. 1) when a charge of an explosive substance explodes inside the vessels. The diameters of geometrically similar vessels and the materials of their walls are indicated in Table 1. In vessels of Type I we used seamless tubing, while in vessels of Type II we used tubing with two welds, each along a generatrix. The thickness of the bases in the Type II vessels was selected on the basis of equal strength in the structure under the action of internal static pressure.

The explosive charge, a sphere of diameter d, was placed at the center of the vessel, and the explosion was initiated from the center. The explosive used was TG 50/50, a melt of TNT (50% by weight) with hexogen (50% by weight), with a density of 1.65 g/cm$^3$. Detonation of 1 g of this explosive produces 1,140 cal. The time required for the generation of full energy in the detonation of such charges is $\tau = d/2D$, where $D = 7.65 \cdot 10^5$ cm/sec is the detonation velocity of the TG 50/50. For the minimum-weight and maximum-weight charges (M = 8 g and 2,400 g) this time is 2.75 $\mu$sec and 18.4 $\mu$sec, respectively.

In the experiment, using the methods of high-speed motion-picture photography and tensometry and also using a coordinate grid on the external surface of each vessel, we recorded the deformation and

TABLE 1. Parameters of the Vessels and Results of the Experiments

| Type of vessel and material of the walls | Diameter of vessels, mm ($\phi$) | Number of experiment | Diameter of charge, mm | M, g | Relative weight of charge | Results of explosion | Type of destruction | Final deformation at central cross section of vessel, % | Initial separation velocity of walls of vessel at central cross section, m/sec |
|---|---|---|---|---|---|---|---|---|---|
| I, steel 20 | 104 | 1 | 21,0 | 8 | 0,006 | Not destroyed | — | 34 | 135 |
| | | 2 | 23,4 | 11 | 0,0083 | Destroyed | Three cracks along a generatrix, of lengths 2$\phi$, $\phi$, and 0.2$\phi$ | 34 | 170 |
| | 426 | 3 | 68,5 | 290 | 0,0032 | Not destroyed* | | 13 | 100 |
| | | 4 | 75,4 | 370 | 0,0041 | Destroyed | Four cracks along a generatrix, of lengths 2$\phi$, 1.5$\phi$, $\phi$, and 0.1$\phi$ | 15 | 110 |
| | 305 | 5 | 41,6 | 62 | 0,0036 | Incipient destruction | One crack along a generatrix, of length 0.1$\phi$, in the region of the weld | 18 | 90 |
| | | 6 | 47,0 | 90 | 0,0052 | Destroyed | One crack along a generatrix, of length 2$\phi$, in the region of the weld | 23 | 130 |
| II, steel 17H1S | 1220 | 7 | 130,6 | 1924 | ~0,0017 | Destroyed | Base ripped off | 7 | 68 |
| | | 8 | 140, | 2400 | 0,0022 | Destroyed | Based ripped off. One crack along a generatrix, of length 1.5$\phi$, in the region of the weld | 12 | 72 |

*One month later a similar charge of explosive completely destroyed the vessel.

Translated from Atomnaya Énergiya, Vol. 38, No. 4, pp. 251-252, April, 1975. Original article submitted July 15, 1974.

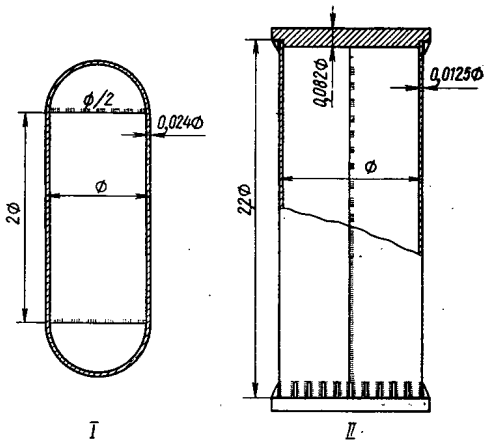


Fig. 1. Schemes of vessels.

destruction of the vessel during the explosion. The instantaneous velocity of separation of the walls of the vessels was fixed by means of a volumetric sensor. The appearance of a through crack in the material of the walls was taken as the criterion for destruction of the vessels. An analysis of the experimental results revealed (see Table 1) the following:

1. Destruction of water-filled vessels which are geometrically similar but are constructed on different scales takes place at different relative weights of explosive charge.* Thus, when the dimensions of the vessels were multiplied by 4 (a change from vessels with diameters of 104 mm and 305 mm to vessels with diameters of 426 mm and 1.220 mm), the relative weight of a destructive charge was found to be half the value for the smaller vessels.

2. The amount of plastic deformation in geometrically similar vessels before destruction takes place depends on the scale of the vessels. When the geometric dimensions of the vessel are multiplied by 4, the relative plastic deformation is reduced by a factor of 2.5.

It should be noted that identical states of stress in the walls of similar vessels are produced by the setting off of explosive charges of equal relative weights. This means that the destruction of vessels of different dimensions takes place at stresses which are substantially different, and this difference cannot be explained simply by a strengthening of the vessel material that results from the change in the rate of loading [1, 2].

The results of this study call into question a criterion used in selecting the maximum admissible weight of explosive charge whose explosion will not cause destruction of a water-filled container, namely, the criterion that the deformations under static loading and explosive loading of the water-filled containers should be equal [3].

The results obtained in this study agree with the results of investigations on the strength of steel vessels and tubes not filled with water when explosive charges are set off inside them [1, 2, 4, 5] and support the view that scale has an effect on the strength characteristics of the vessels. These results must be taken into consideration in the evaluation of accidents in chemical and nuclear reactors.

## LITERATURE CITED

1. A. G. Ivanov, V. A. Sinitsyn, and S. A. Novikov, Dokl. AN SSSR, 194, 316 (1970).
2. A. G. Ivanov, S. A. Novikov, and V. A. Sinitsyn, Fiz. Goreniya i Vzryva, No. 1, 124 (1972).
3. J. Proctor, Exptl. Mechanics, 10, p. 458 (1970).
4. A. G. Ivanov et al., Fiz. Goreniya i Vzryva, No. 1, 127 (1974).
5. A. G. Ivanov et al., ibid., No. 4, 603.

*The relative weight of explosive charge is the ratio of the weight of the explosive charge to the weight of a cylindrical segment of the vessel whose length is twice the vessel diameter.

# SETUP FOR TESTING AND THE CERTIFICATION OF CHEMICAL DOSIMETERS OPERATING ON THE PRINCIPLE OF ABSORBED PHOTON RADIATION DOSE OF $^{60}Co$ AND $^{137}Cs$

V. A. Berlyand, V. V. Generalova, and M. N. Gurskii

UDC 539.12.08

Since standards for the calibration and the periodic testing of chemical dosimeters are not available for the dose range of $10^4$-$10^8$ rad, it is hard to use these dosimeters and the validity of results obtained with these instruments is uncertain.

It is possible to measure the photon radiation dose rate absorbed by certain materials with an accuracy of 1% when the best calorimeters are employed [1]. However, when a transition is made from the dose absorbed by the calorimeter material to the dose absorbed by the material of a chemical dosimeter, the error increases. According to the All-Union scheme for measuring instruments for the absorbed dose rate of ionizing photon radiation, the transfer of the dose rate from a primary State standard which reproduces the unit dose rate absorbed by a reference material (graphite) to a tissue-equivalent material implies an increase in the systematic error to 2.5% and a total error in excess of ±3% [2, 3]. However, in the transition to the dose absorbed by the material of a chemical dosimeter, the error exceeds ±3.5%.

We developed a setup which can be used to calibrate certain chemical dosimeters with a substantially reduced error. The reference setup comprises the isotopic gamma sources MRKh-γ-100 and LMB-γ-1M; a calorimeter set with various absorbers resembling in their composition the most frequently used chemical dosimeters; and measuring and regulating instruments.

The MRKh-γ-100 and LMB-γ-1M units are self-shielding gamma sources in which an almost isotropic field of photon radiation is generated with $^{60}Co$ and $^{137}Cs$ sources which are situated in cylindrical radiation chambers [4] having a volume of 1000 and 300 $cm^3$, respectively.

The chemical dosimeters are calibrated by replacing the calorimeter which measures the dose absorbed under real conditions by a chemical detector. The error which is made in the calibration of the secondary detectors is the result of the errors of the calorimetric measurements and the error which is made in the transition from the dose absorbed by the calorimeter absorber to the dose absorbed by the dosimeter material.

In order to eliminate the errors which are associated with the conversion of the absorbed dose rate from one material to another and in order to bring into account differences in the attenuation of radiation in

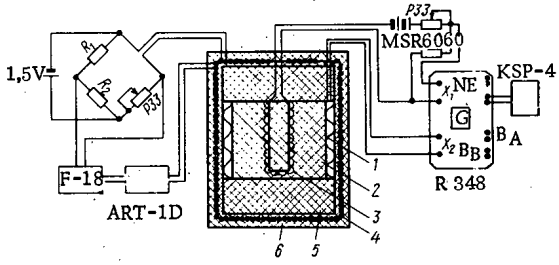


Fig. 1. Block scheme of the calorimeter setup: 1) copper–constantan thermocouple; 2) absorber; 3) manganin wire spiral; 4) thermostat housing; 5, 6) foam plastic.

Translated from Atomnaya Énergiya, Vol. 38, No. 4, pp. 253-254, April, 1975. Original article submitted May 23, 1974; revision submitted November 4, 1974.

TABLE 1. Error Components of the Calorimeter

| Source of error | Magnitude of error, % |
|---|---|
| Measurement of the mass | 0,01 |
| Presence of impurities | 0,3 |
| Measurement of current | 0,02 |
| Measurement of the resitance of the heating element | 0,02 |
| Influence of the heat-meter shell | 1,0 |
| Heat leakage not recorded | 1,3 |

both the calorimeter absorber and the chemical detector, the calorimeter absorber is made of the detector material and has the same form and the same dimensions as the detector.

Since the calorimeter absorber is rather large and since the thermal conductivity of the material of chemical dosimeters is low, an adiabatic or quasi-adiabatic method with a local transducer may lead to considerable errors. The errors originate from the dissimilar distributions of the thermal sources during the irradiation and during the electrical calibration of the calorimeter. Under these conditions one should employ heat flux calorimeters whose readings are independent of the spatial distribution of the heat sources in the absorber material of the calorimeter.

The heat flux calorimeters of the reference setup of absorbers with graphite, polystyrene, and water have the form of a cylinder with the dimensions 22 × 22 mm.

The fluid dosimeter system to be calibrated is inserted into a thin-wall (0.2 mm) polystyrene cylinder of the above dimensions (see Fig. 1).

In order to calibrate the calorimeter in units of absorbed dose, a heater spiral with a diameter of 0.05 mm and a resistance of 150-200 Ω is inserted inside the absorber. The current which flows through the heater element is determined through the voltage drop at an MSR-60 set of reference resistors (accuracy class 0.02) and with the aid of a R348 potentiometer (accuracy class 0.002). The heat flux which issues from the absorber during the irradiation is recorded with a heat-meter which is a set of differential copper–constantan thermocouples connected in series. A thermopile made of a constantan band with a cross section of 0.3× 0.003 mm (the copper was electrolytically applied to the constantan) is kept in good thermal (but not electrical) contact with the absorber of the calorimeter and the housing of the thermostat. A material with a low thermal resistivity (oxide layer and mica sheet with a thickness of 3-5 μ) is for this purpose used as the insulation. The emf of the thermopile is measured with the R348 potentiometer. In order to reduce the influence of temperature fluctuations in the ambient medium, the calorimeter is inserted in a thermostat (aluminum cylinder with a wall thickness of 1 mm, surrounded by a 10 mm thick layer of foam plastic). A copper resistance thermometer inserted in a bridge circuit is used as the measuring transducer in the thermostat. The resistors of the bridge are uniformly distributed over the entire surface of the thermostat housing. The thermostat temperature is kept constant with an accuracy of $10^{-3}$–$10^{-4}$°C by an ART-1D analog temperature regulator built with an F-18 photoamplifier [5].

The changes which the thermal fluctuations produce in the thermal emf of the calorimeter are recorded on the tape of a KSP-4 potentiometer recorder.

The calorimeter calibration, which was made both on a test stand and in irradiation setups, showed that the radiation does not influence the sensitivity of the calorimeter (20-30 mV/W) within the calibration error range (0.3%). The calorimeters can measure an absorbed dose rate of 20-30 mV/W radiation between 0.1 and 100 W/kg (10-10,000 rad/sec).

When the heat flux of the absorbed dose rate of γ radiation was measured with calorimeters in MRKh-γ-100 and LMB-γ-1M irradiation units (50 or 700 rad/sec), the total uncompensated systematic error did not exceed ±1.8% on the 0.95 confidence level; the random error, expressed as mean-square deviation of the result of measurements, did not exceed 0.5% on the 0.95 confidence level. The results of the calorimetric measurements were tested against a standard distribution.

Table 1 lists the values of the remaining systematic error components of the heat-flux calorimeters.

The total error of a measurement of the absorbed dose rate does not exceed ±2% on the 0.95 confidence level in the case of all the calorimeters.

The error in the calibration of the chemical dosimeters does not exceed ±2%. This value can be reduced when the influence of the heat-meter shell is taken into account and when the uncontrollable thermal leakage is reduced. (It is not correct to simply subtract the background of the shell from the total signal, because the irradiation conditions are different in an empty heat-meter shell and in a shell filled with an absorber).

Thus, based on the results of the metrological certification, the setup under consideration can be used as a standard in first-class measurements in which chemical reference dosimeters and normal chemical dosimeters are verified.

## LITERATURE CITED

1. N. S. Shimanskaya, Calorimetry of Ionizing Radiations [in Russian], Atomizdat, Moscow (1973).
2. All-Union State Standard 8.071-73, All-Union Testing Scheme for Measuring Instruments of the Absorbed Dose Rate of Ionizing Photon Radiation [in Radiation [in Russian].
3. All-Union State Standard 8.070-73, Primary State Standard of the Unit of Absorbed Dose Rate of Ionizing Photon Radiation.
4. D. A. Kaushanskii, The MRKh-γ-100 Gamma Source for Microbiological and Radiation-Chemical Investigations [in Russian], Atomizdat, Moscow (1969).
5. V. M. Malyshev, in: Sixth All-Union Conference on Calorimetry [in Russian], Metsnieraba, Tbilisi (1973) p. 549.

# $^{238}$Pu AND $^{239}$Pu CONCENTRATIONS IN THE AIR LAYER CLOSE TO GROUND OF THE PODMOSKOV'E REGION IN 1969-1971

K. P. Makhon'ko, Ts. I. Bobovnikova, A. A. Volokitin, and V. P. Martynenko

UDC 551.510.72

Daily samples of aerosols were collected on FPP-15-1.5 filter cloth with the aid of a filtering station having a throughput of 1900 $m^3/h$ on the ground for the purpose of determining the concentration of plutonium isotopes in the Podmoskov'e region. The samples of each month were combined and the filter cloth was burnt. The ashes were dissolved in a mixture of hydrofluoric acid and nitric acid; the plutonium was transferred into the tetravalent state and extracted with a 5% solution of tenoyltrifluoroacetone in benzene, Finally, the plutonium was deposited on a platinum disk having a diameter of 1 cm. In order to determine the plutonium losses during these operations, known amounts of $^{236}$Pu were initially introduced in the filter ashes and served as marks for the determination of the yield of the analysis.

The concentration of the plutonium isotopes in a sample was measured with an "Amur-1" alpha spectrometer equipped with silicon surface barrier detectors having an area of 1.25 $cm^2$ and a resolution of 160 keV. Measurements were made in the energy range 4-6 MeV. The background of the spectrometer did not exceed 0.02 pulses/hour in this range and the recording efficiency was about 30%.

Figure 1 depicts the results of the measurements of the $^{239}$Pu and $^{238}$Pu concentrations (dashed histogram). The points denote the ratio of the concentrations of these isotopes. It follows from the results that the average annual $^{239}$Pu concentration increased gradually ((5.5, 6.4, 7.0)$\cdot 10^{-17}$ Ci/$m^3$ in 1969, 1970, and 1971, respectively).

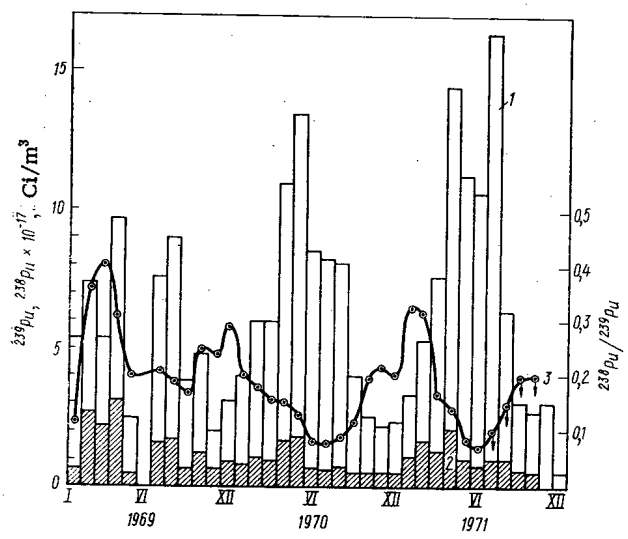


Fig. 1. Concentrations in the atmospheric layer near ground in the region of Podmoskov'e: 1) $^{239}$Pu; 2) $^{238}$Pu; 3) $^{238}$Pu/$^{239}$Pu ratio.

The greatest monthly average concentrations of $^{239}$Pu increased slightly since 1969 and reached in July 1971 values of $16\cdot 10^{-17}$ Ci/$m^3$, whereas in this time the greatest monthly average concentrations of $^{238}$Pu were observed in April 1969 on the level of $3\cdot 10^{-17}$ Ci/$m^3$, followed by a 30% decrease in the next two years. The maximum concentrations of $^{238}$Pu were each year observed in April or May; in the case of $^{239}$Pu, maxima were observed not only in those months but also in July or August, with the maxima being followed by a slight increase in the $^{238}$Pu concentrations. We note for comparison that, according to our results, the maximum concentrations of the global $^{137}$Cs were observed in July in the period 1969-1971. Since the increase in the isotope concentration in the spring-summer period results from the arrival of the isotopes from the stratospheric reservoir, we can conclude that the early April maximum of the plutonium isotope concentration is a consequence of a fallout of relatively coarse particles enriched by $^{238}$Pu from

Translated from Atomnaya Énergiya, Vol. 38, No. 4, pp. 254-255, April, 1975. Original article submitted August 13, 1974.

the atmosphere. Accordingly, the maximum enrichment of aerosol particles with $^{238}Pu$ is observed even earlier, namely in the winter months, as can be inferred from Figure 1. The $^{238}Pu/^{239}Pu$ ratio varied between 0.3-0.4 in winter and 0.07 in summer.

A comparison of the results which to some extent are characteristic of the Eastern part of the Northern hemisphere with the results of the American HASL net for the Western part of the Northern hemisphere* has shown that the level of contamination of the atmospheric layer near ground by plutonium isotopes is about the same in these parts of our planet. For example, the maximum $^{239}Pu$ concentration was observed in the Western part of the hemisphere in 1971, in May and June, with the concentration amounting to $13 \cdot 10^{-17}$ Ci/m$^3$. The annual variation of the isotope concentration is reproduced and even the details appear to some extent. The concentration ratio $^{238}Pu/^{239}Pu$ varied in the USA between 0.06 and 0.36, which is in good agreement with the values which we obtained. There is also agreement between the annual variations of this ratio.

*Fallout Program, Quart. Rep. HASL-257 (1972).

# EVALUATION OF SURFACE ATMOSPHERE CONTAMINATION BY DISCHARGES FROM NUCLEAR POWER STATIONS

V. P. Il'in

UDC 551.510.72

In selecting a site for a nuclear power station, estimates are made of the possible contamination of the surface layer of the atmosphere by radioactive materials discharged through the ventilation stack.

A study was made [1] of a number of methods for calculating atmospheric contamination and it was concluded that there was sufficiently good agreement of the calculated results for surface concentrations which the limits of accuracy specified by the authors.

According to the method of Pasquill and Mead [2], surface concentration ($Ci/m^3$) is given by

$$q=\left(\frac{2}{\pi}\right)^{1/2}\frac{FQ}{\sigma_z ux}\exp\left(-\frac{H^2}{2\sigma_z^2}\right), \tag{1}$$

where Q is the rate of discharge, Ci/sec; u is the wind velocity, m/sec; $\sigma_z$ is the vertical standard deviation, depending on distance and type of turbulence according to Pasquill [2], m; H is discharge height, m; x is the distance from the stack, m; F = 0.01 fn/2$\pi$ is the probability of a given wind direction; f is the frequency of the wind direction in a given sector of the wind rose, %; n is the number of sectors in the wind rose.

Analysis of Eq. (1) shows that the function

$$C(x, H)=\frac{qux}{QF}=\left(\frac{2}{\pi}\right)^{1/2}\frac{1}{\sigma_z}\exp\left(-\frac{H^2}{2\sigma_z^2}\right) \tag{2}$$

forms a series of maxima (Fig. 1) corresponding to the various types of turbulence for a given value of H. The heights of the maxima are the same and have approximately the value

$$C_{max}\approx 1/2H=\text{const}. \tag{3}$$

Considering the continuity of the distribution of atmospheric states over types of turbulence, Eq. (3) can be considered as an equation of an envelope for the family of functions C(x, H) for various atmospheric states.

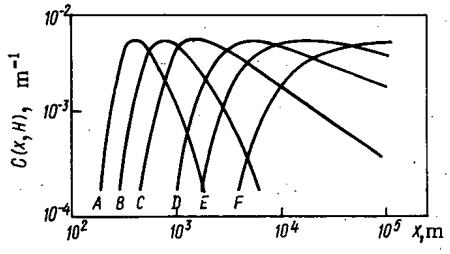


Fig. 1. The function C(x, H) for H = 100 m and various types of atmospheric turbulence according to Pasquill (A-F).

The expression

$$q\leqslant QF/2Hxu. \tag{4}$$

for estimating surface concentrations follows from Eqs. (2) and (3).

Similar consideration of the method of Leichtman and Berlyand, which is given in [3], with the coefficients depending on the state of the atmosphere needed for the calculations gave values of the function $C(x, H)_{max} = qux/QF$ which were 5-30% lower than those given by the Paquill–Mead method. This confirms the validity of Eq. (4), which is an upper limit of surface concentrations within the limits of accuracy and applicability of the methods discussed for parameter ranges $10 \leq H \leq 300$ m and $2H \leq x \leq 10^5$ m.

Translated from Atomnaya Énergiya, Vol. 38, No. 4, pp. 255-256, April, 1975. Original article submitted August 23, 1974.

It is necessary to point out that in Eq. (4), as in all similar equations, one should substitute the average value of $1/u$ for the appropriate wind direction. This quantity may be considerably different from $1/\bar{u}$.

Calculations based on Eqs. (4) and (1) and on data for the frequency of various types of atmospheric turbulence [2] showed that Eq. (4) overestimates surface concentration by factors of no more than 2-3 as a rule. This overestimate can be considered as an acceptable compensation for the inaccuracy of the basic methods (for example, not considering the increase in surface concentration with an inversion layer located above the stack [3]) and also for possible errors in predictions of the amount of discharge from a nuclear power station.

## LITERATURE CITED

1. N. E. Artemova, At. Énerg., 36, 32 (1974).
2. Meteorology and Atomic Energy [Russian translation], Gidrometeoizdat, Leningrad (1971).
3. Contamination of Surface Layer of the Atmosphere with Temperature Inversions [in Russian], Meditsina, Moscow (1969).

# SIMULATION OF ELECTRON BACK-SCATTERING BY A MONTE-CARLO METHOD

P. L. Gruzin and A. M. Rodin

UDC 539.12.172

Differential and integral characteristics were calculated by a Monte-Carlo method for back-scattering of electrons with an energy $E_0 = 200$ keV from semi-infinite aluminum and uranium targets for normal incidence and information was also obtained about the statistics of motion within the target for electrons emerging in the backward direction. The calculations were based on a "discrete energy loss" model which, in contrast to the "continuous loss" approximation [1, 2], makes it possible to include fluctuations in electron energy losses from the relations of Landau theory [3]. In addition, the use of this model provides an opportunity to reduce the consumption of machine time significantly.

According to the "discrete loss" model, the path of an electron in a scatterer is a broken line with segments $\Delta S_i$ at the vertices of which scattering at an angle $\omega_i$ occurs in accordance with the Mott–Rutherford screened elastic-scattering cross sections [4]. An electron moves linearly along a segment of the broken line, losing energy in discrete amounts after traversing a path element $\sum_i \Delta s_i \geq R_L$, where $R_L$ is the distance corresponding to the lower limit of applicability for Landau theory. The value of $R_L$ is defined by

$$R_L = B_L \frac{E_0}{a},$$

which is based on expressions for the most probable energy loss $\Delta E_p$ and the mean energy loss $\Delta E_m$ considering the inequality $I_z \leq \Delta E_p \leq E_0$, where $I_z$ is the average ionization potential of the target medium. In

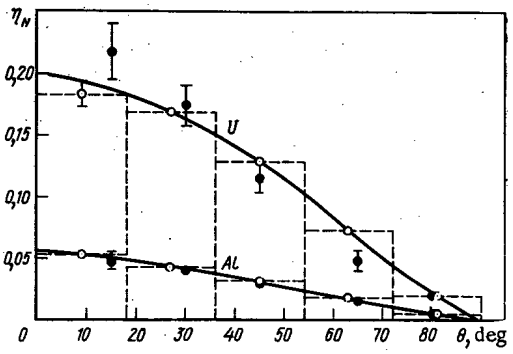


Fig. 1

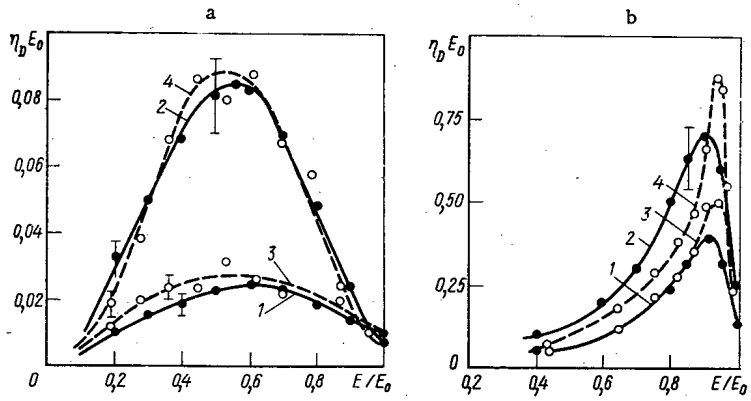


Fig. 2

Fig. 1. Dependence of numerical back-scattering coefficient $\eta_N$ on angle of deflection $\theta$: ○ and solid line) calculation; ●) experiment.

Fig. 2. Energy spectra of back-scattered electrons for aluminum (a) and uranium (b): ——) experiment; 1 and 2) $\theta$ = 65 and 15°; ----) calculation; 3 and 4) $\theta$ = 63 and 18°.

Translated from Atomnaya Énergiya, Vol. 38, No. 4, pp. 256-258, April, 1975. Original article submitted September 4, 1974.

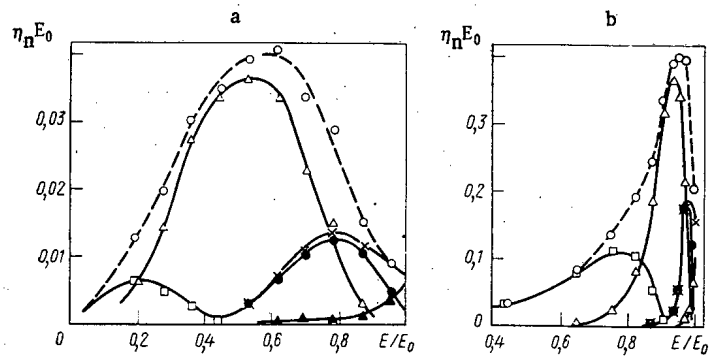


Fig. 3. Energy spectra of components for aluminum (a) and uranium (b). Scattering; ▲) single, $N^{\omega_t=15^\circ}_{col=1}$; ●) plural, $N^{\omega_t=15^\circ}_{col=2-4}$; ×) single + plural, $N^{\omega_t=15^\circ}_{col=1-4}$; Δ) multiple, $N^{\omega_t=15^\circ}_{col=5-20}$; □) diffusion, $N^{\omega_t=15^\circ}_{col>20}$; ○) spectrum of electrons emerging in the backward hemisphere ($\Omega = 2\pi$).

TABLE 1. Contribution of Various Components to Flux of Back-scattered Electrons, %

| Constituent | Al | U | Component | Al | U |
|---|---|---|---|---|---|
| $N$ 15° | 0 | 0 | Single | 3 | 2 |
| $N$ 30° | 6 | 0,5 | Plural | 19 | 8 |
| $N$ 90° | 75 | 42 | Single + plural | 22 | 10 |
| 1 col 90° | 24 | 35 | | | |
| 2 col 90° | 1 | 12 | Multiple | 73 | 47 |
| 3 col 90° | 0,1 | 5 | Diffusion | 5 | 43 |
| > 3 col 90° | 0 | 6 | | | |

the expression given, $a = 0.153\, Z\rho/A\beta^2$ MeV/cm ($\rho$ is the density of the material, A is atomic weight, and $\beta = v/c$) and $B_L$ is a constant depending on the Z of the scatterer and $E_0$ which is $6.1 \cdot 10^{-4}$ for aluminum and $2.15 \cdot 10^{-3}$ for uranium. If an electron emerges from the scatterer in the backward hemisphere having traversed a path $\sum_i \Delta s_i < R_L$ after the usual choice of losses, the energy loss in this element is calculated from the Bethe–Bloch formula for mean loss. The calculations were performed on a BÉSM-6 computer. The machine time used for a single history of an emerging electron was ~1 and ~6.5 sec for uranium and aluminum respectively; the total number of randomly selected trajectories for reflected electrons in each scatterer was over 3000.

The values calculated for the numerical integral back-scattering coefficients for uranium and aluminum (0.55 and 0.14) are in good agreement with experiment [5, 6]. Calculated and experimental curves for the dependence of the numerical differential back-scattering coefficient $\eta_N$ on $\theta$ and spectra of reflected electrons for certain values of $\theta$, where $\theta$ is the angle measured from the normal to the target, are shown in Figs. 1 and 2. As is clear from these figures, the measured and calculated values for aluminum are practically the same. For uranium, some discrepancy apparently resulted from the neglect of bremsstrahlung losses and the use of a value for $B_L$ that was somewhat too low.

Analysis of randomly selected trajectories shows (Table 1) that in the flux reflected from aluminum and uranium there are no electrons for which the angles of deflection $\omega_i$ do not exceed 15° over their entire history (N 15°). For aluminum and uranium the major portion of the reflected flux is made up of electrons which emerge in the backward direction as the result of successive elastic collisions at angles not exceeding 90° (N 90°). At the same time, we find a markedly higher contribution in uranium than in aluminum for constituents which are formed by electrons which undergo scattering at an angle $\omega_i \geq 90°$ one (1 col 90°), two (2 col 90°), three (3 col 90°), and more (> 3 col 90°) times. It is assumed that the single-scattering component ($N^{\omega_t}_{col=1}$) is made up of electrons which during motion in the target are deflected once at an angle $\omega_i$ greater than some threshold angle $\omega_t$. Correspondingly, the plural component ($N^{\omega_t}_{col=2-4}$) consists of electrons which have undergone 2-4 scattering events, the multiple-scattering component ($N^{\omega_t}_{col=5-20}$) of electrons which have undergone 5-20 events, and the diffusion component ($N^{\omega_t}_{col>20}$) of electrons which have undergone more than twenty collisions at angles greater than $\omega_t$. The choice of $\omega_t$ was made in the following manner. It is known that the diffusion component must consist of electrons emerging from a depth $d > d_d$ ($d_d$ is the diffusion depth). According to the results of calculations, a distribution which remains unchanged as d is increased is established at some depth $d_0$ in both scatterers. It has the characteristic

features of diffusion, namely: at a depth of $d > d_0$, the angular distribution of electrons penetrating into the interior of the target obeys the relation $\sim\cos^2\alpha$ ($\alpha = \pi - \theta$) and the corresponding maximum values of the mean scattering angle $\theta$ are 30° and 28° for uranium and aluminum respectively (according to [7], $\theta \approx 33°$). The fraction of electrons emerging from depths greater than $d_0$ was determined from curves obtained for the dependence of electron back-scattering intensity on scatterer thickness. This quantity agreed with $N_{col>20}^{\omega_t=15°}$ within 10%, i.e., $\omega_t = 15°$. As is clear from Table 1, multiple scattering (~47%) and diffusion (~43%) play the main role in the reflection of electrons from uranium for normal incidence of a beam with an energy $E_0 = 200$ keV. For aluminum, the diffusion component is rather small (~5%) and the multiple-scattering component (~73%) provides the main contribution to the reflected flux. The contribution from the single-scattering component is small both for uranium (~2%) and aluminum (~3%). The integral spectrum ($\Omega = 2\pi$) for aluminum and uranium and the corresponding curves for the energy distributions of the components are shown in Fig. 3.

In conclusion, the authors thank A. N. Novikov for valuable discussions, and V. G. Varlamov and P. L. Nevskii for help with programming.

## LITERATURE CITED

1. A. A. Ostroukhov, Fiz. Tverd. Tela, 9, 1744 (1967).
2. I. McDonald, A. Lamki, and C. Delaney, J. Phys. D. Appl. Phys., 4, 1210 (1971).
3. L. Landau, J. Phys. USSR., 8, 291 (1944).
4. G. Moliere, Z. Naturforsch., 2a, 133 (1947).
5. P. L. Gruzin, Yu. V. Petrikhin, and A. M. Rodin, At. Énerg., 33, 779 (1972).
6. T. Tabata, R. Ito, and S. Okabe, Nucl. Instrum. and Methods, 94, 509 (1971).
K. Siegbahn (editor), Alpha, Beta, and Gamma Spectroscopy [Russian translation], No. 1, Atomizdat, Moscow (1969).

# GROUPING OF NEUTRON WIDTHS OF $^{232}$Th p LEVELS

P. E. Vorotnikov

UDC 539.171.4

Recent improvements in mathematical and experimental methods made possible a detailed study of fission cross sections $\sigma_f$ of the heavy elements which are needed for various precise calculations. One of the immediate results was the discovery of a "fine structure" in the fission cross section $\sigma_f$, consisting of a group of resonances with fission halfwidths $\Gamma_f$ much above average [1, 2]. Contemporary theory explains these structures by assuming that the fissionable nucleus has compound states in the intermediate minimum of the double-humped fission barrier, which drastically increases the penetration of this barrier [3]. A comparison of the average $\sigma_f$ structure period and the density of states calculated in the Fermi gas model makes it possible, in particular, to determine the depth of this intermediate minimum. In studied nuclei its bottom has been found to lie 2-2.5 MeV above the ground state of the fissionable nucleus.

The absence of similar phenomena in other decay channels, e.g., in neutron decay, is usually considered as a proof that the $\sigma_f$ structure is of this nature. In fact, since the difference between the nucleus excitation energy E* and the ground state energy in the second minimum $E_{II}$ is less than the neutron binding energy $B_n \gtrsim 5$ MeV, a nucleus in such a minimum cannot emit neutrons so that such states cannot occur in the neutron channel. However, one usually considers only s resonances whose relatively small statistics in the $E_n \lesssim 1$ keV region, where they are easily distinguished from p resonances [4], makes it possible to observe this effect. A study of p resonances clearly demonstrates level groups whose reduced neutron widths $g\Gamma_n^1$ exceed by 1.5-2 orders of magnitude the average widths of levels located between these groups.

Figure 1 shows reduced neutron widths $g\Gamma_n^1$ for p resonances in $^{232}$Th measured in [5]. The figure shows that relatively narrow groups of "strong" levels are located at $E_n \approx 150$, 500, 850, 1100 eV, etc. The distribution of $g\Gamma_n^1$ magnitudes (Fig. 2) is apparently divided into two parts, but the ratios of the number of "weak" levels to the number of "strong" levels, as for fission levels of other heavy nuclei, does not obey the $2I + 1$ rule. The ratio is equal approximately to 6 and not 2, as should be the case for p resonances. From Fig. 3 follows that the distances D between "strong" levels do not follow the simple Wigner distribution. Apart from small D, corresponding to resonances belonging to a single group, one observes very large D associated with spaces between groups. This, as well as the magnitude of $g\Gamma_n^1$, "amplification" and the average distance between groups which, if one uses the Fermi-gas dependence D(E*), requires that the reference point of E* be shifted by approximately 2 MeV, is exactly the same as observed in fission channels of other nuclei.

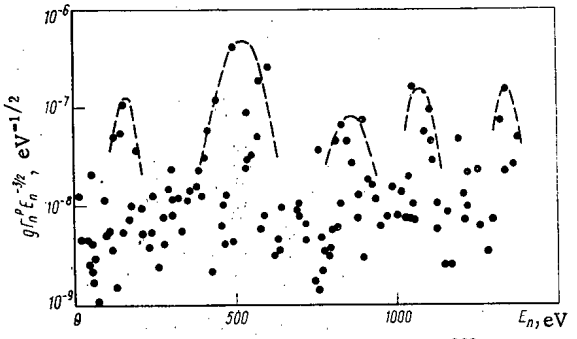


Fig. 1. Reduced neutron widths of $^{232}$Th p resonances.

The most simple and natural explanation of such structures is that they are due to excitations more simple than compound states. Such excitations manifest themselves in other nuclear reactions as input, analog, cluster, and similar states and cause a great local increase of partial widths. As these effects are quite general, we see no reasons for seeking a special explanation in case of fission. Since such effects can be produced by states of different nature, a whole hierarchy of structure can sometimes occur in experiment. For example, structures with periods equal to ~8 [6], ~60 [7], ~500 [8], eV, etc., have been noted in the

Translated from Atomnaya Énergiya, Vol. 38, No. 4, pp. 258-259, April, 1975. Original article submitted August 23, 1974.

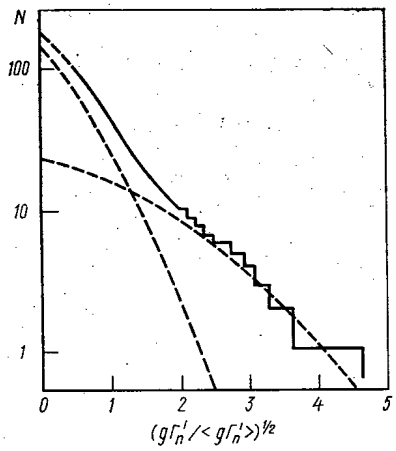


Fig. 2

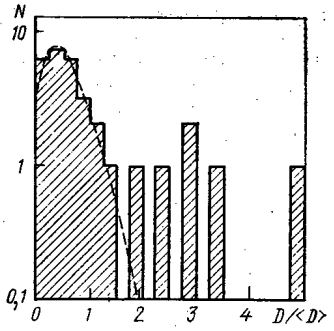


Fig. 3

Fig. 2. Integral distribution of reduced neutron widths of $^{232}$Th p resonances for $E_n < 1400$ eV. Dashed curves show the division into two Porter–Thomas distributions for $\nu = 1$.

Fig. 3. Distribution of distances D between "strong" p resonances ($g\Gamma_n^1 \leq 2.5 \cdot 10^{-8}$ eV$^{-1/2}$). Dashed curve shows the Wigner distribution for small D.

$^{235}$U(n, f) reaction at $E^* \approx 6.4$ MeV, i.e., above the fission barrier. Obviously, not all these structures can be associated with compound states in the intermediate minimum of the fission barrier and require a different explanation.

The results of measurements obtained with a good energy resolution indicate the presence of similar resonance groups in other nuclei, for example in $^{238}$U at $E_n \approx 250$ eV [9].

The presence of p resonance groups with a reduced neutron width $g\Gamma_n^1 \gtrsim 10^{-7}$ eV$^{-1/2}$ must be probably accounted for in calculations and in the interpretation of experimental data. In certain cases, for example at $E_n \approx 100$ keV, they can cause marked spectrum distortion in the passage of a neutron flux through a sample only several millimeters thin.

## LITERATURE CITED

1. D. Paya et al., in: Proc. IAEA Symp. "Nuclear Data for Reactors, 1966," Paris, 17–21 October 1966, Vol. 2, p. 128.
2. E. Migneco and J. Theobald, Nucl. Phys., A-112, 603 (1968).
3. V. Strutinsky and S. Bjornholm, Proc. IAEA Sympos. Nuclear Structure, Dubna (1968), p. 431.
4. P. E. Borotnikov, Yadernaya Fiz., 9, 303 (1969).
5. L. Forman et al., Proc. III Conf. on Neutron Cross Sections and Technology, Knoxville (1971), p. 735.
6. Neutron Cross Sections, BNL-325, 2nd Edition, Suppl. No. 2 (1965).
7. C. Bowman et al., Proc. III Conf. on Neutron Cross Sections and Technology, Knoxville (1971), p. 584.
8. Yu. V. Ryabov and N. Yaneva, in: The Program and Abstracts of the 19th Annual Conference on Nuclear Spectroscopy and Structure [in Russian], Nauka, Leningrad (1969), p. 72.
9. F. Rahn et al., Proc. III Conf. on Neutron Cross Sections and Technology, Knoxville, (1971), p. 658.

# DETERMINATION OF THE PENETRATION OF DECAY PRODUCTS OF RADON INTO THE RESPIRATORY ORGANS BY A DIRECT METHOD

L. S. Ruzer

UDC 621.039.766

The determination of the absorbed doses of internal irradiation of the lungs of mine workers in the case of inhalation of short-lived decay products of radon is an urgent problem. Up to the present time it has been solved by measuring the concentrations of isotopes at the work sites and computing the absorbed dose according to set rates of inhalation and the coefficients of retention of aerosols in the respiratory organs. But the value of the retention coefficient depends on the physicochemical properties of the aerosols and cannot be measured with sufficient accuracy. The value of the rate of inhalation also is rather indefinite, since it depends on the physical load (the nature of the work) and varies within broad limits.

The question of the treatment of the value of the measured concentration is extremely important. The concentration of isotopes in air at the same place is subject to substantial variations. For example, a variation of the intensity of ventilation even for a short period of time leads to a change in the radon concentration of severalfold. Moreover, the content of isotopes directly in the zone of respiration of the miners may differ substantially from the value measured by the usual instruments. Finally, the very concepts of "work place" and "concentration at the work place" are indefinite, since miners are at several work places during their work shift, with variable concentrations of decay products of radon in the mine atmosphere.

Since a measurement of the concentrations at the work places in mines is performed once or twice a month, there can be no precise correspondence between the actual and measured concentrations, and, consequently, it is practically impossible to correctly calculate the individual values of the intake.

The summary error of the calculation of the absorbed doses according to the concentrations is estimated at approximately 5–10-fold in comparison with the actual indices of internal irradiation [1].

In [2–5] a direct method of determining the intake of products of radon into the respiratory organs is described. An analysis of the systematic and random errors of this method showed that the summary error of the measurement in the case of constancy of the concentration of isotopes in the zone of respiration, of the coefficient of retention and respiration rate, determining 0.3 of the value of the permissible intake in a work shift, does not exceed 25% [4].

The systematic errors associated with contamination of the body, work clothes, as well as with the influence of the radon accumulated in the adipose tissues of the abdominal cavity, are eliminated by the introduction of the corresponding corrections. For example, it has been shown that the contribution of $\gamma$ radiation from the region of the abdomen to the total value of the rate of count in measurement of the activity in the lungs 30 min after leaving an atmosphere contaminated with radon does not exceed 5%. The error associated with contamination of work clothes and the body of the worker drops to 15 and 1% of the measured value, respectively, after the work clothes have been taken off and a shower is taken. Random errors associated with geometrical factors, the shift of the equilibrium of RaA, RaB, and RaC, and the stability of the apparatus background, have been analyzed in detail.

We must consider the changes with time in the concentration q, the volume rate of inhalation $v_t$, and the coefficient retention $\varkappa$. The corresponding correction can be introduced experimentally and by calculation.

Translated from Atomnaya Énergiya, Vol. 38, No. 4, pp. 260–261, April, 1975. Original article submitted October 1, 1974.

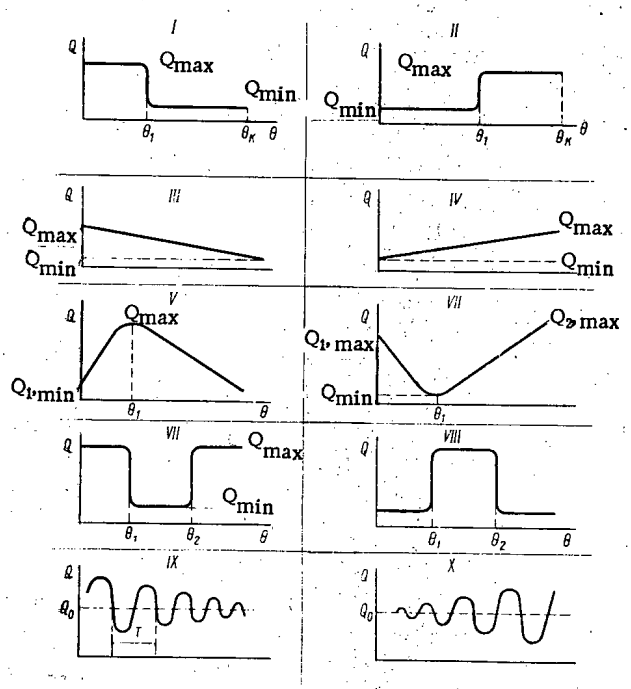


Fig. 1. Forms of functions: I) $Q = Q_{max}$; $0 \le \theta \le \theta_1$; $Q = Q_{min}$; $\theta_1 \le \theta$; II) $Q = Q_{min}$; $0 \le \theta \le \theta_1$; $Q = Q_{max}$; $\theta \ge \theta_1$; IX) $Q = Q_0 \cdot \sin 2\pi t/T$; X) $Q = Q_0 + Qe^{bt} \sin 2\pi t/T$.

In the experimental method, the instrument for measurement by the direct method is placed directly underground close to the work site [4], as a result of which the activity in the lungs of the miners can be measured without any appreciable interruptions in the work.

On the other hand, a consideration of the variations of q, $v_t$, $\varkappa$, and the introduction of the corresponding correction $\delta$ can also be performed by calculation [6].

Let us denote as $Q = qv_t\chi$ the rate of penetration of isotopes into the lungs per unit time. Let us consider the case when Q changes with time. Let us break up the entire time interval of filtration $\theta$ into individual portions $\Delta\theta$, during which Q can be considered constant:

$$\Delta\theta = \theta/k,$$

where k is the multiplicity of division, determined by the required value of the error with which the condition of constancy of $Q_i$ on the portion of the division should be fulfilled.

Let us apply the formulas for the activity in the case of constant Q successively to each interval of division and for each short-lived daughter product of radon. The final expressions for RaA, RaB, and RaC (RaC') will take the form:

$$A_A = \sum_{i=1}^{k} Q_A^i a_A^i(\theta, k), \text{ где } a_A^i(\theta) = \frac{1}{\lambda_A}(1 - e^{-\lambda_A \theta/k})\, e^{-\lambda_A \theta\left(1-\frac{i}{k}\right)};$$

$$A_B = \sum_{i=1}^{k} \left\{ Q_A^i \Phi_B^A\left[\theta/k;\ \theta\left(1-\frac{i}{k}\right)\right] + Q_B^i \Phi_B^B\left[\theta/k;\ \theta\left(1-\frac{i}{k}\right)\right]\right\};$$

$$A_C = \sum_{i=1}^{k} \left\{ Q_A^i \Phi_C^A\left[\theta/k;\ \theta\left(1-\frac{i}{k}\right)\right] + Q_B^i \Phi_C^B\left[\theta/k;\ \theta\left(1-\frac{i}{k}\right)\right] + Q_C^i \Phi_C^C\left[\theta/k;\ \theta\left(1-\frac{i}{k}\right)\right]\right\}.$$

The expressions for $\Phi_B^A$, $\Phi_B^B$, $\Phi_C^A$, $\Phi_C^B$, and $\Phi_C^C$ are cited in [7].

The correction due to a change in the value of Q is conveniently represented in the form:

$$\delta = \frac{\sum_{i=1}^{k} \{Q_A^i [\Phi_B^A(\theta, k) + \Phi_C^A(\theta, k)] + Q_B^i [\Phi_B^B(\theta, k) + \Phi_C^B(\theta, k)] + Q_C^i \Phi_C^C(\theta, k)\}}{\overline{Q}_A [\Phi_B^A(\theta) + \Phi_C^A(\theta)] + \overline{Q}_B [\Phi_B^B(\theta) + \Phi_C^B(\theta)] + \overline{Q}_C \Phi_C^C(\theta)} - 1,$$

where $\overline{Q}$ represents the average values of the rate of penetration of the isotopes into the respiratory system in the time $\theta$. The value of $\delta$ depends on the type of the curve $Q(\theta)$, the ratio $Q_{max}/Q_{min}$, the shift of equilibrium, etc.

For the calculation we selected 10 variations of the function $Q(\theta)$ (Fig. 1), as well as a number of values of the parameters, which reflect the variety of situations arising under practical conditions.

The general values of the parameters for all variations are:

1. $\theta$ = 30; 60; 90; 120; 180; 420 min.

2. Number of divisions: k = 2; 3; 5; 7; 10; 14; 28; 42.

3. $Q_A : Q_B : Q_C$ = 1 : 1 : 1; 1 : 0.8 : 0.6; 1 : 0.6 : 0.4; 1 : 0.5 : 0.5; 1 : 0.4 : 0.2; 1 : 0.3 : 0.1; 1 : 0.5 : 0.05; 1 : 0.1 : 0.05; 1 : 0.1 : 0.01; 1 : 0.05 : 0.01; 1 : 0.01 : 0.01.

4. $Q_{max}/Q_{min}$ = 1.5; 2.0; 3.0; 5.0; 10; 15; 20; 30; 50; 100; 300; 1000.

5. $\left.\begin{matrix}\theta_1/\theta_k \\ (\theta_2-\theta_1)/\theta_k\end{matrix}\right\}$ = 0.1; 0.2; 0.3; 0.4; 0.5; 0.6; 0.7; 0.8; 0.9.

6. $Q_{min}$ = 50 disintegrations/min/min ($q = 10^{-11}$ Ci/liter; k = 0.2; $v_t$ = 10 liters/min).

The calculation was performed on a BÉSM-6 electronic computer [6].

The method of introduction of the correction associated with the change in Q with time presupposes the selection of the function $Q(\theta)$ closest to the real form (variations I-X, see Fig. 1) and a search according to the set values of $Q_{max}/Q_{min}$, $\theta_1$, as well as the other necessary parameters of the correction $\delta$.

The value of the activity (penetration) in the lungs sought, $\bar{A}$, is expressed in terms of the measured value of A as follows:

$$\bar{A} = \frac{1}{1+\delta} A.$$

The degree of error in the determination of $\delta$ depends on the closeness of the selected variant of the distribution to the variant under real conditions. It must be noted that since the correction $\delta$ is largest in absolute magnitude, and that means also the largest difference of A from $\bar{A}$, are given by variants I and II, we can limit ourselves to the maximum value of $\delta$ for these variants. This is also advisable because even in these cases, for $Q_{max}/Q_{min} \leq 30$, the summary error of measurement by a direct method does not exceed 40% at the level of the maximum permissible intakes, which is quite sufficient for practical purposes.

## LITERATURE CITED


1. L. S. Ruzer, Dissertation [in Russian], VNIIFTRI, Moscow (1970).
2. L. S. Ruzer, Byul. Izobret., No. 18 (1964).
3. L. S. Ruzer and S. A. Urusov, At. Énerg., 26, No. 3, 301 (1969).
4. S. A. Urusov, Dissertation [in Russian], In-t Biofiziki. Minzdrav SSSR (1972).
5. A. D. Al'terman, Dissertation [in Russian], Institut Gigieny Truda i Profzabolevanii AMN SSSR, Moscow (1974).
6. Yu. S. Gerasimov and L. S. Ruzer, Methods of Determination of the Content of Radioactive Isotopes in the Human Organism. Materials of the Symposium [in Russian], Izd. Leningr. NII Radiatsionnoi Gigieny MZ RSFSR, Leningrad (1973), p. 58.
7. L. S. Ruzer, Radioactive Aerosols [in Russian], Izd. Komiteta Standartov, Mer i Izmeritel'nykh Priborov Pri Sovete Ministrov SSSR, Moscow (1968).

# NEUTRON ACTIVATION DETERMINATION OF HAFNIUM IN ZIRCONIUM IN THE CASE OF INTERFERENCE FROM FLUORINE

V. V. Ovechkin, A. Z. Panshin, and V. S. Rudenko

UDC 543.53

A rapid neutron activation method of determination of hafnium, based on the recording of the activity of the short-lived isomer $^{179m}Hf$ ($T_{1/2}$ = 19 sec, $E_\gamma$ = 0.217 MeV), is used in analytical practice [1-3].

The large value of the cross section of the $^{178}Hf(n, \gamma)$ reaction (~75 b) on thermal nuetrons permits the use of portable neutron sources: low-voltage generators [2] and isotopic sources [3], for activation in addition to reactors. The induced activity is usually measured with a scintillation $\gamma$ spectrometer according to the photopeak 0.217 MeV.

According to the data of [2], the use of a 14 MeV neutron generator and moderator permits an increase in the activity of the isomer $^{179m}Hf$, and in addition, a substantial lowering of the background of the zirconium matrix, due to the $\gamma$ radiation of $^{89m}Zr$ and $^{89m}Y$, formed from zirconium according to the reactions $^{90}Zr(n, 2n)$ and $^{90}Zr(n, n'p)$. The sample for irradiation is placed in a moderator at a distance of ~4-5 cm from the neutron source, where the flux of thermal neutrons is a maximum [4]. However, at such a distance in the moderator the fraction of neutrons with energy exceeding the threshold of the indicated reactions is still large (12.53 and 8.79 MeV, respectively). On account of the large difference of the energy spectra of neutrons determining the useful and background effects, it is advisable to find the optimum distance from the target, at which more profitable conditions of measurement of hafnium in zirconium are realized.

It should be kept in mind that in the presence of fluorine in zirconium a serious difficulty arises for the measurement of a hafnium impurity on a scintillation $\gamma$ spectrometer according to the photopeak 0.217 MeV on account of the interference from the 0.197 MeV $\gamma$ radiation of the isotope $^{19}O$ ($T_{1/2}$ = 29.3 sec),

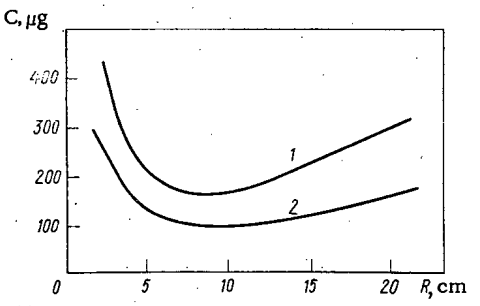


Fig. 1. Dependence of the lower limit of the measurement of hafnium on the position of the sample in the moderator relative to the source: 1 and 2) mean-square error 20 and 30%, respectively.

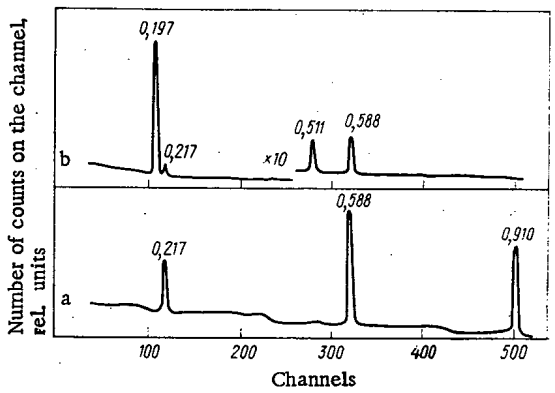


Fig. 2. $\gamma$ spectrum of irradiated samples.

Translated from Atomnaya Énergiya, Vol. 38, No. 4, pp. 261-263, April, 1975. Original article submitted July 15, 1974.

TABLE 1. Hafnium Content in Samples, % by Weight

| Materials | Activation method | Spectral method |
|---|---|---|
| Zirconium | $0{,}8 \cdot 10^{-2}$ | $< 10^{-2}$ |
| Zirconium | $4{,}2 \cdot 10^{-2}$ | $3{,}8 \cdot 10^{-2}$ |
| Zirconium | $6{,}0 \cdot 10^{-2}$ | $5{,}1 \cdot 10^{-2}$ |
| Potassium fluorozirconate | $3{,}0 \cdot 10^{-2}$ | $2{,}8 \cdot 10^{-2}$ |
| Potassium fluorozirconate | $4{,}6 \cdot 10^{-2}$ | $4{,}2 \cdot 10^{-2}$ |

formed in the irradiation of fluorine according to the reaction $^{19}F(n, p)$. The measurement is also hindered by the $\gamma$ radiation of the isotopes $^{16}N$ ($T_{1/2}$ = 7.3 sec, $E_\gamma$ = 6.1 MeV) and $^{20}F$ ($T_{1/2}$ = 11.3 sec, $E_\gamma$ = 1.63 MeV), also formed from fluorine.

In this work we selected the optimum conditions of the determination of hafnium in samples of zirconium using a generator of neutrons with energy 14 MeV and a spectrometer based on a Ge(Li) detector.

As the criterion of optimality we selected the condition of reaching the minimum limit of measurement of hafnium. Determination of the lower limit of the measurement C was performed using the expression

$$C = N/S, \tag{1}$$

where S is the instrument sensitivity of the measurement of hafnium, counts/g of Hf; N is the minimum number of counts from the irradiated sample on account of the recording of $\gamma$ quanta with energy 0.217 MeV, providing for the reaching of a set accuracy.

According to [5], the value of N for a Ge(Li) spectrometer can be determined according to the formula

$$N = A\,[(2n\overline{B} + A^2/4)^{1/2} + A/2], \tag{2}$$

where A is a quantity characterizing the required accuracy; n is the number of channels in the photopeak; $\overline{B}$ is the average background on the channel in the region of the peak, representing the sum of the natural background and the Compton distribution from higher energy $\gamma$ radiation.

The measurements were performed on a 14 MeV neutron generator of the NG-150I type, the rotating target of which provided for a constant value of the neutron flux. Distilled water was used as the moderator (tank with dimensions 60 × 60 × 60 cm). The irradiation chamber in the moderator should be situated at various distances from the target of the neutron generator. For rapid addition of the samples, a pneumatic transport device was used. The induced activity was recorded with a $\gamma$ spectrometer based on Ge(Li) detectors with a sensitive volume of ~38 and ~60 $cm^3$; the resolution according to the $\gamma$ peak 0.217 MeV was ~5 keV. The material to be analyzed was placed in polyethylene ampoules 10 mm in diameter, irradiated for 1 min, and 5 sec after the end of irradiation, the $\gamma$ spectrum photographed for 40 sec on a multichannel analyzer.

Figure 1 presents the experimental dependence of the lower limit of the measurement of hafnium in zirconium on the distance between the irradiation chamber and the target of the generator: at a distance of ~9 cm the value of C is a minimum. Figure 2, *a* cites the $\gamma$ spectrum of a sample of zirconium with a hafnium content of $1.2 \cdot 10^{-2}$% by weight, irradiated at R = 9 cm. In the spectrum a photopeak with energy 0.217 MeV distinctly appears, indicating the presence of hafnium.

In the case of the presence of fluorine in the sample, a $\gamma$ spectrometer based on a Ge(Li) detector reliably resolves photopeaks with energies 0.197 and 0.217 MeV. In addition, the selected geometry of irradiation (R = 9 cm) permits virtual elimination of the background in the region of measurement of hafnium (0.217 MeV), due to the higher energy $\gamma$ radiation from the isotopes $^{16}N$ and $^{20}F$. At the same content of fluorine and hafnium impurities in the sample, the contribution of fluorine in the region of recording is three orders of magnitude lower than that of hafnium.

Thus, the use of a semiconductor detector for the recording and the selected geometry of irradiation permits an analysis of the hafnium content in zirconium or its compounds in the presence of a large content of fluorine. The $\gamma$ spectrum, for example, of a sample of potassium fluorozirconate with a hafnium content of $\sim 5.0 \cdot 10^{-2}$% by weight, is shown in Fig. 2b. The results of measurement of the hafnium content for several samples are contained in the table.

In the measurement of the hafnium content in zirconium according to the $\gamma$ peak with energy 0.217 MeV, the value of the background in this region from the radioisotopes $^{89m}Zr$ and $^{89m}Y$ depends on the size of the semiconductor detector. This also is confirmed by the measurements performed on two different Ge(Li) detectors. At the same intensity of the photopeak 0.217 MeV, recording on the detector with a larger volume leads to an approximately twofold increase in the intensity of the photopeak with energy 0.588 MeV, while the background in the region of 0.217 MeV increases by ~45% in this case.

In work with a detector with smaller volume under the selected conditions of analysis, the lower limit of the measurement of hafnium is $\sim 2 \cdot 10^{-3}\%$ by weight (for a sample of zirconium weighing ~5 g, with a yield of 14 MeV neutrons equal to $\sim 1 \cdot 10^{10}$ neutrons $\cdot$ sec$^{-1}$ and R = 9 cm). A fluorine content in the sample up to tens of percent increases the value of the lower limit of measurement of hafnium to $\sim 1 \cdot 10^{-2}\%$ by weight. It should be noted that the design of the detector used did not permit the sample to be brought to a more sensitive distance than 1 cm during the measurements. By selecting a detector with improved characteristics, the value of the lower limit of measurement of hafnium may be reduced. For example, for a Ge(Li) detector of the well type [6] (the total efficiency for the energy 0.2 MeV is equal to ~20%), according to the calculation, the lower limit of the measurement of hafnium is decreased by an order of magnitude.

The results of the measurements show that the selected conditions and apparatus can be successfully used for the neutron activation analysis of samples of zirconium for the content of hafnium impurities in the presence of fluorine.

The authors would like to express their sincere gratitude to A. A. Luppov for aid in performing the measurements on the generator.

## LITERATURE CITED

1. S. S. Kodiri et al., At. Énerg., 32, No. 5, 428 (1972).
2. V. V. Ovechkin and V. S. Rudenko, At. Énerg., 35, No. 4, 277 (1973).
3. J. Strain and W. Lyon, in: Proc. IAEA Symp. Radiochemical Methods of Analysis, Salzburg, October 19-23; 1964; Vol. 1, p. 245.
4. W. Meinke and R. Shideler, Nucleonics, 20, No. 3, 60 (1962).
5. J. Cooper, Nucl. Instrum. and Methods, 82, 273 (1970).
6. J. Verplanke, Ibid., 96, No. 4, 557 (1971).

# NEUTRON ACTIVATION MEASUREMENT OF THE FLUORINE CONTENT IN URANIUM AND PLUTONIUM

V. I. Melent'ev and V. V. Ovechkin

UDC 543.08.53

The development of instrumental nuclear physical methods of measuring the fluorine content in inactive construction materials, based on activation of the samples with neutrons [1-3], $\gamma$ quanta [4, 5], and charged particles [6, 7], is reported in the literature.

The application of the neutron activation method to samples based on fissioning substances is complicated by the fact that during neutron irradiation an intense delayed $\beta$ and $\gamma$ radiation of the fission products arises [8].

An analysis of the characteristics of the neutron reactions on fluorine [9] and the apparatus $\gamma$ spectrum of irradiated uranium and plutonium (Fig. 1) permits us to conclude that there are advantages in using the reaction $^{19}F(n, \alpha)^{16}N$. The recording of high-energy $\gamma$ radiation of the isotope $^{16}N$ ($E_\gamma \approx 6$ MeV, $T_{1/2} = 7.35$ sec) in the region where the yield of the delayed radiation of the fission products is already small, provides for the possibility of obtaining higher selectivity and reliability of the result of the analysis.

An extremely convenient means of activation is the use of an isotopic source based on the Be($\alpha$, n) reaction, since for the average energy of the emitted neutrons (~5 MeV) the cross section of the $^{19}F(n, \alpha)$ reaction is comparatively large, while the yield of the competing reaction $^{16}O(n, p)^{16}N$ is negligible.

For activation we used an isotopic $^{238}Pu-Be$ source with a yield of $1 \cdot 10^8$ neutrons/sec$^{-1}$, which was placed in a tank (800 × 800 × 1200 mm) with water, surrounded by a concrete shield (400 mm thick). The pneumatic transport system with pneumatic drive of a polyethylene tube with inner diameter 12 mm provided for delivery of the irradiated samples from the zone of activation to the zone of recording in a time $\leq 2$ sec. The induced activity was recorded with a $\gamma$ spectrometer based on an NaI(Tl) scintillator 150 × 150 mm in diameter with a well 33 × 70 mm in diameter, in lead shielding with a wall thickness of 50 mm. The energy region of the recording ($\Delta E = 5.6$-$6.5$ MeV) was selected so as to provide for the greatest limit of detection of fluorine against a background of fission products of the matrix of the sample.

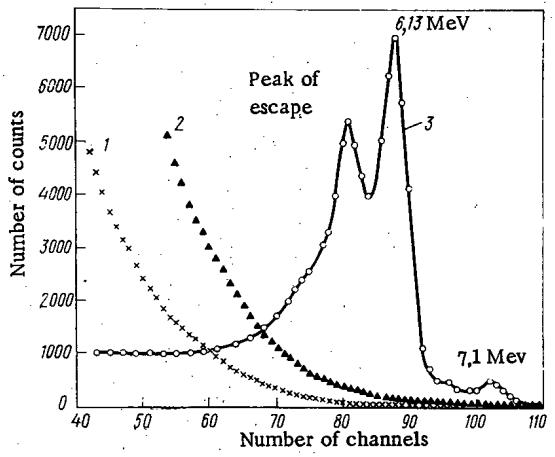


Fig. 1. Apparatus $\gamma$ spectra of irradiated samples: x) uranium (6.06 g); ▲) plutonium (5.36 g); ○) fluorine (2.19 g).

The samples were placed in hermetic polyethylene linings 6 × 17 mm in diameter, after which they were surrounded with cadmium 0.3 mm thick to reduce the level of $\beta$ and $\gamma$ radiation of the fission products, which might be formed in the matrix of the sample during the process of irradiation with thermal neutrons; stainless steel containers were used for transportation.

The fluorine content in the sample was determined according to the formula:

Translated from Atomnaya Énergiya, Vol. 38, No. 4, pp. 263-264, April, 1975. Original article submitted October 24, 1974.

TABLE 1. Results of the Determination of Fluorine in Samples of Uranium and Plutonium

| Sample | Weight, g | F content, % by wt. | |
|---|---|---|---|
| | | introduced | determined by the neutron activation method |
| $UF_4+UO_2$ | 1,983 | 2,337 | 2,16±0,05 |
| $U+(C_2F_4)_n$ | 6,010 | 1,940 | 1,92±0,05 |
| $UF_4+UO_2$ | 1,755 | 1,042 | 1,28±0,05 |
| $UF_4+UO_2$ | 1,6738 | 0,524 | 0,49±0,03 |
| $U+(C_2F_4)_n$ | 6,121 | 0,198 | 0,22±0,03 |
| $U+(C_2F_4)_n$ | 6,501 | 0,082 | 0,08±0,02 |
| $UF_4+UO_2$ | 1,3915 | 0,052 | 0,06±0,01 |
| $UF_4$ | 5,3567 | 24,2 | 23,9±0,5 |
| $PuF_3$ | 0,9969 | 19,2 | 19,2±0,4 |
| $PuO_2+Na_2PuF_6$ | 0,9975 | 2,50 | 2,50±0,04 |
| $Pu+(C_2F_4)_n$ | 5,361 | 1,866 | 1,86±0,06 |
| $Pu+(C_2F_4)_n$ | 5,334 | 0,381 | 0,37±0,04 |
| $Pu+(C_2F_4)_n$ | 5,331 | 0,075 | 0,07±0,02 |

$$C_F(\text{rel}) = \left[\frac{N-N_b}{M} - \frac{C_f}{C_{f.s}}\cdot\frac{(N-N_b)}{M_s}\right] \Big/ n_F + (C_{F.S}C_f)/C_{f.s} \quad (1)$$

where N and $N_s$ are the counts recorded from the test and control samples, respectively; $N_b$ is the background of the detector in the energy region of recording; M, $M_s$ are the masses of the sample and standard (sample with known content of fluorine $C_{F.s}$ and fissioning sample $C_{f.s}$); $n_F$ is the number of counts recorded from 1 g of fluorine and determined by activation of the control samples; $C_f$ is the concentration of the fissioning substance in the test sample, rel. units.

Table 1 presents the results of neutron activation analysis of samples based on uranium and plutonium; each result was obtained from five determinations.

The error in the measurement in the case of introduction of fluorine into the sample was equal to ±0.001 (abs.); the total error of the result of the analysis was determined according to [10]. From Table 1 it follows that the results of neutron activation analysis, within the limits of error, are in good agreement with the amount of fluorine introduced.

The lower limit of detection of fluorine was found according to the criterion $2\sigma$ of the background [11] from the expression

$$m_F(\%) \approx 2(n_f C_f M)^{1/2} 10^2/(n_F M). \quad (2)$$

In the case of time systems of analysis ($t_{irr}$ = 18 sec, $t_{isol}$ = 4 sec, $t_{meas}$ = 16 sec, and $t_{cycle}$ = 1 min), for 30 cycles of irradiation of 10 gram samples of $^{238}U$, we obtained the following values: $n_F$, $N_f$ (uranium), and $N_f$ (plutonium) equal to 37,590, 2280, and 7940 counts, respectively. From this it follows that $m_F$ (uranium) and $m_F$ (plutonium) are equal to $2.5\cdot10^{-2}$ and $4.8\cdot10^{-2}$% by weight, respectively. In this case the background of the detector was equal to 0.4 counts·$sec^{-1}$. Further improvement of the sensitivity of the method can be achieved using more intense neutron sources.

## LITERATURE CITED


1. J. Wing and M. Wahlgren, J. Radioanal. Chem., 3, 37 (1969).
2. N. P. Lisovskii et al., Khim. Prom-st', No. 3, 235 (1971).
3. V. I. Melent'ev, V. V. Ovechkin, and V. S. Rudenko, At. Énerg., 34, No. 1, 35 (1973).
4. S. Ohno et al., Analyst., 95, 260 (1970).
5. C. Engelman and A. Scherle, J. Radioanal. Chem., 6, 235 (1970).
6. I. Jurai et al., Chem. Listy, 64, No. 11, 1121 (1970).
7. M. Gerrard, Isotop. Radiat. Techn., 8, 118 (1970).
8. P. Fisher and L. Engle, Phys. Rev., 134, No. 4B, B796 (1964).
9. I. A. Maslov and V. A. Luknitskii, Manual of Neutron Activation Analysis [in Russian], Nauka, Leningrad (1971).
10. R. I. Alekseev and Yu. I. Korovin, Handbook for Calculation and Treatment of the Results of Quantitative Analysis [in Russian], Atomizdat, Moscow (1972).
11. D. De Soete, R. Gijbels, and J. Hoste, in: Series of Monographs on Analytical Chemistry and Its Applications, Vol. 34, Neutron Activation Analysis, J. Wiley and Sons (1972), p. 536.

# SEMINAR OF THE INTERNATIONAL INSTITUTE OF APPLIED SYSTEMS ANALYSIS IN RELATION TO THE ENERGY PROBLEM

V. I. Mastbaum

A scientific Seminar was held in Moscow in December 1974 by the International Institute of Applied Systems Analysis* in relation to the energy problem.

The leading scientists of this Institute, W. Heffel, T. Kupmans, C. Marchetti, and others, set out their own conception of the power development in the distant future. The principal technical procedure underyling this conception lies in the use of nuclear reactors. However, the conditions governing the use of these reactors and the requirements to be imposed upon them differ from those which have always hitherto been accepted. These characteristics are primarily associated with the changing prospects of power development in the capitalist countries after the energy crisis.

Before the energy crisis there was an extremely widely-held opinion that nuclear reactors would chiefly be required for the production of electrical power. It was pointed out in the Seminar that the shortage of oil and gas and the increasing price of these on the world market would compel western scientists concerned with energy problems to seek new ways of power development. Hence the increasing interest in nuclear power, which is now considered not only as a source of electrical energy but also as a method of producing secondary hydrocarbon fuel.

In the opinion of the Institute's scientists, artificial hydrocarbons should be capable of replacing gas and oil, as well as their processing products, in industry, transportation, and a number of other fields. The Seminar discussed the most promising technological methods of producing synthetic fuel, initially by the gasification of coal to produce hydrogen, methane, and methyl alcohol. However, this process involves mining operations; it is expensive and (what is worse) contaminates the environment. A more promising long-term procedure lies in the production of hydrogen by the electrolytic or thermal decomposition of water. The thermal method is thermodynamically more efficient, but its introduction requires advanced technology relating to the production of high temperatures in the reactor coolants, heat transfer at elevated temperature, and other processes.

The scientists of the International Institute of Applied Systems Analysis indicate that the transition from power based on organic fuel to that based on inorganic fuel will take place in three stages. In the first stage, which will last up until 1985, owing to the inertia of the development process, oil and gas will continue to provide the main basic fuel. In the second stage, which may be completed by the year 2000, fuel will largely be based upon coal, which will be used to produce hydrocarbons replacing oil and gas. The third stage belongs to the next century, and will involve a transition to synthetic hydrocarbons obtained by the decomposition of water. The use of synthetic hydrocarbons will at the same time solve the problem of protecting the environment from contamination.

*The International Institute of Applied Systems Analysis is an International scientific organization, formed in October 1972. Founder members included representatives of the United States, the Soviet Union, the United Kingdom, France, West Germany, Canada, Japan, Poland, Czechoslovakia, and others. The Institute is centered in Vienna. The Soviet Union is represented in the Institute through the Systems-Analysis Committee formed by the Presidium of the Academy of Sciences of the USSR. The Institute develops projects relating to the methodology of systems analysis, biology, power, and other problems.

Translated from Atomnaya Énergiya, Vol. 38, No. 4, pp. 265-266, April, 1975.

The trend toward high-temperature technological processes in the production of secondary hydrocarbon fuel will furthermore demand the creation of the corresponding technological equipment, especially high-temperature reactors. Thus the high-temperature reactor becomes a necessary and essential element in reactor strategy.

In the opinion of the International Institute of Applied Systems Analysis, the development of nuclear power should be based on three types of reactors: light-water, fast, and high-temperature. The first two types are mainly designed for the development of electrical power, the third for technological heat, as required in the production of hydrocarbons.

Light-water reactors are mainly required in the initial period of the development of nuclear power. Secondary nuclear fuel is developed in these as well as in fast reactors; this is required for the annual recharging of existing fast reactors and the initial charging of new ones. In accordance with one of the main reactor strategies, it is important to remember that the screens of fast reactors are partly charged with thorium, which may be converted into the $^{233}U$ required for charging high-temperature reactors. Thorium and waste or natural uranium are required for the functioning of the system. Since the need for enriched uranium will be substantially reduced, it will become economically justifiable to use even expensive uranium ores.

The Institute has developed mathematical models for verifying the practical feasibility of the foregoing reactor strategies under various conditions of power development and various probable times for the adoption of the new types of reactors.

# INTERNATIONAL SEMINAR ON REACTOR NOISE

D. M. Shvetsov

The first International Seminar devoted to the study of noise in nuclear reactors (SMORN-I) was held in Rome between October 21 and 25; 1974. The Seminar was organized by the European–American Committee on Reactor Physics in conjunction with the Italian National Committee on Nuclear Power. Countries not constituting members of these organizations were also invited, especially the Soviet Union, Poland, Hungary, and Rumania. Altogether sixty scientists from more than twenty countries took part in the Seminar and presented some forty papers.

This was the first time such a representative gathering had been convened. Previous conferences and symposia on reactor noise had been of a national or a bi- or trilateral character (national conferences in the USA in 1963 and 1966, the Soviet–Belgian–Dutch symposium in 1967, the All-Union school of physicists concerned with pulse and statistical methods in reactors held in 1967, and so on).

Recent years have seen a considerable growth in the role of nuclear power and the construction of new nuclear power stations; problems of optimum use have accordingly arisen. This in turn demands a comprehensive study of the physical processes taking place in reactors. The watchword of the Seminar was "From critical assemblies to power reactors."

The increasing interest of research workers in "power" noise is shown by the fact that fluctuations in the neutron flux low- ("zero-") power reactors formed the subject of well under half the total number of papers. The general opinion held at the present time is that the question of noise in critical assemblies has, on the whole, now been exhausted. Statistical methods of measuring the kinetic parameters of equipment are now frequently treated as standard. Questions remaining to be solved are mainly of academic interest. The role of experiments on the physical test-bed is diminishing.

The position with noise in power reactors is rather different. The extensive prospects of using the statistical characteristics of nuclear installations in order to monitor the safety aspect and provide early warning of technological breakdown provide the logical basis for the study of reactor noise. On the other hand, the "noise" picture in a power reactor is far more complicated than in a critical assembly. Whereas in a physical reactor the main source of reactivity noise has a uniform ("white") frequency spectrum, in a power reactor there is a great number of sources (temperature, coolant flow, mechanical vibrations, etc.) the spectral composition of which is often extremely "nonwhite." The existence of a large number of feedback relationships makes the problem even more complicated. We are thus still a long way from obtaining a complete picture of the noise in a power reactor. Theoretical and experimental investigations in various countries are therefore now being mainly directed at solving individual, particular problems, many of which are of direct practical interest.

A number of papers presented in the Seminar were devoted to methods of detecting the boiling of the coolant in the active zone in the case of the accidental blocking of the channels. Work of this kind is being carried out in Hungary, Japan, West Germany, the United States, and France. Extrareactor models of boiling channels are being studied, as well as the noise of the neutron flux which arises during the passage of gas bubbles into the active zone of water reactors. During these experiments, fluctuations in temperature and neutron flux are recorded in addition to acoustic noise. Acoustic methods are considered as being the most promising for the detection of boiling in fast reactors containing liquid-metal coolants. Since in any real power reactor there is a severe acoustic background not associated with boiling effects, it is proposed to suppress this by using the mutual correlation between the acoustic noise and fluctuations in the

Translated from Atomnaya Énergiya, Vol. 38, No. 4, pp. 266-267, April, 1975.

neutron flux. In the French fast reactor "Superphoenix," for example, it is proposed to keep a constant check on boiling by reference to the mutual correlation between the acoustic and neutron-flux noise. The use of intrareactor neutron sensors of the DPZ (control and safety devices) type even enables the site of the boiling to be determined. The same sensors are used for monitoring the circulation of the coolant in a boiling reactor by measuring the velocity of the rising steam bubbles, using the mutual correlation of two detectors in different parts of the channel. The results of a measurement of coolant velocity based on the mutual correlation of two thermocouples were presented by Hungarian physicists.

Certain contributions (from the USA and Australia) emphasized the necessity of studying mechanical vibrations in power reactors for monitoring purposes. The use of the corresponding sensors (such as accelerometers) provides information as to the vibrations of the rods due to pressure fluctuations or hydrodynamic effects. In the United States the noise of various sensors (extrareactor neutron chambers and accelerometers) has been studied in order to monitor the displacements of the active zone in water-cooled, water-moderated reactors.

At the same time as these experimental investigations, theoretical research is also being carried out in various countries. In many cases this is of the applied nature and is intended to explain existing experimental data. Specific physical models (usually extremely simple ones) are being constructed to this end, and the coefficients of the corresponding equations are being determined from experimental data. This enables us to obtain such important characteristics as the time constants of the elements of the active zone and the feedback-function parameters. In certain papers some rather more general theoretical questions were discussed, such as those relating to nonlinear effects (Japan and the Soviet Union).

Subsequent investigations into the noise of power reactors should provide material for a more fundamental theoretical analysis. The stimulus for this is the useful information which the noise contains.

We should mention the tremendous amount of work which has been done by the organizing committee of the Seminar under the direction by Professor N. Paccillio and Dr. V. Iorio. Selected papers regarding statistical effects in power reactors will be published in the British journal, Annuals of Nuclear Science and Engineering. The complete collection of papers will be published in Italy.

# THE FIFTH ALL-UNION CONFERENCE ON HEAT EXCHANGE AND HYDRAULIC RESISTANCE IN THE MOTION OF A TWO-PHASE STREAM IN THE ELEMENTS OF POWER MACHINERY AND EQUIPMENT

M. Ya. Belen'kii and V. A. Shleifer

The Conference was held on October 15-18, 1974, in Leningrad, at the initiative of the State Committee of the Council of Ministers of the USSR for Science and Technology, the Academy of Sciences of the USSR, the USSR Ministry of Heavy Power and Transport Machinery Construction, the I. I. Polzunov Central Boiler and Turbine Institute, the High-Temperature Institute of the Academy of Sciences of the USSR, the National Committee on Heat and Mass Exchange, and other organizations.

Those attending the Conference included more than 800 delegates from 168 scientific, construction, and design organizations, industrial enterprises, and institutions of higher education. They heard and commented on 50 survey reports, covering more than 250 scientific studies.

M. A. Styrikovich devoted his introductory report to the prospects of development in the power industry and the utilization of natural resources. N. M. Markov, Director of the Central Boiler and Turbine Institute, emphasized in his statement the importance of rapidly introducing into industry the results of scientific investigations. S. S. Kutateladze, V. M. Borishanskii, and V. I. Golubinskii, who spoke thereafter, discussed some problems of hydrodynamics and heat exchange in two-phase media.

Two sections functioned at the Conference:

1. Heat exchange and hydrodynamics in the boiling of liquids under conditions of free convection. Condensation of vapors and evaporation. Heat exchange and hydrodynamics in the near-critical region.

2. Heat exchange and hydrodynamics in the organized movement of a two-phase stream and rapidly moving vapor-bearing streams. Heat-exchange crisis with free convection and organized movement of coolant (pipes, channels).

In the first section a great deal of attention was devoted to the investigation of the mechanism of boiling. New data were presented concerning break-away diameters, surface characteristics, and growth dynamics of steam bubbles. A great deal of interest was aroused by reports devoted to boiling on ribbed surfaces, in slit channels, and on surfaces with various types of covering. Noteworthy among the reports were those dealing with investigations of heat transfer in the condensation of vapors of various substances, in which the investigators considered new aspects of the mechanism of heat transfer during bubble-boiling of liquids.

Some reports contained an analysis of the operation of power equipment, including in particular the steam generator of the Novovoronezhsk Atomic Power Station, the VK-50 reactor, etc. The results of these investigations made it possible to optimize the area of the steam-generator heating surface and to develop a new method for the design of shell-type boiling reactors.

The second section discussed problems involved in heat exchange and hydrodynamics in the boiling of liquids in pipes, as well as the heat-exchange crisis associated with boiling.

---

Translated from Atomnaya Énergiya, Vol. 38, No. 4, p. 267, April, 1975.

The material presented included extensive experimental material on heat exchange, hydrodynamics, true volumetric vapor content, and the flow boundaries for two-phase media. Today increasing attention is being devoted to the investigation of the local characteristics of two-phase streams by the latest diagnostic methods, which was reflected in many reports.

Great interest was attracted by reports devoted to a very timely problem: the heat-exchange crisis in the steam-generating channels. Investigations dealt with the mechanism by which the crisis arises and obtained relations for calculating the limiting flow rate of the liquid in a film, as well as the intensity of precipitation of drops from the core of the stream onto the wall. It was noted that the data on critical thermal loads presented by a number of authors agreed with one another.

The reports presented at the Conference gave rise to a very fruitful discussion.

The results of the investigations were summed up in a resolution adopted at the closing plenary meeting. It was recommended that scientific organizations should devote more attention to the critical comparison and generalization of experimental material and to the early formulation of recommendations on thermal and hydraulic calculations for power equipment. The Conference declared that the issuing of inter-branch normative materials was advisable. It noted the development of some very promising trends in heat-power engineering.

# SOVIET – FRENCH SEMINAR ON PHYSICS, HYDRAULICS, AND HEAT TRANSFER IN WATER-COOLED, WATER-MODERATED REACTORS

S. A. Skvortsov

During the visit of a French Delegation to Soviet Atomic Centers, a Soviet–French Seminar on the "Physics, Hydraulics, and Heat Transfer of Water-Cooled, Water-Moderated Reactors" was held in the I. V. Kurchatov Institute of Atomic Energy (October 7–10, 1974).

The French Delegation consisted of ten members, eight from the atomic center at Saclay and two from Grenoble.

The French scientists presented ten review papers on computing procedures for water-cooled, water-moderated reactors. These included neutron-physical and thermal calculations of reactors, experimental investigations carried out in critical assemblies, determinations of the isotopic composition of burnt-out fuel, thermohydraulic calculations of fuel assemblies by the cell method, a calculation of the reactor parameters which would apply in a so-called "major emergency" (rupture of the circulation tube), and other problems. These papers gave a general picture of the computing procedures used in France at this time.

The Soviet scientists presented fourteen papers. These discussed, inter alia, the thermalization equations, programs for calculating the thermal-neutron distribution, the experimental study of certain neutron-physical parameters, experimentally-obtained thermohydraulic characteristics of fuel assemblies, transient modes of multichannel systems, the heat-transfer crisis, and methods of increasing the critical loads. The Soviet program of papers was less systematic but contained more new material.

Lively discussions took place at the end of the seminar.

On the final day the French guests viewed the experimental installations of the Institute of Atomic Energy which had been used in the development of water-cooled, water-moderated reactors.

Translated from Atomnaya Énergiya, Vol. 38, No. 4, p. 268, April, 1975.

# WINTER SESSION OF THE AMERICAN NUCLEAR SOCIETY 1974

F. G. Reshetnikov and I. S. Golovnin

The latest session of the American Nuclear Society was held in Washington on October 27-31, 1974, Soviet scientists being invited for the first time.

The American Nuclear Society was organized in 1954 (December) as a scientific and educational institution. The principal aims of the Society were the popularization and stimulation of science in the field of nuclear studies and neighboring aspects of research. The Society promotes the publication of papers by its members, and organizes conferences and symposia; its departments are headed by well-known scientists from the universities and scientific research institutes (laboratories). At the present time the Society has over eleven thousand members, including some nine hundred from forty other countries. The Society enjoys great influence and authority among scientific research undertakings and industrial corporations; it maintains close links with the United States Atomic Energy Commission and with over fifteen hundred corporations and scientific research and educational institutions.

The range of activity of the Society may be judged from this session alone, which was devoted to the problem of fast reactors. Sessions were held in sections – fourteen of these involved at least a thousand participants, who presented some four hundred and fifty papers. In addition to the American scientists and representatives of the United States Atomic Energy Commission, there were scientists from France, the Federal German Republic, Belgium, the Soviet Union, and other countries.

American, French, and West German work programs relating to improved types of fuel, the construction of fuel elements, and radiation tests on fuel and whole fuel elements for fast reactors were set out at this session. Of particular interest in all these programs was the "doubling time," to which western scientists had earlier paid much less attention, and discussions on the most promising fuel for fast reactors – mixed carbides and nitrides – although considerable space was also afforded to the further development of oxide fuel.

The key questions now interesting foreign scientists from the point of view of the optimum construction of fuel elements for fast reactors are: 1) the maximum permissible temperatures in the core; 2) the effective density of the core; 3) the heat-transfer medium in the fuel element (sodium or helium); 4) the geometrical parameters of the fuel element, such as the thickness of the can, the diameter of the core, and the extent of the heat-transfer gap; 5) the permissible linear powers of the fuel elements; 6) ways of reducing the mechanical interaction of the core with the fuel-element can; 7) ways of preventing the carbiding of the can.

The American program for the comprehensive study of carbide and nitride fuel was set up with the intention of choosing between these two forms of fuel by 1979-1980, and then continuing the development and industrial adoption of one of them. It is considered that by 1985 sufficient experience for this purpose will have been gained in relation to the properties of the improved fuel, its reliability, and its economic characteristics.

One serious shortcoming of nitride fuel, of course, is the fact that nitrogen-14 (amounting to 99.62% of natural nitrogen) has a large neutron-capture cross section. In the opinion of the American scientists, however, this fact should in no way reduce interest in nitride fuel, which also has a number of marked advantages. These scientists consider it an entirely practicable and economically justified process to

Translated from Atomnaya Énergiya, Vol. 41, No. 4, pp. 268-269, April, 1975.

engage in nitrogen isotope separation. It is interesting to note in this connection that in the Battelle Institute of Applied Sciences (Columbus, Ohio), which was visited by the Soviet delegation, only mixed nitride fuel is at present being studied.

The French and West German programs devote principal attention to the study of carbide fuel as the more promising material, at the same time acknowledging that, for the first fast reactors, the principal form of fuel remains that of the oxide type.

The western scientists all agree in their estimation of the possible "doubling time" when using carbide fuel: eight to ten years. These scientists have already initiated a considerable complex of investigations into the properties of carbide fuel, including radiation tests, in which the linear loading of the fuel elements is brought up to 1000-1300 W/cm, while France is studying the intrareactor behavior of carbide fuel elements subjected to a loading of 3200 W/cm, achieving a burn-up of 140,000 MW·days/ton.

Great attention was paid in the conference papers to the production of mixed carbides and nitrides. The overwhelming majority of earlier publications had been devoted to the production of carbides and nitrides from oxides. In this forum, however, as never before, the accent was laid upon producing these uranium and plutonium compounds from the metals themselves (rather than the oxides) as original materials. The Battelle Institute, in particular, is studying the technology of producing mixed nitrides from metallic uranium and plutonium only. This is because in this case it is possible to obtain fuel of a specified composition with a minimum content of oxygen and carbon impurities, which has a great effect on the behavior of the core and the efficiency of the fuel elements. It is found, in particular, that more than 0.1% oxygen in the nitride seriously worsens the radiation resistance of fuel elements with nitride cores.

Within the general problem of mixed uranium–plutonium fuel (both carbide and nitride) there is yet another vital problem affecting the technology of its production: how uniform should the uranium and plutonium distribution be? Oxide mixed fuel makes extreme demands on the uniformity of mixing, so that in some countries mixed oxides are obtained by coprecipitation from solutions. This is an expensive and troublesome process. Analogous requirements are imposed upon carbide and nitride fuels as well. The production of these in the form of solid solutions is also an expensive process. The American scientists, however, consider it perfectly acceptable to use a mechanical mixture of uranium and plutonium fuel with a powder size of up to 100 $\mu$. This question is also being studied by West German scientists (Karlsruhe), who have obtained good results on irradiating mechanically mixed carbides up to a burn-up of 8 at.% for a linear power of 990-1300 W/cm. Analogous results were obtained on irradiating mixed oxide fuel prepared by coprecipitation and mechanical mixing in the EBRII reactor.

From the technological point of view the advantages of producing mixed fuel in the form of a mechanical mixture of uranium and plutonium compounds are obvious. This is why so much interest is being evinced in this procedure.

Requirements relating to oxide fuel for the fuel elements of fast reactors were formulated earlier. The new programs consider ways of perfecting this form of fuel, increasing the efficiency of the fuel elements, and ensuring a doubling time of less than fifteen years.

In the United States program, great attention is being paid to the reprocessing of the fuel with a minimum duration of the external cycle (less than a hundred days), since this parameter largely governs the economics of nuclear power. In order to achieve this state of affairs, the question of creating "nuclear parks" in which the whole fuel cycle may be conducted is now being considered. This proposition is also supported from the point of view of the safety of the population and convenience of monitoring in accordance with the Program of Guarantees regarding fissile materials.

This summary illustrates the scope and variety of the program of the 1974 winter session of the American Nuclear Society. Expanded abstracts of the papers appear in a special number of the Transactions of the American Nuclear Society, 19, No. 1 (1974).

# SECOND INTERNATIONAL SCHOOL ON THE TECHNOLOGY OF THERMONUCLEAR REACTORS

L. I. Rudakov

The Second International School devoted to the study of pulsed thermonuclear reactors was held in Italy from September 11 to 22, 1974. Taking part in the work of the school were some forty-five physicists and engineers from Europe, the United States, and Japan.

The first week in the work of the school was devoted to a discussion on the state of research and the latest achievements in the field of pulsed systems. H. Bodin and R. Carruthers (Culham Laboratory, England) gave a detailed analysis of toroidal pinches with large values of $\beta = 8\pi nT/B^2$, stellarators with large $\beta$, and the so-called reverse-magnetic-field pinches. The Culham physicists adopted a well-defined line in all their lectures and discussions, emphasizing the fundamental advantages of systems with a large $\beta$ value over those of the tokamak type. The first advantage lies in the relatively low value of the magnetic fields for the same plasma pressures. In these systems nitrogen-cooled rather than superconducting magnets may be employed. The second lies in the fundamental possibility of achieving ignition of a D–T mixture by ohmic heating alone.

Great interest was evoked by K. Bruckner's lectures devoted to the use of powerful lasers for compressing and igniting the D–T mixture, in which he set out the United States' idea of using lasers for initiating the reaction in the D–T mixture, gave a theoretical description of the compression process, discussed the basic problems and difficulties of this approach, and reported the results of two years experimental research in the KMS organization in relation to the compression of a D–T mixture in a glass envelope, initiated by a laser pulse. These results will be considered below.

The second week in the work of the school was devoted to a discussion on technological and engineering problems associated with pulsed systems. F. Ribi (USA), described a plan for a thermonuclear reactor based on a toroidal Θ pinch. This would appear to be the most fully-developed project for a pulsed thermonuclear reactor in existence at the present time. The reactor comprises a toroidal pinch 50 m in radius, with a radius of the first wall of the chamber equal to 50 cm; the pinch is thermally insulated and held for 100 msec by a longitudinal magnetic field of 110 kG. The total magnetic energy of the system is $10^{11}$ J. The main technical and technological difficulties encountered in setting up such a system will be associated with the rapid shock-wave heating phase, when a magnetic field of tens of kilogauss has to be created in the chamber in the order of a microsecond. This magnetic field has to penetrate through the sectioned lithium blanket, and there is a serious problem of electrical insulation and the prevention of break-down in the blanket sections. Another technological problem is associated with the material of the blanket wall. The properties of the gas blanket in systems of the Θ pinch type formed as a result of the injection of gas with a density of $10^{14}$ cm$^{-3}$ in the region between the hot plasma and the wall were discussed. The blanket serves to reduce the flux of energetic charged particles from the plasma to the wall and the likelihood of wall rupture.

F. Ribi indicated that work is being successfully carried out at this moment in the Scyllac with a view to checking the theoretically-predicted large-scale helical instabilities of the toroidal Θ pinch and stabilizing their feedback; he expressed the conviction that by using feedback and the wall effect to suppress magnetohydrodynamic instability it should be possible within the next couple of years to achieve prolonged retention of hot plasma in a Θ pinch and to establish the possibility of reaching thermonuclear conditions in a toroidal Θ pinch.

---

Translated from Atomnaya Énergiya, Vol. 38, No. 4, pp. 269-271, April, 1975.

G. Rostagni (Italy) and T. James (United Kingdom) gave an analysis of the present state and future prospects of creating large thermonuclear systems with energies of tens and hundreds of gigajoules and powers of over 1000 MW.

In four lectures read by A. Fraaz (USA) and S. Forster (West Germany) a systematic analysis of the thermonuclear situation was presented and two fundamental schemes were proposed for the construction of a laser-based thermonuclear reactor. In the BLASCON thermonuclear reactor proposed by A. Fraaz, rotating lithium fills the whole of the explosion chamber and forms the working substance in the ordinary high-temperature thermodynamic cycle. Injection of the target and the laser beam takes place into the funnel formed by the rotation of the lithium, in which bubbles are specially created in order to soften and absorb the shock waves from the thermonuclear explosion. Experiments have been carried out in Oak Ridge with a Plexiglas sphere full of rotating water containing air bubbles to simulate the BLASCON system. The experiments show that in such a system the intensity of the shock wave and the stresses in the wall may be reduced to a reasonable level.

In the Saturn system proposed and developed in West Germany by a group of scientists under the leadership of S. Forster it is proposed to take off the energy and reproduce the tritium in the ordinary way with the aid of a lithium blanket comprising a large number of modules set together in the form of a honeycomb on the surface of a sphere (the explosion chamber with a diameter of 10-20 m).

The author of this idea sees the advantage of such a system in the possibility of continuously replacing the modules without stopping the operation of the station in order to separate the tritium and repair the modules.

G. Rebeux (France) and K. Kompa (West Germany) discussed the state of thermonuclear research with special reference to the possibility of obtaining powerful laser pulses in order to initiate thermonuclear reactions. These authors consider that before 1980 several installations will have been made with an energy of 3-10 kJ, using light in the nanosecond range. The prospects of obtaining pulses of more than 100 kJ with an efficiency of around 10% is not yet quite clear. Great hopes are laid upon gas lasers, which have a high enough efficiency, but a search will have to be made for high-efficiency gas lasers with an adequately short wavelength.

L. Rudakov considered the prospects of using powerful beams of relativistic electrons to initiate thermonuclear reactions. Electron-beam technology even now permits the construction of a system working at a level of $10^7$ J in a pulse 5-100 nsec long. This is sufficient to set up a thermonuclear experiment with a shell target. The basis for such designs is the success of the KMS physicists, who experimentally demonstrated the fundamental possibility of achieving stable compression of D–T plasma with a heavy (envelope). L. Rudakov also laid down the basic principles underlying the conception of a thermonuclear-explosion reactor (At. Énerg., 36, 258 (1974)). According to this concept, at each shot (discharge) into the chamber, a thick lithium liner is injected together with the fuel. In this way the load on the chamber walls may be considerably reduced and the lithium plasma (at a temperature of about 10000°K) used in various schemes for producing electrical energy at a very high efficiency.

The final lecture came from the representative of the Commission of the European Community, R. Hancocks, who discussed plans for the development of thermonuclear research in the Community. Expenditure and the number of scientists and engineers occupied with thermonuclear research will increase continuously up to the 90's. In the next five years it is proposed to spend 500 million dollars. The total cost of the program up to the year 2000 is estimated as 6000 million dollars. The number of engineers and physicists occupied in the program should double by 1980-1985 and the thematic aspect should contract to one or two lines of procedure. The mainstay of the next five years will be based on the program of toroidal quasi-steady-state systems. Pulsed systems will be developed with a time shift of five to seven years.

K. Bruckner presented the results of two years experimental research in KMS on verifying the feasibility of the severe compression of D–T plasma by a laser-pulse accelerated envelope. A French laser was used for this purpose. The target was a spherical glass envelope 1.5-5 $\mu$ thick and 20-200 $\mu$ in diameter filled with D–T to a pressure of hundreds of atmospheres. The compression was effected by means of a specially-shaped triangular laser pulse ~100 nsec long with an energy of ~100 J. Some 50 J were directed straight on to the target. No more than 30% of the incident energy was reflected from the target. Thus up to 25 J was absorbed in the plasma of the corona. Measurements with a camera-obscura in x-ray illumination showed that the glass plasma of the envelope compressed the D–T mixture by 125 times. Of the 25 J absorbed by the corona, 1 J passed into the energy of the compressing envelope. The measured

rate of compression of the inner layers of the envelope was approximately $4.10^7$ cm/sec, while the camera-obscura-measured degree of compression corresponded to a final density of $6 \cdot 10^{24}$ cm$^{-3}$ and a life-time of the compressed state equal to $10^{-11}$ sec. Thus in this experiment $n\tau = 6 \cdot 10^{13}$ sec/cm$^3$, while the temperature of the compressed D–T mixture approached ~1.5 keV. A neutron yield up to $4 \cdot 10^5$ neutrons per pulse was recorded.

From the x-ray measurements the electron energy distribution function in the corona was determined. When the flux of incident power in the light exceeded $10^{15}$ W/cm$^2$, the electron distribution function comprised a two-temperature distribution with a main temperature of ~1 keV and a temperature tail of the order of 10 keV. This indicates that for large power fluxes collective effects develop in the corona. However, the theoretically-predicted strong reflection of the incident light was not detected under these conditions.

The symmetry of the compression was established in experiments in which a small quantity of a substance with a large Z was added to the D–T mixture. For an asymmetry of the incident flux below 10% the strong x-ray emission of the compressed core at the stage of maximum compression was then symmetrical, which indicated that there was no intermingling of the envelope material with the D–T mixture. The degree of compression of the envelope was measured and expressed as a function of the asymmetry of the incident light, and these results were compared with the results of two-dimensional numerical calculations. The comparison showed, firstly, that the law of thermal conductivity and the value of the thermal conductivity in the corona corresponded to the classical case, and secondly that, even if self-generation of the magnetic fields in the corona existed, the value of the magnetic field was quite small and had no effect on the thermal conductivity.

The main assertion of K. Bruckner, based on calculations and experiments carried out in KMS, lay in the fact that these experiments genuinely simulated a full-scale thermonuclear explosion. Such gas-dynamic parameters as the temperature of the corona, the degree of compression, and the flux of the incident laser light power will be preserved in a large-scale explosion. Increasing the mass of the target requires a proportional energy increase. However, in order to achieve a positive output with a 10% laser efficiency, it is essential to have at least hundreds of kilojoules in a nanosecond pulse.

Thus any advances in the program of obtaining a thermonuclear reaction by means of a laser will depend very much on the progress of laser technology and an increase in laser efficiency.

# FIFTH IAEA CONFERENCE ON PLASMA PHYSICS AND CONTROLLED NUCLEAR FUSION RESEARCH

V. A. Chuyanov

The Fifth IAEA Conference on Plasma Physics and Controlled Nuclear Fusion Research was held in Tokyo, November 11-15, 1974. About 500 delegates from more than twenty countries participated, as well as a number of guests and observers. 47 reports, which summarized more than 180 papers, were given, as well as several individual papers.

There has been considerable interest in tokamak studies in recent years. 62 papers were devoted to this topic (26 experimental, 30 theoretical, and 6 engineering designs for thermonuclear reactors). The experimental papers can be arbitrarily divided into two groups: (a) experiments on devices of increasing size and (b) new plasma heating methods and diagnostics to permit "untying" of the plasma parameters and to study the physics of the processes involved in more detail.

Among the work in the first group are the experiments on the French TFR tokamak, the most powerful tokamak at this time. In this device discharges with currents of up to 300 kA lasting up to 0.5 sec are attained with a magnetic field of 50 kG and a plasma column diameter of 40 cm. The mean plasma density is $4 \cdot 10^{13}$ cm$^{-3}$; the mean electron temperature, 1 keV (up to 2.5 keV in the center); the hydrogen ion temperature in the center, 1 keV; and the energy confinement time, up to 17 msec. Studies of the dependence of the plasma parameters on the discharge current have shown that the energy balance of the ion component is correctly described by neoclassical thermal conductivity and charge exchange. The ion temperature increases monotonically with the discharge current. However, the expected substantial increases in the electron temperature and the energy confinement time as the current is increased beyond 200 kA do not occur. Whether the observed saturation with current is the first sign of future difficulties or whether the appropriate operating regimes at high currents have not yet been found is not clear at present. Another puzzle raised by the experiments on TFR is the absence of impurity buildup on the axis of the discharge, which according to classical assumptions and the experimental results on the T-4 tokamak should be expected for such long discharge durations. In TFR, however, the effective charge does not rise above 4. The analysis of the accident with TFR in June, 1973, is of considerable interest. At that time, during a 150 kA discharge in a plasma of density $6 \cdot 10^{12}$ cm$^{-3}$ the vacuum chamber wall was burnt through. It appears that at densities below $10^{13}$ cm$^{-3}$ the "runaway" electron instability produces electrons with energies of up to 50 keV, trapped in local mirrors originating in the inhomogeneity of the toroidal field between the coils. These electrons are propelled into the wall due to their drift in the inhomogeneous field. The energy released is localized in an area of about 1 cm$^2$ and reaches 200 J over the discharge, which is sufficient to destroy a wall of thickness 0.5 mm.

Among the work in the second group, we should evidently first note the experiments on electron cyclotron heating in the TM-3 machine (Institute of Atomic Energy), where a ratio of plasma pressure to current magnetic field pressure, $\beta_{pol}$, considerably greater than unity has been attained. This shows that the previously observed universal relation $\beta_{pol} = 1$ is defined by the physics of Ohmic heating, not by the physics of confinement.

Neutral beam injection heating was studied on two tokamaks, "Ormak" (Oak Ridge, USA) and ATC (Princeton, USA). In all cases, when injection is tangential in the direction of the current, heating is observed in good agreement with theoretical predictions. When injection is against the current in "Ormak," heating is not observed and there is a noticeable general deterioration in the plasma parameters. The reason is apparently poor confinement of the injected ions and their escape to the walls with release of gas and impurities. This is confirmed by the fact that injection against the current at lower particle energies,

Translated from Atomnaya Énergiya. Vol. 38, No. 4, pp. 271-273, April, 1975.

when confinement should be better, is successful in ATC. Perpendicular injection (when one might expect even poorer confinement of fast ions trapped in local mirrors) also gives negative results on ATC.

Experiments on the Japanese tokamaks, JFT-2 and JFT-2A, dealt with the interaction of the plasma with the walls. Experiments with a moveable diaphragm were carried out on JFT-2 to examine the role of the diaphragm in the entry of impurities, the formation of the discharge, and plasma equilibrium. However, the speed of opening the diaphragm, up to 9 m/sec, was not sufficient. The plasma boundary always succeeded in moving beyond the diaphragm because of diffusion. The JFT-2A tokamak is intended for studies of an axially symmetric divertor. Experiments on this machine began just before the conference and the only thing that can be said up to now is that the divertor does not interfere with the formation of the discharge.

It should be noted that impurities in tokamaks were one of the main themes of the theoretical studies. Detailed computations of the influx and ionization of impurities were presented at the conference and various methods were proposed for eliminating them, such as with RF fields.

The experimental results on stellarators were not unexpected. Both in Kharkov and in Garching (FRC) it was shown that particle losses are described by the neoclassical theory while heat transfer is increased and obeys the pseudoclassical theory as in tokamaks. It was shown that heat transfer is proportional to the square of the electron Larmor radius in the total poloidal field, i.e., including the field from the helical windings, so that the rotational transform, supplemented by the helical windings, improves confinement. This allows us to await with optimism the results of experiments on new, larger stellarators, comparable in size to tokamaks, which will be built in the near future.

An analogous situation holds with open mirrors as well. It was expected that before the conference the large, new Livermore (USA) 2XII-B machine, with injection of a powerful deuterium atom beam (20 keV, up to 600 A) into a target plasma prepared by adiabatic compression, would be running. During the conference the device was in the stages of physical startup, so the first results, which to a considerable degree will determine the thermonuclear future of this approach, should appear in 1975.

Many papers dealt with high beta systems: toroidal theta-pinches and various combinations of Z and theta pinches. As an example of a general result we may say that in all cases, with one or another method, it has been possible to obtain toroidal equilibrium at large beta, including in current free systems ("high beta stellarators"). Further progress will depend on success in the fight with instabilities. We shall dwell in more detail on the results from the most powerful experiment of this type, "Scyllac" (Los Alamos, USA). "Scyllac" is a theta pinch closed into a torus of radius 4 m. The first experiments on the closed torus were completed just before the conference. To compensate for toroidal drift in "Scyllac" a combination of a bumpy ($l = 0$) and a helical ($l = 1$) magnetic fields, obtained by special profiling of the walls of the theta pinch coils, was used. This combination makes it possible to obtain toroidal equilibrium and to avoid the outward drift of the plasma along the radius of the torus. The lifetime of 6-10 $\mu$sec is determined by an instability of the first azimuthal mode, $m = 1$. Higher modes do not appear. To stabilize the $m = 1$ mode a magnetic feedback system has been prepared for now. Another method of stabilizing long wavelength oscillations might be to not use adiabatic compression as a heating method but to shift to shock heating. In this case the plasma would occupy a large part of the chamber and the stabilizing effect of the metal wall on the $m = 1$ mode should suffice for stability. At present, this method of heating is being studied in a linear system.

At this conference, as opposed to previous ones, very much attention was paid to microexplosions produced by high power lasers and relativistic electron beams. The results of calculations of laser compression of multilayer targets were first communicated at the conference. These complicated targets do not change the required total energy of the laser pulse, but do substantially reduce the necessary peak power and make it possible to avoid complicated time profiling of the pulse power.

In the paper by the research group at the firm KMS (USA) experiments on the compression of D–T targets with a glass shell were described. Hollow glass spheres of diameter 30-700 $\mu$, with wall thicknesses of 0.5-12 $\mu$, and filled with a D–T mixture at a pressure of up to 100 atm, were spherically symmetrically compressed using two laser beams reflected from ellipsoidal mirrors. The target was suspended at the common focus of the two mirrors by an aluminum oxide thread of diameter 3 $\mu$. The energy of the laser beam delivered to the target was as high as 240 J. The desired pulse shape was selected by combining a series of pulses of duration 30 $\mu$sec delayed by various amounts. The width of the total pulse of the half power level was 0.03 to 1.0 nsec. The radiant power at the surface of the target reached $4 \cdot 10^{15}$ W/cm$^2$. The best results were obtained for a target of diameter about 70 $\mu$ with a wall thickness of ~0.9 $\mu$

and a D–T pressure of 13-18 atm. In this case ~50 J reached the target, of which about 10 J were absorbed. Under these conditions the plasma temperature in the target reached ~1·3 keV according to soft x-ray measurements. X-ray pinhole photographs indicate a fivefold reduction in the diameter of the target, i.e., a 125-fold volume compression. Up to $4 \cdot 10^5$ neutrons were produced in each pulse. The compression, temperature, and neutron yield are in good agreement.

A large number of papers, from the USSR, the USA, Japan, France, and Great Britain, were devoted to various nonlinear effects which occur when powerful light beams interact with a plasma. The general conclusion of these papers may be formulated as follows: in agreement with theoretical predictions, anomalous reflection and absorption, production of higher harmonics and fast particles, and other nonlinear effects are observed both in simulation experiments with "rarefied" plasmas and microwaves and directly upon illuminating targets with a powerful light beam; however, the harmful consequences of these effects for thermonuclear experiments are, apparently, not as significant as it seemed based on earlier theoretical work.

Experiments with relativistic electron beams are at an earlier stage than laser experiments. However, the successes in beam focusing described at this conference (Sandia, USA; Institute of Atomic Energy, USSR) make it possible to hope that in the near future this method will compete seriously with laser compression. The first experiments on the compression of a hollow gold sphere with an electron beam were described in a paper from Sandia Laboratories (USA). It appears that sufficiently good compression symmetry may be obtained even using only a single beam. At present, it is possible to do experiments with beams of up to $10^{12}$W power, which is one or two orders of magnitude less than that necessary to test the critical physics problems of thermonuclear ignition. To obtain such large powers will apparently require synchronized multichannel systems. At Sandia an accelerator with six synchronized pulse forming lines for $10^{13}$ W at an energy of 1-3 MeV is being built.

On the whole, the conference showed that thermonuclear research is proceeding successfully in all directions and everywhere has reached, or will soon reach, the stage of critical experiments to determine the thermonuclear "future" of one or another approach.

The next IAEA Conference on Plasma Physics and Controlled Nuclear Fusion Research will be held in Munich (FRG) in 1977. Thus, it has been decided to hold these conferences every two years rather than every four.

# CONFERENCE ON THE SPECIALIZATION IN THE PRODUCTION OF ACCELERATORS

L. G. Zolinova

In November 1974 the Conference on the Sharing of Work in the Development and Production of Accelerators for Low and Medium Energies for Industrial, Medical, and Scientific Use took place in Warsaw. Specialists of the German Democratic Republic, Poland, the USSR, and Czechoslovakia and representatives of the "Interatominstrument" participated in the Conference.

The participants of the Conference exchanged information on the accelerators which are developed and supplied by several Socialist countries (see Table 1), analyzed the specifications of the accelerators and the possibilities of increasing their performance characteristics, and discussed recommendations on the international Socialist sharing of work in the development and production of accelerator technology.

The analysis of the specifications has shown that the accelerators which are supplied and which are being developed basically correspond to the requirements set by industry and medicine. The conference recommended that both the energy and the intensity of betatrons be increased, that the size and weight of linear accelerators (particularly those for defectoscopy) be decreased, and that the neutron yield of the neutron generators be increased 5-10 times (from $2 \cdot 10^{11}$ to $10^{12}$ neutrons/sec). Interest in microtrons for defectoscopy and medicine was noted.

TABLE 1. Accelerators for Low and Medium Energies, Supplied and Developed by Socialist Countries

| Country | Model, type | Designation | Basic parameters | | Additional information | State |
|---|---|---|---|---|---|---|
| | | | energy, MeV | intensity, radiation dose | | |
| German Democratic Republic | Directly acting EVA-500 | Irradiation in vacuum | 0,020—0,040 | 500 mA, 30 mrad at 2 m/sec | | Produced for internal needs of the country |
| | Directly acting EVA-200 | Irradiation in vacuum | 0,022 | Two emissions of 160 mA each, 8 mrad, at 1 m/sec | | Development will be finished in 1976 |
| Poland | Betatron B-30-S | Activation analysis | 8–34 | 100 R/min·m (gamma radiation) | Mobile, x-ray | In production |
| | Betatron | Medicine | 34 | 150 R/min·m (gamma radiation) | Mobile therapeutic | Development will be finished in 1976 |
| | Linear | Physics research | 4–8 | | Standing-wave accelerator | In development |
| | Microtron with linear gap (race track) | Activation analysis | 15 | 50 μA | Can be used for x-ray diffraction work | In development |
| USSR | Directly acting "Elektron," models 3,4, and "Avrora." | Radiation chemistry, sterilization, defectoscopy, activation analysis | 0,3–0,7 | 1–20 mA | Has local biological shield and can be operated on normal industrial premises | In production |

Translated from Atomnaya Énergiya, Vol. 38, No. 4, pp. 273-274, April, 1975.

TABLE 1. - (continued)

| Country | Model, type | Designation | Basic parameters: energy, MeV | Basic parameters: intensity, radiation dose | Additional information | State |
|---|---|---|---|---|---|---|
| USSR | Directly acting NG-150I | Activation analysis | 0,15 | 3mA (deuterons) $2 \cdot 10^{11}$ neutrons/sec | Ion beam current 3 mA on the target; ion beam diameter 5-25 mm on the target | In production |
| | Compact cyclotron | Activation analysis | 5-20 (protons) 3-10 (deuterons) 8-26 (helium ions) | 300 μA (internal) 50 μA (external) | Can be equipped with a system for the production of shortlived isotopes | In production |
| | Linear electron accelerators | | | | | |
| | LUÉ-8-5 | Sterilization of medical preparations and articles | 4-12 | 5-7 kW | Can be provided with targets for bremsstrahlung and can be used for activation analysis | In production |
| | LUÉ-8-5V | | 8-10 | 5 kW | | |
| | LUÉ-10-20 | Defectoscopy of thick parts | 10 | 5000 R/min·m, 200 μA on a target | Thickness of the material inspected with radiation: 50 mm during 10 min at a sensitivity of 1% | In production |
| | LUÉ-15M | Radiation therapy, static (±120°), rotational, and tangential-rotational (±15°) treatment | 10-20 | 300 rad/min (gamma radiation), 1000 rad/min (electrons) at a distance of 1 m from the target | Irradiated field 300 × 300 $mm^2$ gamma radiation), 200 x 200 $mm^2$ (electrons); provided with a therapeutic chair which allows the accurate adjustment of the field of irradiation; provided with a programming unit for multi-field irradiation in given directions and with a given dose | In testing |
| | Microtron ST | radiation treatment activation analysis | 20 | Average power and beam current 0.5 kW, 25 μA, 8000 R/min·m, $10^{11}$ neutrons/sec, 35 R/min | Pulse frequencies 50, 100, 200, and 400 Hz | In construction |
| | Betatron B5M-25 | Medicine, can be used also for other purposes | 7-25 (x-ray radiation) 18-23 (electron radiation) | | Betatron head can be shifted in vertical direction within 1200-1800 mm from the level of the field and rotated around the horizontal by 120° | In construction |
| Czechoslovakia | Betatron B-2-10(100) | Defectoscopy | 22 | 30 R/min·m | The intensity measured in the centre of the beam at a distance of 1 mm amounts to 70 R/min | Built |
| | Betatron B-10 | Medicine | 4-19 | 30 R/min·m | The radiation dose rate is 400 R/min for a radiation field up to 12 x 12 cm | Two built; a third is being produced |

The participants of the Conference were of the opinion that an international sharing of work in the planning and production of accelerators for low and medium energies must be established in accordance with the following nomenclature: betatrons B-30-S (Poland), B5M-25 (USSR), B-2-10(100) and B-10 (Czechoslovakia); linear accelerators LUÉ-8-5, LUÉ-8-5V, LUÉ-10-2D, and LUÉ-15M; microtron ST; NG-150I neutron generator; directly acting accelerators "Élektron"; and compact cyclotron (USSR).

M. N. Zizin, B. A. Zagatskii, T. A. Temnoeva, and L. N. Yaroslavtseva

# AUTOMATION OF REACTOR CALCULATIONS*

Reviewed by V. P. Kovtunenko

The book under review is the third publication in the series, "The Physics of Nuclear Reactors." It is devoted to a question that had not previously been discussed so widely in Soviet Literature. Now, in the period of the widespread introduction of third generation electronic computers, problems of the automation of reactor calculations are urgent and are of substantial interest.

The task that programmers have taken and which has ultimately led to the creation of modular systems, is clearly shown in the introduction. The large number of foreign modular systems now being used are an example. A survey of several of them (ARC, JOSHUA, NCCS, CARONTE, CODNUC) is given in the second chapter. Principal schemes of systems, relationships among moduli, means of introduction of the user with the system, and libraries of moduli are cited. The principles of construction of modular systems are preliminarily outlined in the first chapter. The organization of a modular system with a universal monitor is considered in greater detail. The third chapter is devoted to the first domestic modular system for neutron-physical calculation of a reactor (the FIKhAR system), designed by the authors of this book. The algorithmic language developed for the formulation of the problem is described in detail; standard notations of the quantities for the calculation of the reactor, the construction of a monitor for the organization of the computing process, and the composition and requirement for the library of moduli are cited.

The last chapter gives a brief comparative analysis of several modular systems from the standpoint of utilization of electronic computers, operational systems, languages of the systems, computational moduli and program assignments, interfaces and other parameters.

The Appendix cites standard notations of quantities for neutron-physical calculation of a reactor, as well as a list of moduli of the FIKhAR system. Unfortunately, the book does not discuss programs that we class in the second generation – complexes. Substantial experience has been accumulated on the creation and use of complexes, and they are now the basic means of automation of reactor calculations.

It should also be noted that the library of moduli of the FIKhAR system does not contain a number of moduli essential for the calculation of thermal reactors. Despite the shortcomings noted, the book is very useful and is written in good language. It will attract great attention to the problem of the automation of reactor calculations and should promote a joining of efforts of interested persons and organizations in further work on the creation of modular systems.

*Atomizdat, Moscow, 1974.

Translated from Atomnaya Énergiya, Vol. 38, No. 4, p. 277, April, 1975.

A. A. Luk'yanov

# MODERATION AND ABSORPTION OF RESONANCE NEUTRONS*

Reviewed by V. M. Mikhailov

The book under review on the moderation and absorption of resonance neutrons fills an important gap in the systematization and generalization of the results obtained in this important division of reactor physics, since the well-known monograph by L. Dresner on resonance neutrons, published more than 10 years ago is seriously obsolescent. A substantial fraction of the investigations during these years have been directed to the development of methods of calculation of resonance absorption of neutrons. These include: refinement of the methods of narrow and broad resonances, creation of the method of intermediate resonance, determination of the mutual influence of resonances and interference of potential and resonance scattering. Another part of the investigations was aimed at studying new macroscopic effects associated with the resonance structures of cross-sections, in particular, peculiarities of the diffusion of neutrons, important for calculations of rapid and intermediate steps. The achievements obtained as a result of these investigations have found reflection in the book under review.

The book has five chapters. The first chapter gives information from theoretical nuclear physics, as well as certain experimental data on the variation of the cross-sections of nuclear reactions in the region and intermediate energies. In particular, two methods of description of the cross-sections are cited: in single-level and multi-level representations, considering Doppler broadening of the resonances, as well as statistical data on the distribution of the resonance parameters, permitting an estimation of the cross-sections in the region of unresolved resonances.

The second chapter cites the basic premises of neutron physics: determination of the neutron distribution function, various forms of the kinetic equation and its approximations, and the equation for the value of neutrons. Expressions are also cited for the scattering function in elastic and inelastic interaction.

Thus, in the first two chapters the problem of neutron moderation is presented in the most general form, and approaches towards its solution are cited in the following chapters.

The third chapter is devoted to resonance absorption in a homogeneous medium. Here the peculiarities of the formation of the spectrum are cited in the case of cross-sections that depend smoothly on the energy and closely separated resonances. It was shown how depending on the ratio between the width of the resonance and the average energy loss during scattering, approximate approaches to the solution of the problem are constructed. The influence of such factors as Doppler broadening of the resonances, interference of the levels, deviation of the spectrum from an asymptotic structure, etc., are discussed individually.

As one of the advantages of the book we should note the indication of the values of the errors of the approximations considered, as well as quantitative estimates of correction effects. Some attention should have been paid to methodological difficulties in the determination of the upper energy limit of the resonance integral. If, as is described in the book, the limit is raised up to the energy of fission, then with sufficiently rigorous requirements for accuracy, the question arises of the demarkation of the value of the probability of avoiding resonance absorption and the coefficient of multiplication on fast neutrons. Another way might be to select the boundary somewhere below the threshold of fission on fast neutrons and simultaneously below the region of inelastic deceleration. Such an approach would also be convenient because

*Atomizdat, Moscow, 1974.

Translated from Atomnaya Énergiya, Vol. 38, No. 4, pp. 277-278, April, 1975.

most of the calculation methods are based on elastic scattering. However, in this case difficulties arise in the use of the experimental data. On the other hand, the latter question in itself requires a more profound consideration. The "ideality" of the determination of the value of the effective resonance integral (in the case of a Fermi spectrum!) leads, on the one hand, to a complex procedure of treatment of the measurements, and on the other hand forces a cautious approach to its use in calculations of real apparatuses. The fourth chapter discusses the influence of the heterogeneous structure of the medium on resonance effects. After the classical approaches to the solution of the problem, by Gurevich–Pomeranchuk and Vigner, permitting the isolation of the characteristic geometrical parameter in the value of the resonance absorption, a more general approach is given, from which both approximations follow as particular cases. Great attention is paid to the theorem of equivalence of the resonance absorption in heterogeneous and homogeneous media, which simplifies the construction of the calculation schemes and the systematization of the experimental data.

The content of the fifth chapter consists of peculiarities of the consideration of resonance effects in the calculation of rapid and intermediate reactors. A multi-group approach, which necessitates averaging of the cross-sections with respect to resonance within the limits of individual groups, corresponds to the increased requirements for accuracy of the calculation of the space-energy distribution of neutrons. The book discusses the general theory of obtaining the group constants and certain classical schemes. On the whole, the book does not claim to present the entire abundance of calculation methods, proposed for calculations in the resonance region. But it did successfully accomplish its own aim – to acquaint the reader with the modern level of analytical consideration of the problem of the moderation of resonance neutrons and the calculation methods that have found wide use in the practice of calculations of reactors, both in our country and abroad.

E. F. Cherkasov and V. F. Kirilov

# RADIATION HYGIENE*

Reviewed by O. M. Zaraev

The book under review, which was published under the editorship of Academician of the Academy of Medical Sciences of the USSR, F. G. Krotkov, was written as a text book designed for the sanitary-hygiene faculties of medical institutes. Radiation hygiene as an independent discipline has been taught at these faculties for more than 10 years; therefore, the publication of the first textbook is an important event. The authors – great specialists in radiation hygiene – have successfully coped with the vigorous accumulation of new data and with the insufficient degree of development of a number of questions. They were able to coherently and compactly present extensive and varied material, and also to keep a sense of proportion in the construction of individual sections.

The first three chapters acquaint the reader with the basic stages in the development of Soviet radiation hygiene, necessary information from nuclear physics, and general information on the effects of ionizing radiation on the organism, beginning with the primary mechanisms of radiation damage up to the biological responses of the human organism. The authors devote the small fourth chapter to a characterization of natural sources of ionizing radiation; in it they cite the basic information on the natural radiation background, as well as the doses formed in the tissues and organs of man by radiations of natural sources.

Of great interest is the fifth chapter of the textbook, which discusses the maximum permissible levels of radiation as the basis for ensuring radiation safety. The authors discuss in detail the basic stages of development of the concepts of permissible levels of irradiation, the factors determining their repeated lowering, and give a scientific substantiation for the maximum permissible dose of external and internal irradiation, as well as a number of other criteria, standardized by NRB-69.

The sixth chapter of the book discusses the principles of protection in work with radioactive substances and other sources of ionizing radiations. The description of the principles of protection on the basis of the generally accepted division of sources into open and closed enabled the authors to present these principles in an accessible form, while in the section "Principles of Protection Work with Open Sources," they were able to formulate them in an original manner. The classification of objects that carry a potential hazard of contaminating the working environment with radioactive substances, presented by the authors, merits definite attention, although its arbitrariness, dictated by the purpose of the book, is quite obvious.

The seventh chapter contains materials on the protection of the external environment: a characterization of the potential sources of contamination; information on the behavior of radioactive substances; a hygienic characterization of radioactive contaminations; methods of detoxification of radioactive wastes and methods of their burial, and, finally, problems of the sanitary service are described.

Thus, the book presents the basic hygienic aspects of radiation safety at the modern level.

It should be noted that the book does not at all present particular problems of labor radiation hygiene. The advisability of publication of data on the density of fallout of radioactive substances in 1957-1967 is doubtful, since for practical workers they will be chiefly of historical interest, and moreover, have been presented in detail in special publications. The small volume of the book did not enable the authors to present information on the variety of methods and instruments used in radiation monitoring sufficiently completely. There are some remarks on the selection of the material, which, however, are debatable.

*Meditsina, Moscow, 1974.

Translated from Atomnaya Énergiya, Vol. 38, No. 4, p. 278, April, 1975.

Despite the shortcomings noted, the book may be considered a successful attempt to create a modern textbook in radiation hygiene. It will be useful not only for students, but also for engineering and technical workers, employed in the provision of radioactive safety.

# The Plenum/China Program

**Research in the medical, life, environmental, chemical, physical, and geological sciences from the People's Republic of China**

The 15 major scientific journals published in China since the Cultural Revolution are being made available by Plenum in authoritative, cover-to-cover English translations under the Plenum/China Program imprint.

These important journals contain papers prepared by China's leading scholars and present original research from prestigious Chinese institutes and universities. Their editorial boards are affiliated with such organizations as the Chinese Chemical Society, the Academia Sinica in Peking and its Institutes, and the Chinese Microbiological Society.

The English editions are prepared by scientists and researchers, and all translations are reviewed by experts in each field.

| Journal Title | No. of Issues | Subscription Price |
|---|---|---|
| Acta Astronomica Sinica | 2 | $65 |
| Acta Botanica Sinica | 4 | $95 |
| Acta Entomologica Sinica | 4 | $95 |
| Acta Genetica Sinica | 2 | $65 |
| Acta Geologica Sinica | 2 | $75 |
| Acta Geophysica Sinica | 4 | $95 |
| Acta Mathematica Sinica | 4 | $75 |
| Acta Microbiologica Sinica | 2 | $55 |
| Acta Phytotaxonomica Sinica | 4 | $125 |
| Acta Zoologica Sinica | 4 | $125 |
| Geochimica | 4 | $110 |
| Huaxue Tongbao — Chemical Bulletin | 6 | $95 |
| Kexue Tongbao — Science Bulletin | 12 | $175 |
| Scientia Geologica Sinica | 4 | $125 |
| Vertebrata PalAsiatica | 4 | $95 |

*For further information, please contact the Publishers.*

**SEND FOR YOUR FREE EXAMINATION COPIES**

plenum

PLENUM PUBLISHING CORPORATION
227 West 17 Street, New York, N.Y. 10011
In United Kingdom 8 Scrubs Lane, Harlesden, London, NW10 6SE, England

Declassified and Approved For Release 2013/09/25 : CIA-RDP10-02196R000400050002-4